

**Bench-mark morphodynamic
model Ameland Inlet -
Kustgenese 2.0 (ZG-C2)**



**Bench-mark morphodynamic model
Ameland Inlet -
Kustgenese 2.0 (ZG-C2)**

dr. E.P.L. Elias

1220339-008

Title
 Bench-mark morphodynamic model Ameland Inlet -
 Kustgenese 2.0 (ZG-C2)

Client	Project	Reference	Pages
Rijkswaterstaat Water, Verkeer en Leefomgeving	1220339-008	1220339-008-ZKS-0001	70

Keywords
 Kustgenese 2.0; Ameland inlet; morphodynamic modelling; Delft3D

Summary

Making predictions on the future state and development of complex morphodynamic systems such as the Wadden Sea is not a trivial task. Process-based models, such as the Delft3D model system, that actually describe the underlying physics of the morphodynamic systems are therefore essential. Delft3D has been under development at Deltares since the early 1990's and has been applied in various tidal inlet studies, including Ameland inlet, in the past. These studies show that process-based model suites like Delft3D have reached the stage that they can be used successfully to investigate tidal inlet processes and greatly improve our fundamental understanding of the processes driving sediment transport and morphodynamic change.




The bench-mark study specifically aims to identify which trends and patterns in morphodynamic behaviour can or can't be reproduced. The model results presented in the bench-mark simulation show that morphodynamically stable simulations over a timescale of 5 to 10 years can be obtained with Delft3D. The use of a parallel online approach, in combination with a low-resolution model grid, allows us to run with acceptable computational times.

A qualitative comparison of bed-levels reveals a major short-coming of the bench-mark model. The modelled morphodynamic response overpredicts the measured changes of the ebb-tidal delta; the ebb-tidal delta develops beyond observed limits. However, the comparison of the observed trends shows, in the bench-mark simulation and all sensitivity tests, that the model is capable of reproducing the dominant trends. Conceptual descriptions show that wave-dominated ebb-tidal deltas tend to be pushed closer to the inlet throat. In the model, it is likely that the balance between the offshore directed tidal component, and the onshore directed wave-driven transports is not resolved accurately enough.

By selecting a highly efficient bench-mark model we can easily implement, test and verify new insights, model developments and advances as these are obtained in the Kustgenese 2.0 project. The research presented in this study forms part of the Kustgenese 2.0 project, subproject ZG-C1 and ZG-C2 and directly contributes to research questions SVOL-ZG-01, SVOL-ZG-02, SVOL-ZG-03, INGR-ZG-01, INGR-ZG-02.

Referenties

Plan van Aanpak Kustgenese 2.0 versie januari 2017. Bijlage B bij 1220339-001-ZKS-0005-vdef-r-Offerte Kustgenese 2.0. Deltares, 27 januari 2017.

Version	Date	Author	Initials	Review	Initials	Approval	Initials
1.0	29-05-2018	Dr. ir. E.P.L. Elias		Prof. dr. ir. Z.B. Wang		Drs. F.M.J. Hoozemans	

State
 final

Samenvatting

Achtergrond

Deze rapportage “bench-mark studie morfologische modelering Zeegat van Ameland” maakt deel uit van het deelproject ‘Systeemkennis Zeegaten’ van het Kustgenese 2.0 onderzoek naar de lange-termijn kustontwikkeling. Het vergroten van onze kennis over zeegatsystemen is belangrijk om vragen te kunnen beantwoorden over de zandvraag van de getijbekkens van de Waddenzee. Deze zandvraag wordt gezien als een substantiële verliespost voor zand uit het kustfundament en is daarom een belangrijke parameter om het benodigde suppletievolume te berekenen wat nodig is voor het onderhoud van het kustfundament. Daarnaast is systeemkennis van getijbekkens ook nodig om vragen te beantwoorden over de mogelijkheden van grootschalige ingrepen rondom zeegaten waaronder mogelijke suppleties in de buitendelta.

Belangrijkste resultaten

De resultaten van deze studie laten zien dat stabiele morfologische simulaties van het Amelandse Zeegat over de middellange termijn mogelijk zijn. Met behulp van een lage-resolutie model en een efficiënte rekenmethode (parallel online) is het mogelijk om morfologische berekeningen te maken op een tijdschaal van 5 -10 jaar. De resultaten van deze berekeningen laten een stabiele ontwikkeling van de bodem zien. Op de grote schaal van het gehele systeem, blijven de dominante kenmerken van een zeegat systeem (de karakteristieke buitendelta, geulen, platen, bekken en eilanden) behouden en realistisch van vorm.

Een tweede belangrijke conclusie van de bench-mark studie, ondersteunt door een serie gevoeligheidssommen, is dat het model de geobserveerde (grootschalige) trends in buitendelta gedrag goed lijkt te reproduceren. Het model reproduceert de erosie van de Boschplaat, de verplaatsing en vervorming van het eb-schild naar de Kofmansbult, de oostelijke verplaatsing van Akkepollegat en de versterking van het buitendeltafront. Hoewel, het gedrag van de buitendelta wel gereproduceerd lijkt te worden, is dit op de schaal van de individuele geulen en platen niet direct zichtbaar.

Een belangrijke geconstateerde tekortkoming is de overschatting van de morfologische veranderingen (o.a. de gemodelleerde buitendelta strekt zich te ver zeewaarts uit). Een simpele verklaring voor de overschatting van de buitendeltaontwikkeling kan misschien al gevonden worden in “basiskennis” van zeegaten. In principe wordt de vorm van een buitendelta bepaald door de verhouding tussen golf-energie en getij-energie. Golf-gedomineerde systemen worden dichter naar de keel van het zeegat gedrukt en getij-gedomineerde systemen strekken zich juist verder zeewaarts uit. Getij en golven vormen de primaire aandrijving achter de gemodelleerde bodemveranderingen, maar beide zijn sterk geschematiseerd. Het lijkt logisch een nader onderzoek uit te voeren naar de geldigheid van de schematisaties.

Een belangrijke conclusie van deze studie is ook dat de rekentijd van het “bench-mark” model beperkt is. Dit maakt het mogelijk uitgebreid gevoeligheidsonderzoek uit te voeren over de middellange tijdschalen. Dit maakt het ook mogelijk modelverbeteringen, nieuwe inzichten en metingen verkregen tijdens de uitvoering van Kustgenese 2.0 direct door te voeren en door te rekenen in het model.

Een vertaling van de inzichten naar de onderzoeksvragen van Kustgenese 2.0

Dit rapport is een inventarisatie van de huidige staat van het model en heeft daardoor een ondersteunende functie. Dit rapport levert op dit moment geen directe beantwoording van de onderzoeksvragen. De toekomstige modelering welke uitgevoerd gaat worden met dit model (of een verbeterde versie), geeft wel direct antwoord op de vragen in Tabel 1. Uitzondering hierin is zand en slib. Op dit moment is er nog geen bijdrage van slib in het model geïmplementeerd.

Tabel 1: Overzicht onderzoeksvragen Kustgenese 2.0

Code	Onderzoeksvraag	
SVOL-01	Wat zijn de drijvende (dominante) sedimenttransportprocessen en -mechanismen en welke bijdrage leveren ze aan de netto import of export van het bekken?	JA
SVOL-02	Hoe beïnvloeden de morfologische veranderingen in het bekken en op de buitendelta de processen en mechanismen die het netto transport door een zeegat bepalen?	JA
	Hoe zetten deze veranderingen door in de toekomst, rekening houdend met verschillende scenario's voor ZSS?	JA
SVOL-03	Wordt de grootte van de netto import of export beïnvloed door het aanbod van extra sediment in de kustzone of de buitendelta?	JA
SVOL-04	Wat zijn de afzonderlijke bijdragen van zand en slib aan de sedimentatie in de Waddenzee, als gevolg van de ingrepen en ZSS? En wat betekent dat voor het suppletievolume?	NEE
INGR-01	Hoe beïnvloedden de ontwikkelingen van een buitendelta (inclusief de verandering van omvang) de sedimentuitwisselingen tussen buitendelta, bekken en aangrenzende kusten en welke consequenties en/of randvoorwaarden levert dat voor een suppletieontwerp?	JA
INGR-02	Is het, op basis van beschikbare kennis van het morfologisch systeem, zinvol om grootschalige suppleties op buitendeltas te overwegen?	JA

Contents

1	Introduction	1
1.1	Background	1
1.2	Main objectives of this study.	1
1.3	Research Approach	2
1.4	Report setup	3
2	An analysis of the recent morphodynamic changes at Ameland inlet (1999-2016)	3
2.1	Introduction	3
2.2	Bathymetry of the ebb-tidal delta	3
2.3	Morphodynamic changes between 1999 and 2016	4
3	The Delft3D morphodynamic model of Ameland Inlet	8
3.1	Basics of Delft3D Online Morphology	8
3.2	Main components of the sediment transport model	9
3.3	Morphodynamic updating and concepts of morphological acceleration	11
3.3.1	Tide-averaging approach.	11
3.3.2	Online or morphological factor approach	12
3.3.3	Parallel online approach (also called mormerge)	13
3.4	Settings for the Ameland Inlet model application	14
3.4.1	Introduction	14
3.4.2	Model Grids	15
3.4.3	Bathymetry and bed composition	16
3.4.4	Boundary conditions; Tides	17
3.4.5	Boundary conditions: Waves	20
3.5	Additional model parameter settings	22
4	An evaluation of previous model results	27
4.1	Roelvink and Steijn (1999)	27
4.1.1	General description	27
4.1.2	Model Results	28
4.2	De Fockert (2008)	31
4.2.1	General description	31
4.2.2	Model results	32
4.3	Teske (2013)	38
4.4	Jiao (2014)	40
4.4.1	General description	40
4.4.2	Model results	41
5	Results for the bench-mark morphodynamic model simulation of Ameland Inlet	44
5.1	Introduction	44
5.2	Model Results	45
5.3	Sensitivity Testing	49
5.3.1	Effect of wave climate	49
5.3.2	Effect of individual wave heights on long-term morphology	53
5.3.3	Effect of sediment transport tuning factors	55
5.3.4	Effect of initial bathymetry	57
5.3.5	Effect of reduced tides	60
5.4	Discussion	62

5.5	Next steps in Kustgenese 2.0 research	63
5.5.1	Validate the morphological tide	63
5.5.2	Validate the Morphological wave-climate schematisation	63
5.5.3	Grid resolution	64
5.5.4	Sediment transport tuning factors.	64
5.5.5	Initial bed composition.	64
5.6	Concluding Remarks	64
6	References	65

1 Introduction

1.1 Background

It is well known that the largest sediment losses in the Dutch sediment budget occur along the North Sea coastline of the Wadden Sea Area. The processes behind this sediment import are not fully understood to make quantitatively accurate predictions. An essential part of the Kustgenese 2.0 (KG2) program is to develop tools that are capable of reproducing the morphodynamics of tidal inlets. Such tools are indispensable to better understand the natural processes, make predictions of future changes due to e.g. climate change and the related sea-level rise and anthropogenic influence, and to help support sustainable and resilient future coastal management of these systems including large scale nourishments.

Making predictions on the future state of complex morphodynamic systems such as the Wadden Sea is not a trivial task. Large-scale tidal-inlet systems exhibit a range of morphodynamic features that act and interact on different time and spatial scales. Behaviour on the larger scales, do not seem to accurately capture the observed changes in the Dutch Wadden Sea (Elias et al. 2006; Elias et al. 2012). Process-based models that actually describe the underlying physics of the morphodynamic systems are therefore essential. One of the tools available to address questions on the time-scales of years to decades for complex tidal inlet systems is the Delft3D model system. Delft3D has been under development at Deltares since the early 1990's and has been applied in various tidal inlet studies, including Ameland inlet, in the past. These studies show that process-based model suites like Delft3D have reached the stage that they can be used successfully to investigate tidal inlet processes and greatly improve our fundamental understanding of the processes driving sediment transport and morphodynamic change.

The research presented in this study forms part of the Kustgenese2 project, subproject ZG-C1 and directly contributes to research questions SVOL-ZG-01, SVOL-ZG-02, SVOL-ZG-03, INGR-ZG-01, INGR-ZG-02.

1.2 Main objectives of this study.

The bench-mark study presented in this report specifically aims to identify which trends and patterns in observed morphodynamic behaviour can or cannot be reproduced. This approach is only feasible due to the increased efficiency of the numerical models and computer hardware. Typically, morphodynamic model studies were cumbersome and time-consuming due to the long runtimes involved. Runtimes over a week (to weeks) were no exception. This imposed a major limitation on the amount of runs that can be made. Very often the model can only be run once or twice. Especially if model results deviate from what is expected (not uncommon in morphodynamic models), this leaves a lot of uncertainty in the interpretation of the results.

The main objective of this report is to document the results of a bench-mark, morphodynamic model simulation for Ameland inlet. The existing Delft3D model suite and available Ameland model application form the basis of this bench-mark study. In addition to the bench-mark we aim to:

1. identify and summarize the existing (relevant) morphodynamic model studies of Ameland inlet,
2. identify strongpoints and weakness of the bench-mark model, and
3. provide recommendations for the next steps in the KG2 research.

1.3 Research Approach

One of the major pitfalls in morphodynamic modelling is to assess the model skill by only quantitatively comparing model results and measurements. A clear example is given in the study of Lesser (2009), but his conclusion is valid for most morphodynamic studies performed to date. Lesser demonstrated through agreement between modelled and measured morphodynamic behaviour of Willapa Bay, that a process-based numerical model could reproduce the most important physical processes in the coastal zone over medium-term (5 year) timescales. Most of the observed general patterns are reproduced, but the magnitude and/or precise location of these changes are not accurately predicted. In his case the Brier Skill Score, an objective score to measure the model performance results, is a negative value. This in essence means, that the model skill is worse than simply predicting that no morphological change occurs. Extensive tweaking of parameter settings, initial inputs, and boundary conditions to “custom fit” the model to the observations is an often used and accepted method to improve the model skill. With “tweaking” an optimal hind-cast result may be achieved, but in the process, you may have altered the underlying dynamics of the model to such an extent that these are no longer representative of the natural processes.

Such approach is not followed in this bench-mark study. We use a qualitative assessment by comparing model results with morphological developments and trends identified from data. The assessment is founded on understanding of system behaviour and morphodynamic processes, but is – as expert judgement – inherently subjective in nature.

The study of Lesser (2009) also showed that the “observed general patterns are reproduced”, which indicated that underlying processes and mechanisms are most-likely well captured. Such findings are confirmed by other morphodynamic inlet studies. Van der Weegen (2009), Dastgheib (2012), Lesser (2009) and Elias (2006) demonstrate the usefulness of the Delft3D process-based model to study inlet morphodynamics on a wide variety of temporal and spatial scales. Each of these studies used a carefully selected research and model schematization strategy. By using different assumptions and schematizations, simulations over the appropriate spatial and temporal scales can be made. Both short-term, quasi-realtime models (Elias 2006; Elias and Hansen 2012) and the long-term models (Van der Weegen 2009; Dastgheib 2012) seem to produce useful results.

As part of the Kustgenese modelling study we will introduce a method to quantify model performance over a variety of different time- and space scales, and model objectives. A well-quantified skill can be determined for the (short-term) hydrodynamics. By using the various parameters measured during the Kustgenese campaigns, in addition to existing datasets, a clear skill score can be defined. For hydrodynamics this is a straightforward and well-known approach. A similar comparison between model results and Kustgenese measurements can be followed for short-term sediment transport using the Sonar, bed-form and bed composition data. This will require the development of correct evaluation metrics and analysis methods. Parts of such methods and analysis are available in literature, but parts will also need to be developed (in collaboration with the SEAWAD PhD's) given the uniqueness of the Kustgenese campaign.

The definition of an accepted skill based scoring for morphodynamics needs to be part of the Kustgenese study. We envision that this skill score is a combination of quantitative and qualitative metrics. With improved model performance and more accurate prediction advanced brier skill score analysis may be a metric that can be used to quantify performance.

A quantitative metric can be based on the scoring of reproduction of trends. In this benchmark study examples of such scoring are presented.

1.4 Report setup

Following this introduction, in **Chapter 2** of this report we provide a brief overview of the recent morphodynamic changes over the 1999 – 2016 timeframe. An elaborate overview of the data and analysis of underlying processes is provided in Elias (2017a, b). Chapter 2 focusses on the main trends in bathymetric changes that we aim to reproduce in the morphodynamic simulations. The focus is on the recent timeframe 1999-2016 that is seen as representative for the present-day dynamics. **Chapter 3** provides a brief overview of the Delft3D morphodynamic model, and the settings and assumptions underlying the model application for Ameland Inlet. The focus in this Chapter is not to fully explain the equations, but provide essential background to understand some of the assumptions and parameter settings that were used in this study. Overviews of the morphodynamic model results of the studies of Steijn and Roelvink (1999), De Fockert (2008), Teske (2013), Jiao (2014) and Bak (2017) are provided in **Chapter 4**. These studies produced morphodynamic predictions on timescales of 5 to 10 years. The differences between the results as a result of various model settings, approaches and underlying assumptions can already teach us valuable lessons on the strong points and weaknesses of the Delft3D model. Results for the benchmark study are presented in **Chapter 4**. In this chapter we also present results of initial sensitivity testing of various parameter settings and assumptions. This testing allows us to provide more useful recommendations for future research. We conclude by a discussion of the results, concluding remarks and recommendations or next steps in **Sections 5.4 to 5.6**.

2 An analysis of the recent morphodynamic changes at Ameland inlet (1999-2016)

2.1 Introduction

An extensive summary of the recent morphodynamic changes at Ameland inlet is presented in Elias (2017a), while the data is presented in Elias (2017b). In this Chapter, we provide a brief analysis of the dominant changes that are relevant to and therefore will be used to evaluate the performance of the bench-mark model. Section 2.2 provides a brief overview of the dominant channels and shoals. In Section 2.3 an overview of the bathymetric changes since 1989 is presented.

Note that all bathymetric data is gridded to the morphodynamic model grid to allow a fair comparison with the model results. This model resolution is lower compared to the original DEM (Digital Elevation Model) data, therefore the figures presented here contain less detail compared to the reports of Elias (2017a,b).

2.2 Bathymetry of the ebb-tidal delta

Figure 2-1 provides an overview of the location of the main channels and shoals in 1999 (A) and 2016 (B). Both bathymetries show similar characteristics, with a deep main ebb-channel Borndiep along the west coast of Ameland, and in 1999 a smaller channel (Boschgat) between Borndiep and island of Terschelling. In 1989, Westgat still formed a pronounced channel, with a continuous connection to Boschgat. This connection was not present in the 1999 and 2005 bathymetries. Since 2008, Westgat connects directly to Borndiep. The changes in Westgat must have had a pronounced influence in the Boschgat region. In 2016 the connection between Boschgat and Westgat is formed by a shallow platform (at approximately -5m NAP) dissected by several smaller channels or ebb- and flood chutes. The large shoal, in the middle of the inlet, between Boschgat and Borndiep is called Robbeneiland (eiland is the Dutch name for island). Boschgat connects to the main channel Westgat on the ebb-tidal delta, and splits into multiple smaller channels in the basin. The eastern tip of Terschelling island is called Boschplaat.

The ebb-tidal delta is formed by a large shallow shoal area (Bornrif) to the east of Akkepollegat. Akkepollegat is the outflow of Borndiep and the main ebb-channel on the ebb-tidal delta. Since 1989, the distal part of the channel has narrowed and started to migrate eastward. Especially during the last 10 years this locally reshaped the outer margin of the ebb-tidal delta (see next section). In 1989, the Strandhaak Bornrif had just connected to Ameland and the alongshore, pre-dominant eastward migration of the Strandhaak has locally dominated the behaviour of the shoreline since. This natural "Zandmotor" has supplied the (downdrift) coastline with sand since attachment. On the ebb-tidal delta a new shoal area Bornrif Bankje started to show around 2008, and the landward displacement of this shoal introduced large morphodynamic changes along the northeast margin of the ebb-tidal delta. West of Akkepollegat a large ebb-chute and shield formed, that resulted in shoal building on the Kofmansbult. This evolution became increasingly dominant in the 2008-2016 bathymetries.

2.3 Morphodynamic changes between 1999 and 2016

The morphodynamic changes since 1999 are displayed in Figure 2-1C and in detail in Figures Figure 2-2 and Figure 2-3. The focus here is on the morphodynamic evolution since 1999. The reason for this is two-fold. Firstly, the goal of the modelling presented in this study is to capture the relevant morphodynamic evolution for the present-day ebb-tidal delta. In 1989 there was still a two-channel system present; it is likely that the behaviour is different from the one-channel system observed since 1999. Secondly, some questions arise about the validity of the 1989 bathymetry wherein especially Westgat is remarkably straight and deep.

The main morphologic developments that can be observed during the 1999-2016 timeframe include:

1. Erosion of the Boschplaat. The entire tip of the island of Terschelling has eroded and the coastline retreats. This erosion is a continuous and ongoing process over the entire timeframe.
2. Sedimentation of Boschgat. Since 1999 Boschgat (in the inlet) transformed from a channel to a shallow shoal area with a depth of around -5m NAP. The infilling of the channel resulted in a considerable accretion. The platform itself remains fairly stable at an overall depth of -5 m, but smaller channels and ridges periodically introduce areas of erosion and sedimentation. These areas vary over the years.
3. Eastward migration of the basin part of the Boschgat channel and shoal formation to the west of the channel. The basin part of the Boschgat channel has migrated to the east and a secondary small channel emerged along the Boschplaat. The shoal area in between these two channels has considerably grown in height and size.
4. Westward migration Borndiep. On the large scale Borndiep has been fairly stable in size and position, but a considerable amount of accretion has occurred seaward and landward of the inlet. In the inlet gorge the channel has eroded the shoal Robbeneiland, which indicates a slight westward outbuilding of the channel.
5. Accretion of Akkepollegat. Large accretion has occurred along the western margin of Akkepollegat and in the channel centre. The latter occurred especially in the more recent timeframe between 2008-2016.
6. Scour of the ebb-tidal delta front and eastward rotation of the outflow of Akkepollegat.
7. Localized sedimentation due to rotation Akkepollegat and a deformation of the ebb-shield facing the channel.
8. Formation of an ebb-shield on the Kofmansbult shoal. The formation of a large ebb-chute and ebb-shield resulted in large areas of erosion and sedimentation towards the Kofmansbult. Initially, this process started between Westgat and the Kofmansbult, but by 2011 the ebb-chute and shield had migrated onto the Kofmansbult and dominate the changes of the shoal area since.
9. Accretion central part of Bornrif.
10. Formation and landward/ eastward migration of Bornrif Bankje.
11. Eastward migration, areas of erosion and accretion Bornrif Strandhaak.
12. Large (channel) variability in the basin.

A distinct difference in the behaviour of the central part of the ebb-tidal delta can be observed around 2008. Prior to 2008, a larger shoal area extended along the western margin of Akkepollegat after infilling of Westgat. In the bathymetry of 2008, we first observe the formation of the ebb-chute that deforms the shoal into a characteristic ebb-shield. The growth and seaward displacement has increasingly influenced the developments of the ebb-tidal delta. The increasing influence on the outflow of Akkepollegat has resulted in a deformation of the Akkepollegat channel and the surrounding shoal areas.

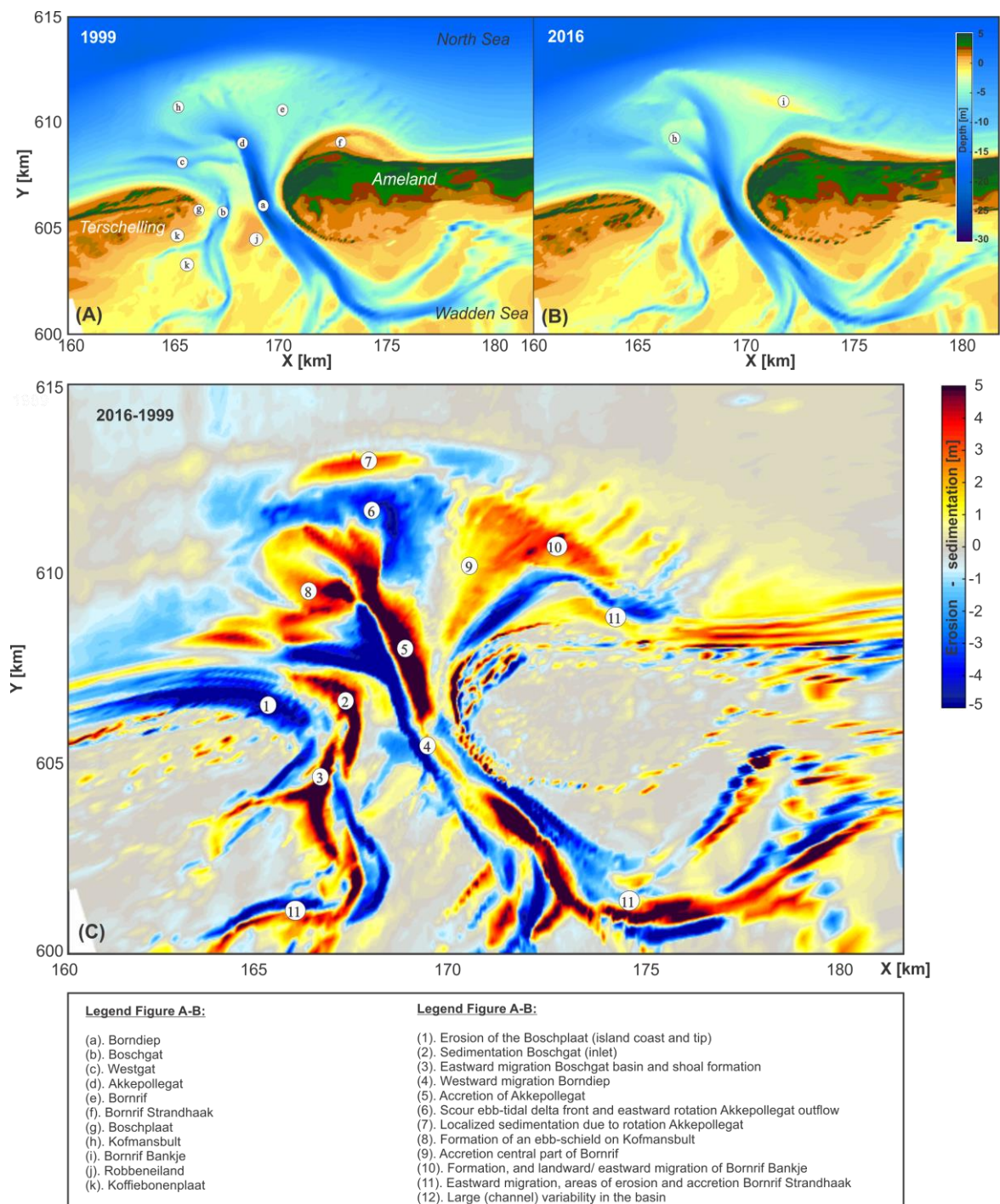


Figure 2-1: Measured bed level in 1999 and 2016 (A,B). (C) Observed bathymetric change between 1999 and 2016. Note that bed level data is gridded on the morphological model grid and therefore only bathymetric changes that can be resolved by the model are shown.

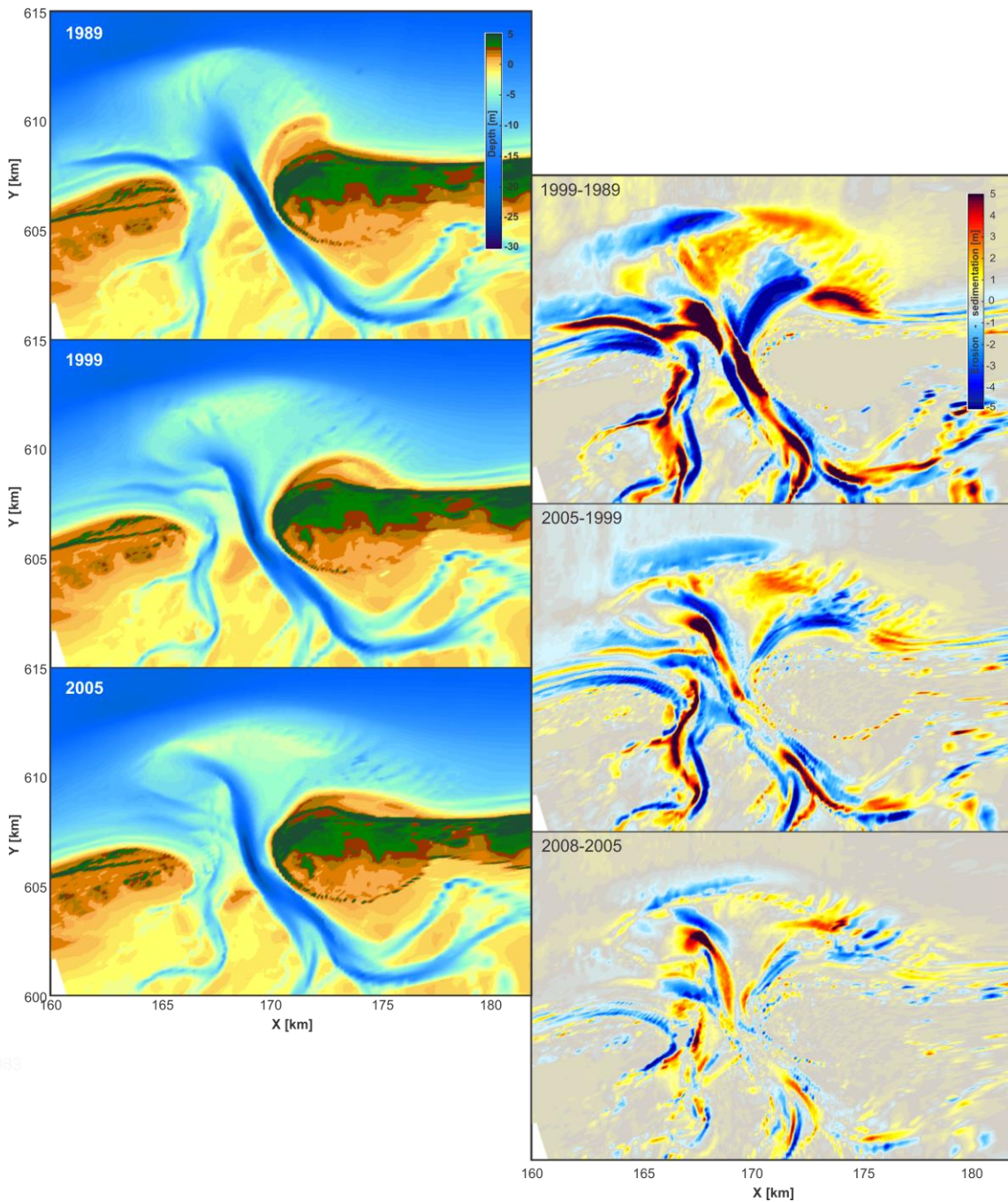


Figure 2-2: Observed bed-levels in 1989, 1999 and 2005 (left panels, top to bottom) and bathymetric changes (right panel) between 1989-1999, 1999-2005 and 2005-2008. Note that bed level data is gridded on the morphological model grid and therefore only bathymetric changes that can be resolved by the model are shown (> 100m).

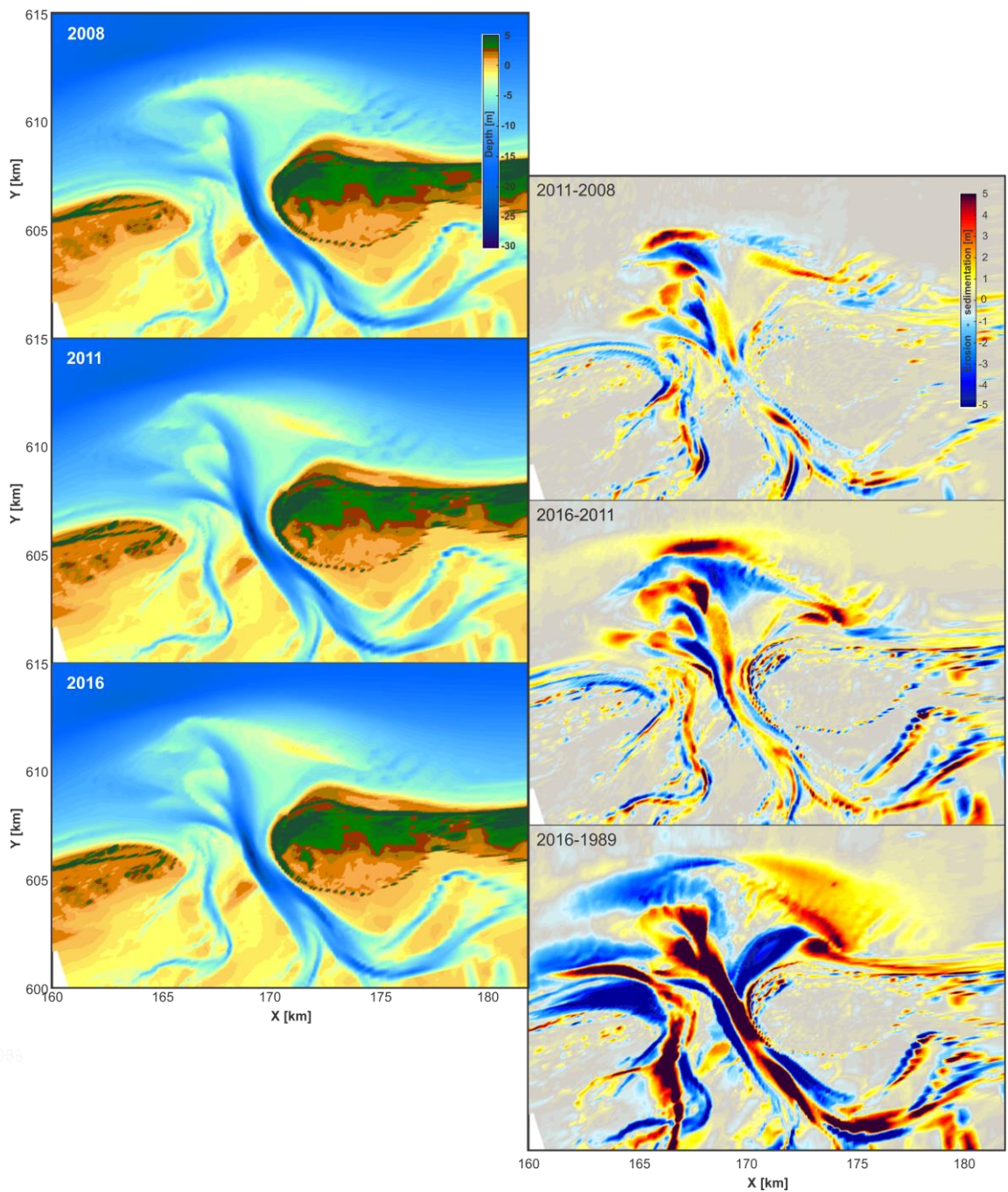


Figure 2-3: Observed bed-levels in 2008, 2011 and 2016 (left panels, top to bottom) and bathymetric changes (right panel) between 2008-2011, 2011-2016 and 1989-2016. Note that bed level data is gridded on the morphological model grid and therefore only bathymetric changes that can be resolved by the model are shown (> 100m).

3 The Delft3D morphodynamic model of Ameland Inlet

3.1 Basics of Delft3D Online Morphology

The main components of Delft3D Online Morphology are the coupled Delft3D-Wave and the Delft3D-Flow modules (see Figure 3-1 for principal overview). Delft3D-Flow forms the core of the model system simulating water motion due to tidal and meteorological forcing by solving the unsteady shallow-water equations that consist of the continuity equation, the horizontal momentum equations, the transport equation under the shallow water and Boussinesq assumptions. Vertical accelerations are assumed minor compared to gravitational acceleration (shallow water assumption) reducing the vertical momentum equation to the hydrostatic pressure relation. By specifying boundary conditions for bed (quadratic friction law), free surface (wind stress or no wind), lateral boundaries (water level, currents, discharges) and closed boundaries with free-slip conditions at the coasts, the equations can be solved on a staggered grid using an Alternating Direction Implicit method (Stelling 1984; Leendertse, 1987). The flow and sediment transport equations are resolved on the flow time-step.

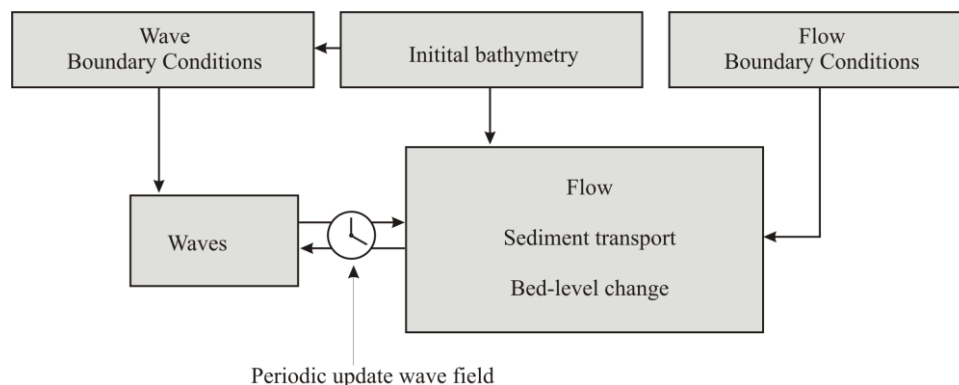


Figure 3-1: Schematic overview of Delft3D.

Wave effects, such as enhanced bed shear stresses and wave forcing due to breaking, are integrated in the flow simulation by running the 3rd generation SWAN wave processor (Version 40.72ABCDE). The SWAN wave model is based on discrete spectral action balance equations, computing the evolution of random, short-crested waves (Holthuijsen et al., 1993; Booij et al., 1999; Ris, 1999). Physical processes included are: generation of waves by wind, dissipation due to white-capping, bottom friction and depth induced breaking, and, non-linear quadruplet and triad wave-wave interactions. Wave propagation, growth and decay is solved periodically on subsets of the flow grid. The results of the wave simulation, such as wave height, peak spectral period, and mass fluxes are stored on the computational flow grid and included in the flow calculations through additional driving terms near surface and bed, enhanced bed shear stress, mass flux and increased turbulence. Wave processes are resolved at the wave time-step, which is typically every 10 to 60 minutes.

3.2 Main components of the sediment transport model

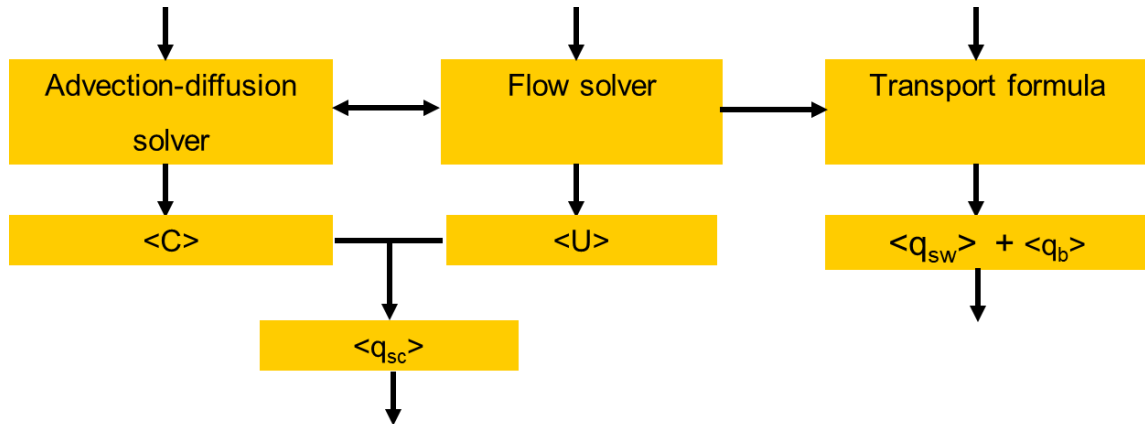


Figure 3-2: Schematic overview of the sediment transport equations in Delft3D.

In this study the Delft3D Online Morphology model was used to resolve the flow and sediment transport patterns dynamically. At each computational time step, Online Morphology supplemented the flow results with sediment transports using the TR2004 transport formulation (Van Rijn, 2007a,b,c,d). The main advantages of integrating the sediment transport into the Flow solver are:

- Simple timekeeping as the flow and sediment transport computations are at the same time-step (less user error).
- Allows for the implementation of sediment – flow interactions (such as turbulence damping and density currents).
- Allows for robust and simple dry-bank erosion formulations, drying and flooding and non-erodible layers.
- Creates robust and stable morphodynamic simulations as the bed is updated simultaneously with the flow and sediment transports.

The Delft3D implementation of this formula follows the principle description of Van Rijn (1993), wherein a distinction is made between bed load and suspended load transports (see Figure 3-2). Bed load transports represent the transport of sand particles in the flow boundary layer in close contact with the bed surface. Suspended sediment transport is computed by the advection-diffusion solver. The Delft3D implementation of this formulation follows the principle description of Van Rijn (1993), separating suspended load (S_s) and bed load (S_b) components. See Van Rijn (1993; 2000; 2002, 2007a,b,c,d) specifically for the transport formulations, and Walstra and Van Rijn (2003) and Lesser (2004) on details of the implementation.

The suspended sediment transport is computed by the advection-diffusion solver, wherein the effect of sediment in suspension on the density is added. A source (D) and sink (E) relation describes the sediment exchange with the bed:

$$D = f_{SUS} \eta 0.015 \rho_s \frac{d_{50}}{a} \frac{\tau_a^{1.5}}{D^{0.3}} \left(\frac{\beta^{VV} / \sigma_c}{\Delta z} \right) \quad (3-1)$$

$$E = c_{kmx} \left(\frac{\beta^{VV} / \sigma_c}{\Delta z} + w_s \right) \quad (3-2)$$

For simulations without waves $\beta = 1 + 2 \left[\frac{w_s}{u_{*s}} \right]^2$, including waves β is replaced by $\beta_{eff} = 1 + (\beta - 1) \frac{\tau_c}{\tau_w + \tau_c}$. The f_{SUS} factor allows the user to calibrate the suspended load transport contribution to the bed-level changes.

Bed load transports (S_b) represent the transport of sand particles in the wave boundary layer in close contact with the bed surface; below the reference level a . Simulations including waves use the approximation method of Van Rijn (2002) to include an estimate of the effect of wave orbital velocity asymmetry:

$$|S_b| = \eta 0.006 \rho_s w_s \left(\frac{\sqrt{(v_R^2 - U_{on}^2)}}{(\rho_s / \rho - 1) g d_{50}} \right)^{0.5} \left(\frac{(\sqrt{(v_R^2 - U_{on}^2)} - v_{cr})^2}{(\rho_s / \rho - 1) g d_{50}} \right)^{0.7} \quad (3-3)$$

The bed-load transports are split in a current-related component ($S_{b,c}$) acting in the direction of the Eulerian velocities, and wave-driven part ($S_{b,w}$) in the direction of wave propagation, and an additional wave-related suspended sediment transport is added to account for wave asymmetry effects:

$$|S_{s,w}| = 0.2 \frac{U_{on}^4 - U_{off}^4}{U_{on}^3 + U_{off}^3} 0.007 \rho_s d_{50} \frac{\sqrt{(v_R^2 - U_{on}^2)}}{(\rho_s / \rho - 1) g d_{50}} \quad (3-4)$$

Bed load transports are modified to account for longitudinal and transverse slope effects using approximations based on Bagnold (1966) and Ikeda (1982) respectively.

a	reference height
Δz	the vertical distance from the reference level a to the centre of the reference cell
C_{kmax}	the mass concentration in the reference cell
w_s	is the sediment settling velocity (m/s).
f_{sus}	is a calibration coefficient (default 1)
η	relative availability of the sediment fraction at the bed
Ta	dimensionless bed shear stress (Van Rijn, 1993, 2000).
D^*	dimensionless particle diameter (Van Rijn, 1993, 2000).
τ_w, τ_c	bed shear stresses due to waves and currents ()
v_{cr}	critical depth-averaged velocity for imitation of motion (Shields)
v_R	magnitude of the
U_{on}	is the high-frequency near-bed orbital velocity due to short waves in the direction of wave propagation (m/s)

To describe sediment characteristics, additional formulations are included to account for: density effects of sediment in suspension (Eckart, 1958), settling velocity (Van Rijn, 1993), vertical diffusion coefficient for sediment, suspended sediment correction vector and sediment exchange with the bed. The elevation of the bed is dynamically updated at each computational time-step by calculating the change in mass of the bottom sediment resulting from the sediment transport gradients. A series of tuning parameters (such as f_{SUS} , f_{SUSW} , f_{BED} , f_{BEDW}), allows for the calibration of the individual contributions of the suspended load transports, the bed-load transports, and the wave-driven suspended and bed load transports before bed elevation updating. Table 3-1 presents an overview of recent studies and settings of the calibration parameters. Note that these settings are the result of calibrations to produce best results for each of these studies. Depending on the assumptions made in the model

development, different settings are needed. A general correspondence between the studies is the reduced settings for the f_{SUSW} and f_{BEDW} . This indicates that the wave related contribution to the sediment transport is overestimated by the sediment transport formulations. The most recent study of Luijendijk et al. (2017) also indicates that sediment transport in general is overestimated (f_{SUSW} and $f_{BEDW}= 0.5$).

Table 3-1: Overview of calibration factors as applied in recent studies (based on Bak, 2017)

Topic	Study	f_{SUS}	f_{BED}	f_{SUSW}	f_{BEDW}
Modeling of Ameland inlet	Bak (2017)	1.0	1.0	0.7	0.3
Modeling of Ameland inlet	Jiao (2014)	1.0	1.0	0.2	0.2
Modeling of Ameland inlet	Wang (2015)	1.0	1.0	0.0	0.0
Sand engine	Tonnon et al (2009)	1.0	1.0	0.2	0.2
Sediment demand Dutch coast	Van der Spek (2015)	1.0	1.0	0.2	0.2
Tidal inlet Sri Lanka	Duong (2015)	1.0	1.0	0.0	0.0
Sand Engine	Luijendijk et al (2017)	0.5	0.5	0.2	0.2

Lesser (2004) provides a complete overview of model testing under a range of (simple) validation cases. These cases include:

- theoretical results, such as the development of sediment transport under flow conditions, the modelling of an equilibrium longitudinal bed slope from a plane bed, and the simple case of sediment settling from suspension.
- laboratory datasets, such as reproducing a flume experiment with downstream migrating trench, the formation of bars and channels in a curved flume with spiralling flow, and reproducing sediment concentration profiles under the action of waves and currents.
- Case studies, such as the wave-driven deformation of a sediment hump, and tombolo formation behind an emergent shore-parallel breakwater.

Hibma (2004), Elias (2006), Lesser (2009), van der Wegen (2009) and Dastgheib (2012) present recent morphodynamic model applications.

3.3 Morphodynamic updating and concepts of morphological acceleration

Process-based models like Delft3D Online Morphology compute the hydrodynamic processes and associated sediment transports at each computational time step. Typically, such time step ranges between 0.1 and 1 minute. The morphodynamic changes on the scale of e.g. an ebb-tidal delta system take place on timescales of years to decades. One of the fundamental aspects of morphodynamic modelling is to bridge the gap between the hydrodynamics and associated sediment transports, and the morphodynamic changes. Roelvink (2006) provides a detailed overview of various coastal morphodynamic evolution techniques. Roelvink discusses 3 different strategies: (1) Tide averaging approach, (2) Online or morphological factor approach (Delft3D online), and (3) Parallel online approach (mormerge).

3.3.1 Tide-averaging approach.

The underlying assumption in the tide-averaging method is fact that morphological changes occur on time-scales that are an order of magnitude larger than the change in the hydrodynamics. The influence of the morphodynamic changes are thus negligibly small; such changes hardly affect the hydrodynamics or sediment transports. Under this assumption it is

acceptable to assume a fixed bed during the tide cycle, compute the sediment transports over the tide cycle and fixed bed, and use the (gradients in) tidally-averaged transport to compute the bed elevation change. By using a continuity correction, a further reduction in computational time can be achieved. The underlying assumption of the continuity correction is that the flow pattern and rate remain similar (see Figure 3-3 and Roelvink 2006 for details).

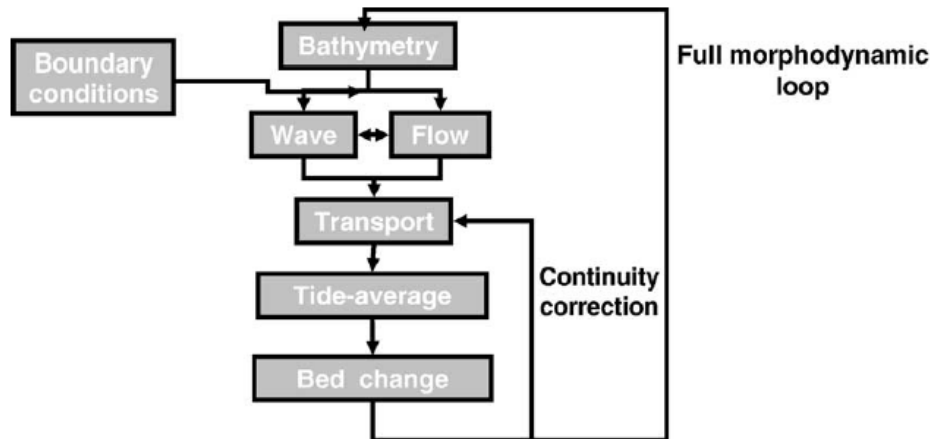


Figure 3-3: Schematic overview of the tide averaging approach (from Roelvink, 2006).

The studies of Hartsuiker and Wang (1999), Roelvink (1999) and Stein and Roelvink (1999) are all based on the tide-averaging approach. Herein the flow model was run at a 60s time step. Waves had a 12-minute recurrence interval. Sediment transports were computed with the Bijker and Soulsby-van Rijn formulations at 5-minute intervals using a 5 continuity steps between hydrodynamic updates. The total simulation period obtained was 7 years. See Chapter 4.1 for an evaluation of the morphodynamic results.

3.3.2 Online or morphological factor approach

The development of the Delft3D Online Morphology model (Lesser et al. 2004) allows for a different method of model schematizations. Online morphology supplements the flow results with sediment transport computations; at each computational time step flow, sediment transport and the associated bed-level changes are computed. Before the bathymetric changes are included in the model a morphological factor can be applied.

$$\Delta t_{morphology} = f_{MOR} \cdot \Delta t_{hydrodynamic} \quad (3-5)$$

With a morfac (f_{MOR}) of 1 the bed level changes correspond directly with the computed sediment transport gradients (so-called brute force simulations). By increasing the f_{MOR} the depth changes are increased, which basically corresponds to the morphological changes over a longer time interval (more tide cycles). The underlying concept is similar to the elongated tide concept of Latteux (1995). The f_{MOR} factor can be used as the time scales related to the morphological changes are several orders of magnitude larger than the time scales of the water motion. An important assumption underlying this concept is that nothing irreversible happens within an ebb or flood phase, even when all changes are multiplied by a factor. As a result, there are maximum limits to this factor, and results can only be evaluated after each complete tidal cycle (or a complete number of tidal cycles). Figure 3-4 provides a schematic depiction of the method

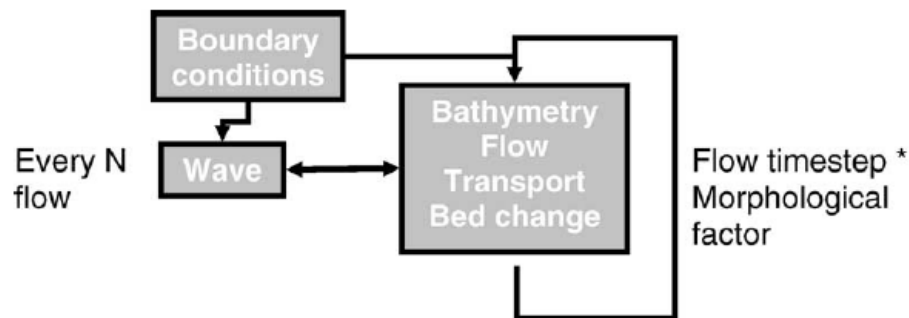


Figure 3-4: Schematic overview of the online morphodynamic model (from Roelvink, 2006).

The major advantages of the online morphology method include:

- (1) the bottom evolution is computed in small time steps but still allows for long morphodynamic simulations;
- (2) all short-term (hydrodynamic, wave and sediment-transport) processes are coupled at flow time-step level;
- (3) drying or wetting becomes more straight forward;
- (4) no continuity correction is required and therefore processes in shallow water are represented more accurately.

Extensive validation is presented by Lesser et al. (2004) and Lesser (2009). In the study of Teske (2013), summarized in Elias and Teske (2015), the online morphology model is used to test the morphological development of the Ameland inlet using the Van Rijn (1993) and Van Rijn (2007) sediment transport relations. Tide only simulations were performed over 2-years of hydrodynamic time using a morfacc of 50. The model results illustrate the morphodynamic response for 100 years of bed-level change (see Chapter 4-3 for results).

3.3.3 Parallel online approach (also called mormerge)

The recent studies of De Fockert (2008), Jiao (2014) and Bak (2017) use the parallel online method to compute the morphodynamic changes in Ameland inlet. The parallel online method is further development of the standard online approach. As explained in Roelvink (2006): “The parallel online approach (or mormerge) assumes that the hydrodynamic conditions vary much more rapidly than the morphology can follow. If the time interval within which all different conditions (ebb, flood, slack, spring tide, neap tide, NW storm, SW wind, etc.) may occur is small relative to the morphological timescale, these conditions may as well occur simultaneously. This leads to the idea that we may as well let simulations for different conditions run in parallel, as long as they share the same bathymetry that is updated according to the weighted average of the bottom changes due to each condition. The flow scheme of this approach is given in Figure 3-5. In this scheme the simulation is split into a number of parallel processes, which all represent different conditions; at a given frequency all processes provide bottom changes to the merging process, which returns a weighted average bottom change to all processes, which then continue the simulation. The parallel execution of the different processes lends itself to an efficient implementation on a series of PCs or Linux cluster. One can now design the different processes to keep each other in check, for instance by assigning a different tidal phase to different conditions, so that ebb and flood transports counteract each other at all times. This reduces the amplitude of short-term changes and thus allows the use of much higher morphological factors.”

In the study of De Fockert (2008) morfac values of 180 and 270 are used (see Chapter 4.2). Sensitivity testing by Bak (2017) reveals negligible influence of the morfac on morphodynamic results up to 600 (note that the grid resolution of Bak is half of the grid resolution of De Fockert). Two important factors play a role that allow the use of these high morfac values. Firstly, each wave condition is scaled with the probability of occurrence before applying the bed level update. In essence this reduces the applied effective morfac. Since storm events occur less frequent, the probability of occurrence is lower and this results in a larger reduction of effective morfac. Secondly, a phase shift in the start of the individual conditions ensures that ebb and flood transports counteract. The bed level changes are based on the net effect of the complete tidal cycle rather than the gross sediment transports. Since the net changes are significantly smaller this allows the use of a much larger morfac. In the study of Bak (2017), 12 wave conditions are used and a phase shift of 1/12 of the tidal period is imposed. Without phase shift, instabilities occur with a morfac of 200, with phase shift morfac values can increase to 600 before bed level changes are influenced.

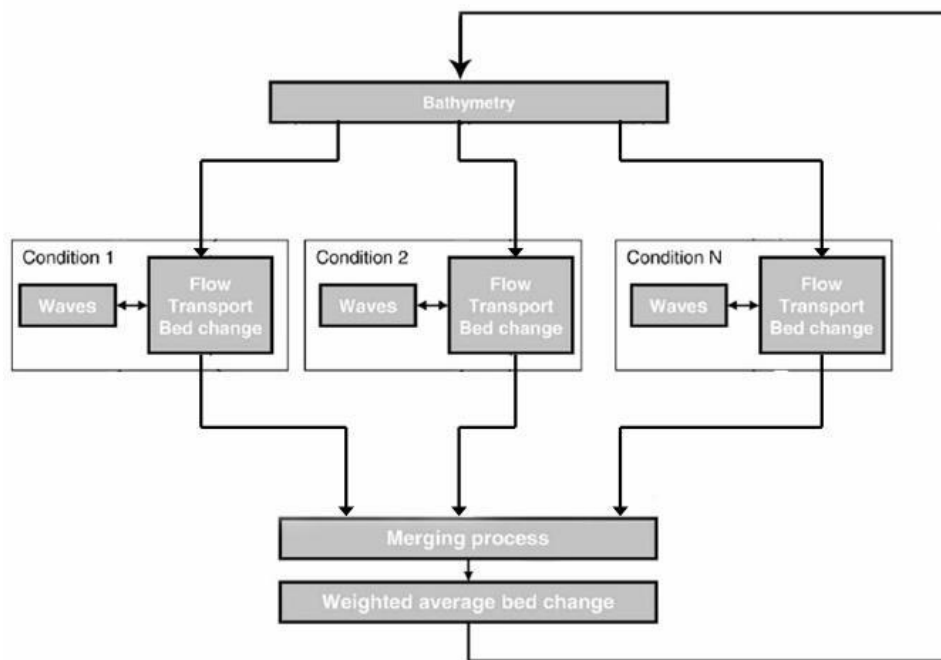


Figure 3-5: FLOW-scheme of the 'parallel online' approach (De Fockert 2008, modified after Roelvink, 2006).

In the present benchmarking study, we use the schematisation of Bak (2017). The hydrodynamic time step is set at 30s. Wave coupling takes place in 60 minute intervals. The wave climate is schematized by 12 wave conditions that are all run in parallel. Between each parallel simulation a 1/12 tidal length of a phase shift in the water level boundary conditions is imposed. The morfac is set to a value of 600, which means that each morphodynamic year is represented by a 14.6 hour hydrodynamic computation.

3.4 Settings for the Ameland Inlet model application

3.4.1 Introduction

Over the last 2 decades morphodynamic models have been used to study Ameland inlet. One of the first model studies was the study of Wang (1995), that used a simplified model grid. The basis of the present day Ameland model is formed by the studies of Hartsuiker and Wang (1999), Roelvink (1999) and Stein and Roelvink (1999) using the Delft3D MOR model system.

In 2008, De Fockert converted the grids into the Delft3D Online Morphology model that is still used today. The online-sediment version of the model has been continuously improved and tested with most relevant studies being Teske (2013), Jiao (2014), Wang (2015, 2016) and recently Bak (2017). The settings of the latest study (as presented by Bak, 2017) are used for the benchmarking study presented in this report.

3.4.2 Model Grids

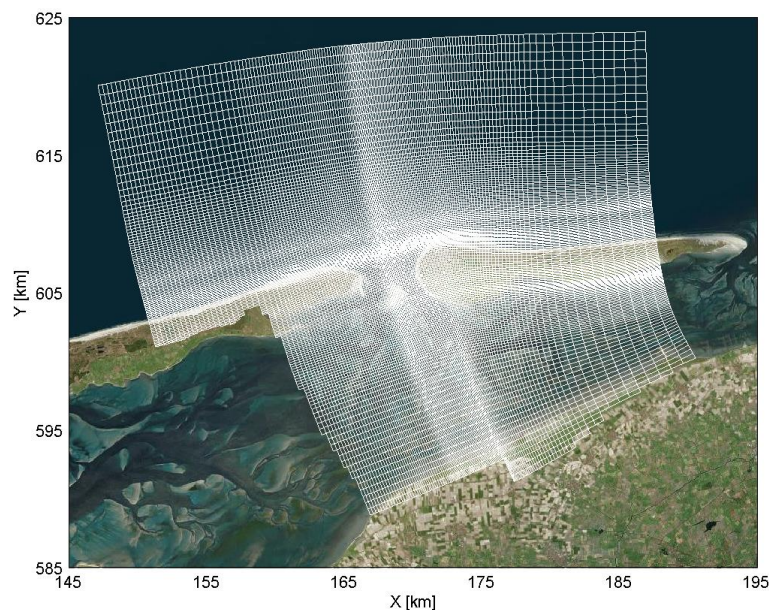


Figure 3-6: Ameland model grid used for the benchmarking study.

Figure 3-6 illustrates the computational grid used for the hydrodynamic and morphodynamic model simulations. The fundamentals of this grid are still based on the study of Roelvink and Steijn (1999) although the version shown here has half the resolution compared to the original. The model boundaries are chosen outside the area directly controlled and influenced by the inlet processes. The seaward boundary is located roughly along the -20m contour¹. This contour is often considered to form the transition between the morphological active (landward) and inactive (seaward) area. The boundaries to the west and east are located halfway of the island of Terschelling and near the end of the island of Ameland. These locations sit well outside the ebb-tidal delta, and along the island coasts relatively undisturbed coastal profiles are present with a gently sloping foreshore and (multiple) breaker bars in the surfzone. In the basin the boundaries are chosen along the tidal divides, and along the mainland coast of Friesland.

A high-resolution and a low-resolution variation of this grid is present. The model grid used in this benchmarking study has a 174x162 grid cells, varying from 60m by 80m in the inlet to 600m by 700m offshore. The grid cell sizes vary smoothly over the domain thereby fulfilling criteria for orthogonality (below 0,02) and smoothness (variation in grid cell size < 10%). This resolution of 60x80m in the inlet seems coarse relative to the features that we are trying to

¹ This means that this model cannot be used for studying the sediment transport over the seaward boundary of the coastal foundation, which is one of the other research questions for the Kustgenese 2.0 long term coastal development research. Aligning these model developments is in progress.

model. However, the models results of De Fockert (2008), using the high-resolution version of the grids (348x324 grid cells with a resolution of 30x40 m in the inlet), did not show a significant improvement between the higher and lower grid resolution. Both domains are capable of producing stable model simulations, and they both shows strong points and weaknesses on the scale of the ebb-tidal delta. Since, the computational runtime is directly proportional to the number of grid cells used in the model domain the lower resolution grids are more efficient to run, allowing for more sensitivity testing and analysis. Increasing the number of grid cells by a factor 2 (keeping the grid resolution similar), will increase the runtimes by a factor 2 as well. However, increasing the resolution by a factor 2, results in a runtime that is at least a factor 8 higher. The number of computational points increases by a factor 4. A factor 2 reduction in size, reduces the computational time-step by a factor 2 in order to retain a similar courant number. The wave model grid has similar dimensions as the flow grid but is extended slightly along all sea boundaries to avoid boundary instabilities.

3.4.3 Bathymetry and bed composition

Bathymetry

The bed schematisation for the model depends on the model iteration. In principle the Vakloedingen datasets are used to compile complete bathymetries. An extensive description of the available datasets is presented by Elias (2017b). Figure 2-2 and Figure 2-3 present an overview of the vakloedingen gridded to the model domain. The Quickin program (Delft3D) has been used to construct these bathymetries. Since the model resolution is significantly lower than the resolution of the Vakloedingen a simple averaging method (nearest point) was used to generate the model bathymetries. As an initial bathymetry for the benchmark study the 2016 depths have been used.

Bed composition

In addition to the hydrodynamic boundary conditions, the bed composition can have a major effect on the morphodynamic simulation. Based on 100-year schematised model simulations for Ameland inlet, Elias and Teske (2015) conclude that a uniformly applied realistic fraction distribution (containing 100-400 μm sand) did not improve channel stability compared to the homogenous bed as the fine sediments are eroded from the system rapidly and deposited on the ebb-tidal delta. However, adding a coarser sediment fraction (or starting from an initial equilibrium fraction distribution) tends to stabilize the runs efficiently. For realistic simulations of the complete inlet system, graded sediments are likely essential due to the increased, more genuine, morphological response in both energetic and non-energetic areas. Similar conclusions are reached by Dasgheib (2012) for Texel inlet. In this study, best results were obtained using a "logical initial sediment size distribution" that is based on the modelled bed-shear stresses derived from pre-simulation runs.

Based on a series of sensitivity tests Bak (2017) derived an initial bed composition map for the Ameland inlet (Figure 3-7). Starting from an initial 4 fraction (100, 200, 300 and 400 μm) distribution, that has varying characteristics for the morphodynamic elements. The main channels consist of respectively a mixture of 0, 30, 40 en 40% of the fractions, the basin has a 40%, 40%, 20% and 0% distribution. The distribution for the offshore area contains 30, 30, 30, 10 % of the fractions. The tidal flats near the Frisian coast consist of 100 μm (80%) and 200 μm (20%) only. Prior to the morphodynamic simulations, additional simulations are made to generate the "model equilibrium" bed composition (Figure 3-7, right). In these simulations all forcing processes are included, but no bed-level change is allowed. Even in the absence of bed-level change, the bed composition will be updated. Figure 3-7 (right panel) shows the end result

after 17.5 years of simulation. This composition maps is used as input for the bench-mark simulation.

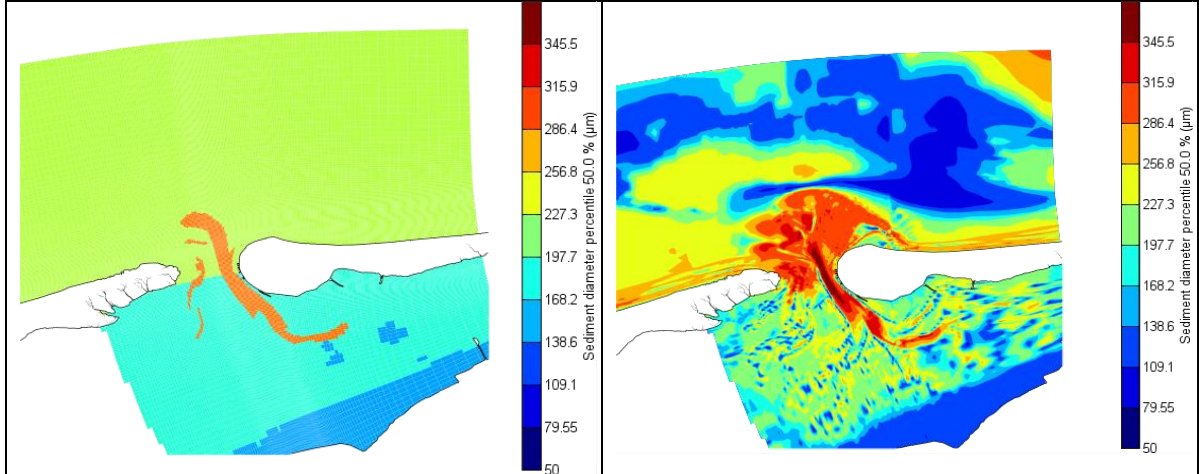


Figure 3-7: Sediment diameter distribution (d_{50}) at the start of the simulation (left) and after 17.5 years of simulation incl. tides, wind and wave-driven processes (right).

3.4.4 Boundary conditions; Tides

De Fockert (2008) and Jiao (2014) both use the basic principle of Latteux (1995) to derive the morphologic representative tide. However, the Fockert uses bed-level changes in the analysis, while Jiao focusses on the sediment transports through the inlet gorge (see Figure 3-9 for locations). In his conclusions, De Fockert mentions that hindcast simulations show that the morphological tide overestimates the transports through the Borndiep compared to the neap-spring cycle. One of the goals of the study of Jiao was to improve the morphodynamic tide schematization. The approach follows the following steps:

- (1) Calculate the total sediment transport over the full spring-neap cycle, and determine the tide-averaged residual (\bar{S}_l).
- (2) Calculate the running average over a double tide (24 hours 50 minutes) to take daily tidal inequality into account.

$$\bar{T}_l(t) = \frac{1}{T} \int_{t+0.5T}^{t-0.5T} (T_i(t)) dt$$

- (3) Determine the ratio between the total residual transport and the double tides:

$$W(t) = \frac{1}{N} \sum_{i=1}^N \frac{\bar{S}_l}{\bar{T}_l(t)}$$

- (4) Determine the difference between the total residual transport and the reference transport for each location. Determine the root mean square error.

$$E_{RMS}(t) = \sqrt{\frac{1}{N} \sum_{i=1}^N \left(\frac{W(t) \cdot \bar{T}_l(t) - \bar{S}_l}{\bar{S}_l} \right)^2}$$

Tides were schematized by reducing a typical full monthly spring/neap tidal cycle into a morphologically representative 24.8 hour tidal cycle. The morphodynamic tide of Bak (2017) is based on the analysis presented by Jiao (2014) and briefly described in this section. The underlying hydrodynamic tide is derived by nesting of the Ameland model in the Wadden Sea model (Figure 3-8). An extensive description of the validation and calibration of the Wadden Sea model is given in de Graaff (2009).

The seaward (northern) boundary of the Ameland model was subdivided in 8 sections and prescribed by the water levels. The eastern and western boundaries were defined through a Neumann (water-level gradient) condition. Using the Delft3D nesthd1 routine the boundary locations were transformed to observation locations in the Wadden Sea model. The Wadden Sea model was run over a 1.5 month timeframe (16 October – 1 December 2010) and results saved at the observation points were transferred back to the locations of the Ameland boundary points using the Delft3D nesthd2 routine. Astronomic time-series at the boundary points were derived using the t-tide toolbox (Pawlowicz et al, 2002). These astronomic time-series form the basis of the morphological tide.

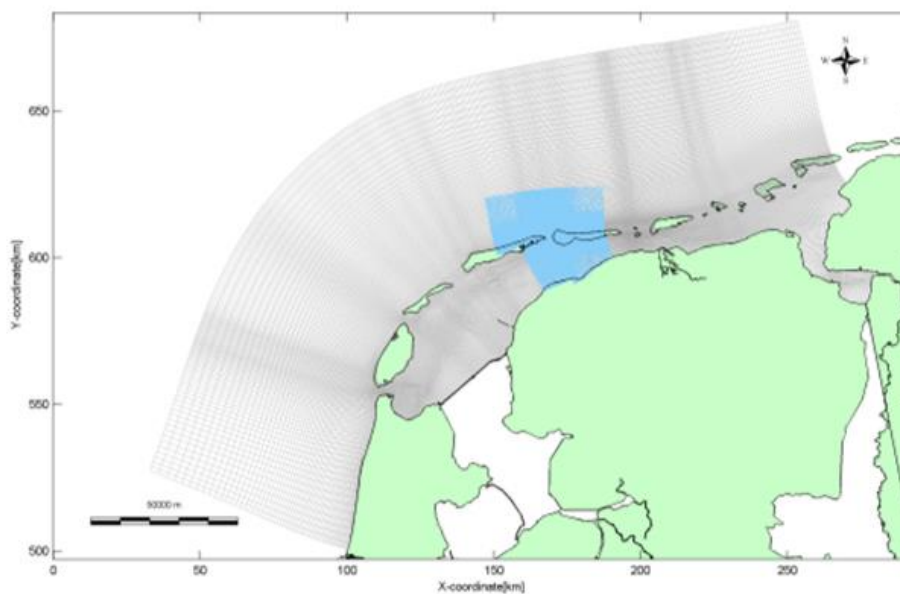


Figure 3-8: Nesting of the Ameland model grid (blue) in the Wadden Sea model (gray).

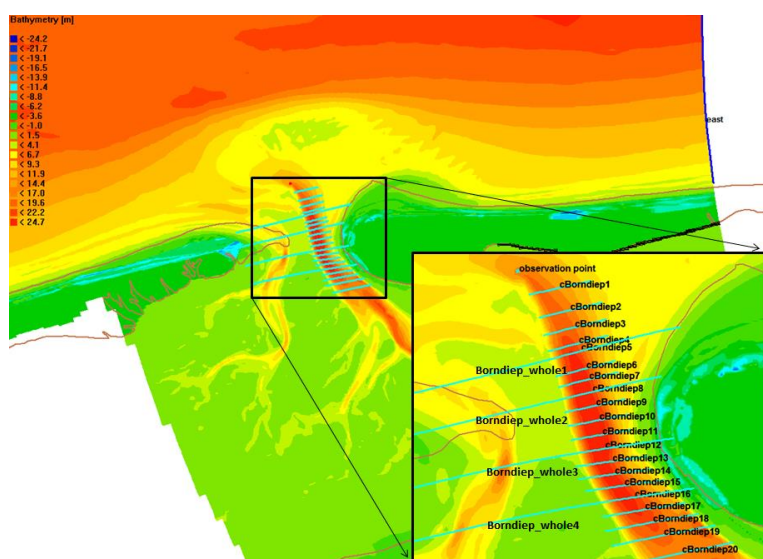


Figure 3-9: Overview of the locations of the cross-sections used in the morphological tide analysis.

The results for selected cross-sections are shown in Figure 3-10. On the x-axis the selected tides are presented. Since the analysis is based on the running average and results are stored in 5-minute intervals over a 29 day (double) spring-neap cycle, 9000 averaged results are present. Results are shown for all cross-sections (1-20), the cross-sections in the central part of Borndiep (10-20) and in the offshore part (1-10). The red lines represent the weight factor and the blue lines the RMS errors. Green points indicate an RMS error < 1%.

Through this method, in the central inlet gorge (transects 10-20), 4 tides (2450, 2596 and 2859) can be selected with RMS < 15 and a weight factor close to 1. Tides 900, 2730, 4546 and 6750 best represent the sediment transport on the seaward part of the ebb-tidal delta (transects 1-10). As an additional step, for each of the selected tides the harmonic constituents were determined and a simulation over a full spring-neap cycle was made. Comparison of the individual simulations with the reference case based on (1) sediment transports through the inlet gorge, and total transport patterns in selected domains reveals that tide 2850 produces the most accurate representation (Figure 3-11). This tide was then selected as the morphological tide for the simulations.

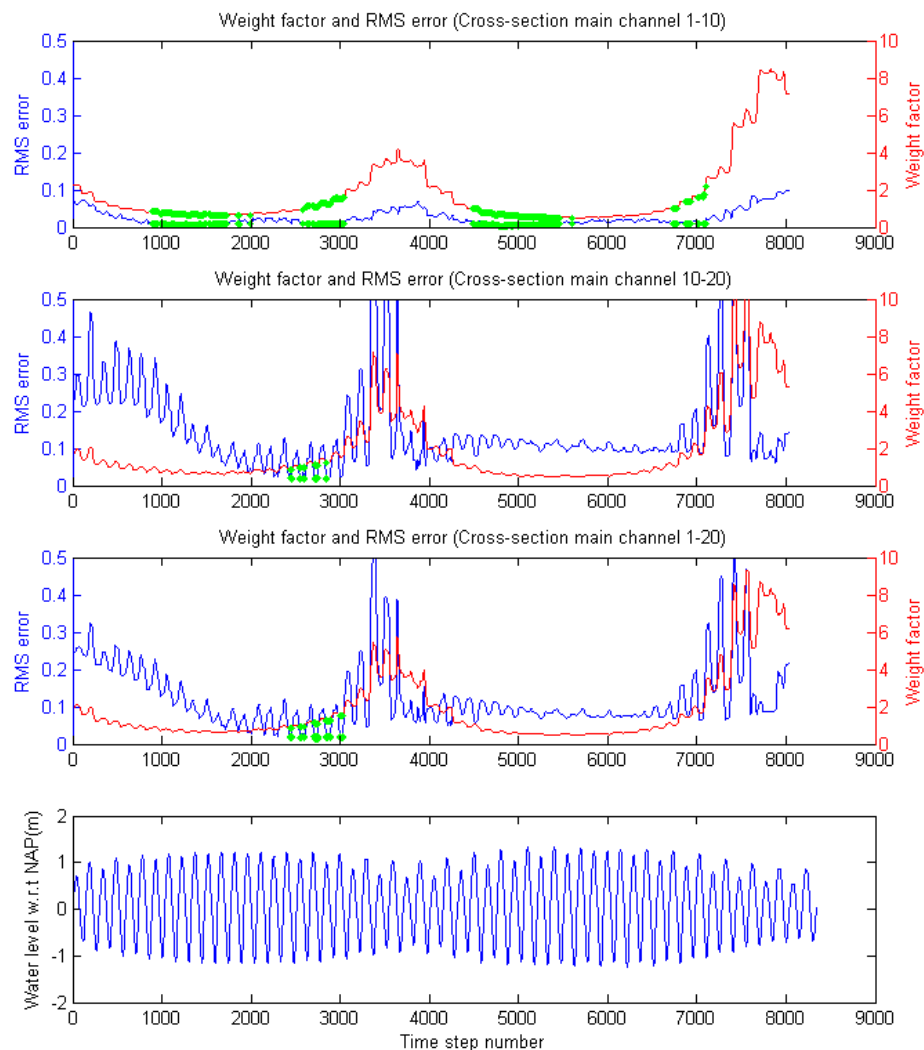


Figure 3-10: Resulting time series of weight factor and RMS Error, for cross section 1-10; cross section 10-20; cross section 1-20, and the water levels in the inlet (from top to bottom).

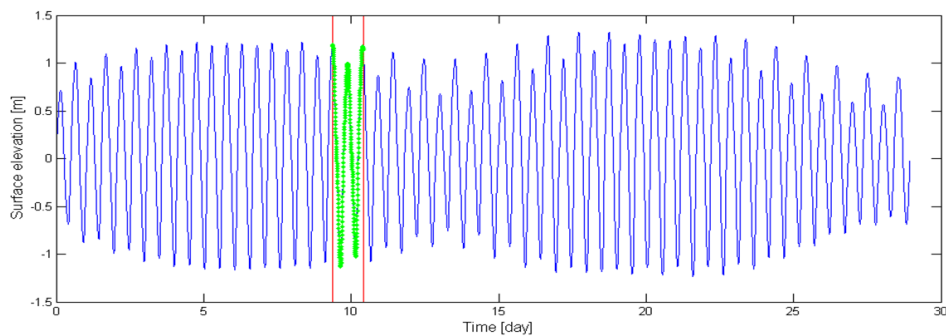


Figure 3-11: Selected morphological tide (in green).

3.4.5 Boundary conditions: Waves

The goal of deriving a morphodynamic wave climate is to derive a set of wave conditions that adequately represent the full wave climate. Elias (2017) showed that due to the relative short record of observations at the Ameland buoys and missing data early summer, when the buoys are out of the water for maintenance, it is not possible to create a long-term representative wave climate for these buoys. Comparing the wave direction and wave heights between Eierlandse Gat (ELD), Schiermonnikoog (SON) and the Ameland wave buoys shows that SON best resembles the Ameland wave record with a close correlation in height and direction. Both Steijn and Roelvink (1999) and De Fockert (2008) use the SON wave buoy data to derive a morphodynamic wave climate schematization.

Steijn and Roelvink (1999) – SR1999

Steijn and Roelvink (1999) bin the 1979–1991 wave data in 0.5 m wave height increments and 30° directional bins. Wave period is not included in the wave climate schematisation, but is derived as a relation of the significant wave height: $T_{m02} = 3.5 + 0.9 \cdot H_s$ for $H_s < 2$ and $T_{m02} = 3.6 \cdot H_s$ for $H_s > 2$. The peak wave period is approximated with $T_p = 1.25 \cdot T_{m02}$.

For each of the wave conditions an approximation of the longshore sediment transports along the coast of Terschelling (Boschplaat), along the coast of Ameland, in the Wesgat and in the Akkepollegat channel is made using the CERC or Bijker transport formula. A distinction is made between small wave heights ($H_s < 2.0\text{m}$) and storm waves ($H_s > 2.0\text{m}$). Waves from the easterly (offshore) direction ($-30^\circ - 180^\circ$) are schematised into 1 morphological wave height. For each of these clusters of wave heights the total weighted sediment transports are computed and a set of wave conditions is chosen that best represents the total sediment transports (see Table 3-2).

Table 3-2: Wave climate schematisation SR1999 derived by Steijn and Roelvink (1999).

Parameter	West	North-west	North-east
H_s [m]	2.8	1.2	1.3
Direction [°]	311	333	23
T_{m0} [s]	6.02	4.58	4.67
T_p [s]	7.53	5.73	5.84
W_{vel} [m/s]	9	4	6.5
W_{dir} [°]	311	333	23
Probability [%]	14	43	21

- Note that 22% of the times no waves are present (tide only).

De Fockert (2008) – DF2008

Since 2008, the wave schematisation as derived by De Fockert (2008) has been used as a default. De Fockert uses the SON wave data over the period 1989-1999 as a basis. The wave climate is grouped in 0.5 m wave height increments ranging between 0.25 and 8.25m, and 30° directional bins. Wave heights smaller than 0.25m, and the offshore wave directions between 75° and 240° are excluded from the analysis (8.7% of the data). In total this results in 126 unique wave conditions. The OPTI method (Roelvink, Personal Communication) was used to derive a representative morphodynamic wave climate. This method contains the following steps:

1. For each wave condition, sediment-transports and morphological change were determined through a stand-alone simulation.
2. A ‘target’ morphodynamic change map is built from the weighted contributions of all (126) simulations.
3. The “OPTI” optimization routine eliminates the least important contribution, determines new weight-factors for the remaining simulations, and determines the error between the target and “optimized” results

A morphological wave-climate consisting of 12 wave conditions (see Figure 3-12) was chosen as the best representation of the full wave climate. The total error between target and optimized wave climate is less than 3.5%. This wave schematisation was also used for the bench-mark study.

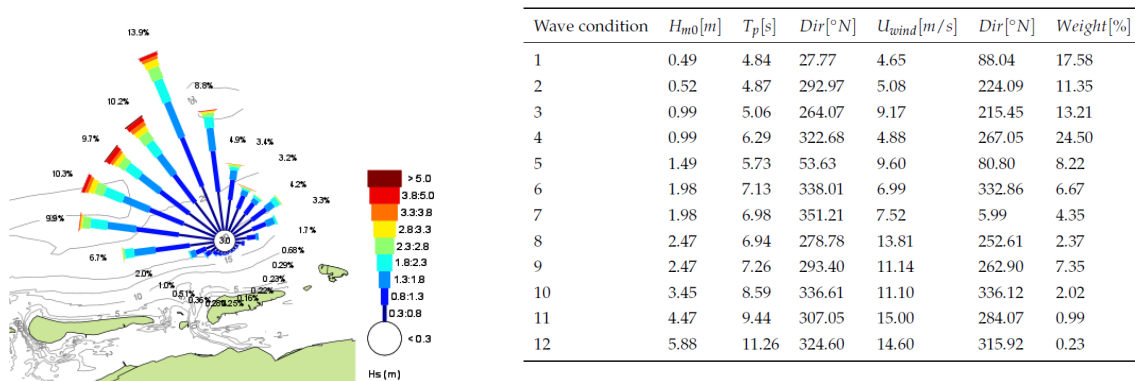


Figure 3-12: Morphological wave climate at Ameland Inlet. Left figure shows the 126 wave conditions used as input for the morphodynamic wave climate.

3.5 Additional model parameter settings

A summary of the key parameter settings is provided in Table 3-3.

Table 3-3: Summary of the main model parameter settings

Module	Parameter	Value domain	Description
Flow	Filcco	ame_low.grd	Hydrodynamic grid
	Anglat	53	Latitude of the mode centre (deg)
	MNKmax	175 163 1	Grid dimensions in M, N and k direction
	Thick	100	Thickness of the sigma layers (2DH)
	Fildep	ame_2016.dep	Depth file
	ltdate	2010-10-16	Reference date of simulation
	Tunit	M	Time unit (minutes)
	Tstart	0.0000000e+000	Start time after ltdate in minutes
	Tstop	8.7600000e+003	Stop time after ltdate in minutes
	Dt	0.5	Flow time step (s)
	Tzone	0	Timezone in relation to GMT
	Sub1	W	Flag to activate process - Wind
	Sub2	CW	Flag to activate process - Waves
	Namc1	Sediment100_mm	Sediment fraction [1] definition in sed file
	Namc2	Sediment200_mm	Sediment fraction [2] definition in sed file
	Namc3	Sediment300_mm	Sediment fraction [3] definition in sed file
	Namc4	Sediment400_mm	Sediment fraction [4] definition in sed file
	Filwnd	ame.wnd	File with wind data
	Zeta0	0	Initial condition water level (m)
	C01	0	Initial sediment concentration (kg/m ³) fraction [1]
	C02	0	Initial sediment concentration (kg/m ³) fraction [1]
	C03	0	Initial sediment concentration (kg/m ³) fraction [1]
	C04	0	Initial sediment concentration (kg/m ³) fraction [1]
	Filbnd	ame.bnd	File with boundary locations
	FilbcH	ameland2850_ neumann0.bch	File with harmonic boundary conditions file
	FilbcC	ame.bcc	File with transport boundary conditions file
	Rettis	120	Thatcher-Harleman return time at surface [10 values]
	Rettib	120	Thatcher-Harleman return time at bed [10 values]
	Ag	9.81	Gravitational acceleration (m/s)
	Rhow	1023	Water density at background temperature and salinity
	Tempw	0	Background water temperature
	Salw	0	Background salinity
	Rouwav	#FR84#	Bottom stress form. due to wave action [Fredsoe]
	Wstres	2.4999999e-003	Wind stress coefficient [1] at 0m windspeed;
		2.4999999e-003	Wind stress coefficient [2] at 100m windspeed
		2.4999999e-003	Wind stress coefficient [3] at 100m windspeed
	Rhoa	1.0	Air density
	Betac	0.5	Parameter spiral motion [not activated]
	Equili	N	Flag for computation spiral motion
	Roumet	C	Roughness formulation : Chézy coefficient
Ccofu	63	U-component of Chézy coefficient	
Ccofv	63	V-component of Chézy coefficient	
Xlo	0	Ozmidov length scale	
Vicouv	1	Horizontal eddy viscosity [m ² /s]	
Dicouv	1	Horizontal eddy diffusivity [m ² /s]	

	Htur2d	N	Flag for HLES sub-grid model
	Filsed	ame.sed	Definition file sediment characteristics
	Filmor	rif4.mor	Definition file morphology
	Iiter	2	Number of iterations in cont.eq.
	Dryflp	YES	Flag for extra drying and flooding
	Dpsopt	MAX	Option for check at water level points
	Dpuopt	MOR	Option for check at velocity points [equals MIN]
	Dryflc	0.10	Threshold depth drying and flooding
	Dco	-999	Marginal depth in shallow area's
	Tlfsmo	600.0	Time interval to smooth hydrodynamic bnd conditions
	Forfuv	Y	Flag horizontal Forester filter
	Forfww	N	Flag horizontal Vertical filter
	Sigcor	N	Flag to activate anti-creep
	Trasol	Cyclic-method	Numerical method for advective terms
	Momsol	Cyclic	Numerical method for momentum terms
	Filsta	ame.obs	File with observation points (history output)
	Filcrs	ame.crs	File with cross-sections (history output)
	FImap	0 - 180 - 8760	Time information to print map output (min)
	Flhis	0 - 180 - 8760	Time information to print history output (min)
	Flpp	0 - 180 - 8760	Time information to write communication file (min) for flow-wave coupling
	Flrst	1440	Time interval to write restart file
	Additional key-words in Flow file		
	WaveOL	Y	Flag to activate online wave coupling
	Cstbnd	yes	Boundary condition: water level offshore and lateral
	SMVelo	GLM	Lagrangian velocity fields
	TraFrm	vanrijn07.frm	Flag to activate VanRijn 2007 transport form. (-2)
	Bdf	Y	Switch for dune height predictor
	Bdfrou	vanrijn07	Roughness height predictor -vanrijn07
	BdfRpC	1.0	Ripple calibration factor
	BdfRpR	0.0	Ripple relaxation time
	BdfMrC	1.0	Mega-ripple calibration factor
	BdfMrR	0.0	Mega-Ripple relaxation time
	BdfDnC	1.0	Dune calibration factor
	BdfDnR	2880.0	Dune relaxation time
	BdfOut	Y	Flag to activate writing dune height/length and/or bedform roughness height data
	SdfD50	0.00025	Default sediment diameter for bedforms if not defined
	Trtrou	Y	Trachytope option activated
	Trtdef	vanrijn07.trt	Definition file trachytopes (105 - bedforms quadratic)
	TrtDt	2.0	Time step in minutes for updating roughness and resistance coefficients based on trachytopes.
Module	Parameter	Value	Description
Wave General	FlowFile	ame.mdf	Name of mdf-file containing FLOW input.
	SimMode	stationary	Simulation mode: stationary
	DirConvention	nautical	Direction specification convention
	ReferenceDate	2010-10-16	Reference date
	WindSpeed	13.5	wind speed at time point (overwritten by wavecon)

Constants	WindDir	307.5	wind direction at time point (overwritten by wavecon)	
	WaterLevelCorrection	0.0	Overall water level correction	
	Gravity	9.81	Gravitational acceleration (default)	
	WaterDensity	1025	Density of water (default)	
	NorthDir	90	Direction of north relative to x axis (default)	
	MinimumDepth	5.0000001e-002	Minimum water depth below which points are excluded from the computation	
Processes	GenModePhys	3	Generation mode for physics	
	Breaking	true	Flag to activate depth-induced breaking model	
	BreakAlpha	1.0	Coefficient wave energy dissipation in the B&J model	
	BreakGamma	0.73	Breaker parameter in the B&J model	
	Triads	true	Flag to activate non-linear triad wave-wave interactions	
	TriadsAlpha	0.1	Alpha coefficient for triads (default)	
	TriadsBeta	2.2	Beta coefficient for triads (default)	
	BedFriction	jonswap	Bottom friction formulation	
	BedFricCoef	0.067	Coefficient for bottom friction (default)	
	Diffraction	false	Flag to activate diffraction	
	DiffracCoef	0.20	Diffraction coefficient (default)	
	DiffracSteps	5	Number of diffraction smoothing steps (default)	
	DiffracProp	true	Include adaption of propagation velocities	
	WindGrowth	true	Flag to activate exponential wave growth	
	WhiteCapping	Westhuysen	Formulation for white capping	
	Quadruplets	true	Flag to activate quadruplet wave-wave interactions	
	Refraction	true	Flag to activate refraction is activated for waves propagation in spectral space	
	Numerics	FreqShift	true	Include frequency shifting in frequency space
		WaveForces	dissipation 3d	Computation method of wave forces
		DirSpaceCDD	0.50	Discretisation in directional space (default)
FreqSpaceCSS		0.50	Discretisation in frequency space (default)	
RChHsTm01		0.02	Relative change of Hs or Tm01 relative to local value	
RChMeanHs		0.02	Relative change of Hs relative to model wide value	
RChMeanTm01		0.02	Relative change of Tm0 relative to model wide value	
PercWet		98	Accuracy criteria iterative computation (default)	
MaxIter		15	Max number of iterations for convergence (default)	
Output		UseHotFile	true	Write and read hotstart files
	MapWriteInterval	0	Interval for writing data to map file(s) in minutes	
	WriteCOM	true	Write results to communication file(s)	
	COMWriteInterval	30	Interval for writing data to com. file(s) in minutes	
Domain	Grid	amewave.grd	File name of computational grid	
	FlowBedLevel	2	Use and extend flow bed level	
	FlowWaterLevel	2	Use and extend water level	
	FlowVelocity	2	Use and extend velocity fields	
	FlowWind	2	Use and extend flow wind fields	
	BedLevel	ame_2016_wave.dep	File name of computational bed level grid	
	DirSpace	circle	Directional space	
	NDir	24	Number of directional bins	
	StartDir	0.0	Start direction in case of sector directional space	
	EndDir	0.0	End direction in case of sector directional space	
	FreqMin	0.05	Lowest discrete frequency	
	FreqMax	1.0	Highest discrete frequency	

Boundary	NFreq	18	Number of frequencies
	Output	true	Write map file for current domain
	Name	Boundary 1, 2,3	Boundary name [3 boundaries]
	Definition	orientation	Definition type
	Orientation	north, west, south	Boundary orientation
	SpectrumSpec	parametric	Spectrum specification type
	SpShapeType	jonswap	Spectrum shape type for parametric specification
	PeriodType	peak	Wave period type for parametric specification
	DirSpreadType	power	Directional spreading type for parametric specification
	PeakEnhanceFa	3.30	Peak enhancement factor for Jonswap spectrum
	GaussSpread	9.999998e-003	width of spectral distribution for gaussian spectrum
	WaveHeight	from wavecon file	Time-varying input from wavecon file
	Period	from wavecon file	Time-varying input from wavecon file
	Direction	from wavecon file	Time-varying input from wavecon file
DirSpreading	from wavecon file	Time-varying input from wavecon file	
Files	Parameter	Value	Description
Mor Morphology	EpsPar	false	Vertical mixing distribution according to van Rijn
	lopKCW	1	Flag for determining Rc and Rw
	RDC	0.01	Current related roughness height (on
	RDW	0.02	Wave related roughness height (only
	MorFac	600	Morphological scale factor
	MorStt	1440	Spin-up interval to start morf updating
	Thresh	0.25	Threshold sediment thickness
	MorUpd	true	Update bathymetry during FLOW simulation
	EqmBc	true	Equilibrium sand concentration profile at inflow bnd
	DensIn	false	Include effect sediment conc. on fluid density
	AksFac	0.50	van Rijn's reference height = AKSFAC
	RWave	2.0	Wave related roughness = RWAVE * estimate ripple height
[Underlayer]	AlfaBs	1.0	Streamwise bed gradient factor for bed load transport
	AlfaBn	20.0	Transverse bed gradient factor for bed load transport
	Sus	1.0	Multiplication factor for suspended transport
	Bed	1.0	Multiplication factor for bed-load transport
	SusW	0.20	Wave-related suspended sed. Transport factor
	BedW	0.20	Wave-related bed-load sed. Transport factor
	SedThr	1.0	Minimum water depth for sediment computations
	ThetSD	1.0	Factor for erosion of adjacent dry cells
	HMaxTH	0.20	Max depth for variable THETSD.
	FWFac	1.0	Vertical mixing distribution according to van Rijn
	CaMax	0.05	Max sediment concentration criteria
	DzMax	0.05	Max bed level change criteria
	Multi	true	Flag for running parallel conditions
	NeuBcSand	true	Neumann boundary conditions for Sand
	IUnderLyr	2	Flag for underlayer concept
	ExchLyr	false	Switch for exchange layer
	TTLForm	1	Transport layer thickness formulatio
	ThTrLyr	0.5	Thickness of the transport layer
MxNULyr	10	Number of underlayers (excluding fin	
ThUnLyr	1	Thickness of each underlayer	
UpdBaseLyr	1	Update baselayer thickness and composition	

	IniComp	morlyr.inb	Input file for bed composition
Sed	Cref	1600	CSoil Ref. density for hindered settling calc.
	IopSus	1	susp. sediment size depends on local flow and wave
[Sediment]	Name	sediment100_mm	Name of sediment fraction [1]
	SedTyp	Sand	Type of sediment
	RhoSol	2650	Specific density sediment (kg/m ³)
	SedDia	1.0000000e-004	d50 median grain diameter sand (μm)
	CDryB	1600	Dry bed density (kg/m ³)
	IniSedThick	10	Initial sediment layer thickness at bed
	FacDSS	1	FacDss * SedDia = Initial susp. sediment diameter
[Sediment]	Name	Sediment200_mm	Name of sediment fraction [1]
	SedTyp	Sand	Type of sediment
	RhoSol	2650	Specific density sediment (kg/m ³)
	SedDia	1.0000000e-004	d50 median grain diameter sand (μm)
	CDryB	1600	Dry bed density (kg/m ³)
	IniSedThick	10	Initial sediment layer thickness at bed
	FacDSS	1	FacDss * SedDia = Initial susp. sediment diameter
[Sediment]	Name	Sediment300_mm	Name of sediment fraction [1]
	SedTyp	Sand	Type of sediment
	RhoSol	2650	Specific density sediment (kg/m ³)
	SedDia	1.0000000e-004	d50 median grain diameter sand (μm)
	CDryB	1600	Dry bed density (kg/m ³)
	IniSedThick	10	Initial sediment layer thickness at bed
	FacDSS	1	FacDss * SedDia = Initial susp. sediment diameter
[Sediment]	Name	Sediment400_mm	Name of sediment fraction [1]
	SedTyp	Sand	Type of sediment
	RhoSol	2650	Specific density sediment (kg/m ³)
	SedDia	1.0000000e-004	d50 median grain diameter sand (μm)
	CDryB	1600	Dry bed density (kg/m ³)
	IniSedThick	10	Initial sediment layer thickness at bed
	FacDSS	1	FacDss * SedDia = Initial susp. sediment diameter

4 An evaluation of previous model results

4.1 Roelvink and Steijn (1999)

4.1.1 General description

In this study an extensive morphodynamic validation of Delft3D MOR was carried out over the time frames 1989-1993 and 1993-1996. The main parameters of the morphodynamic model are provided in Table 4-1. Model results are summarized in Table 4-2, Figure 4-1 and Figure 4-2.

In addition to the morphodynamic predictions, a range of sensitivity studies was performed. Roelvink (1999) provides the following main conclusions:

- The effect of spiral flow may be important but a quasi-3d approach to take these into account did not improve results.
- There is a large effect of the transport formulation used. A comparison between Bijker and Soulsby-Van Rijn formulations showed the following differences:
 - Much more tendency for Bijker to flatten out the morphological features such as channels.
 - Much less activity for Bijker in the flood basin
 - In Soulsby-Van Rijn the development of the plan view of the inlet was much more in accordance with the observed developments.
 - All features became too pronounced in the Soulsby-van Rijn simulations.

Table 4-1: Parameter settings Ameland model Roelvink and Steijn (1999).

Parameter	Value or remarks
Model system	Delft3D MOR
Grid dimensions	109x147
Number of cells	16023 (13054 active)
Tidal Schematisation	Based on harmonic analysis os 24hr50m
Flow boundary condition	Water level
Bed composition	1 Fraction ($d_{50} = 200 \mu\text{m}$)
Timestep flow model	60 s
Roughness	Manning 0.026 (uniform)
Horizontal viscosity	1.0 m ² /s
No. wave runs per hour	5 (every 12 minutes)
No. wave conditions	4 + no wave condition
Wave coefficients	HISWA golfmodel Bijker GAMS = 0.70 ALFA = 0.50
Wind	Real wind conditions
Transport formulation	Bijker or Soulsby-Van Rijn.
Transport Time step	50 times 15 minutes on com-file, time step = 5 minutes
Number of steps between hydrodynamic updates	5
Duration of simulation	7 years
Morphodynamic timestep	Automatic, Courant number 0.8

4.1.2 Model Results

Table 4-2: Comparison of measured and modelled morphodynamic changes (see Figure 4-1 for numbering; note that this numbering deviates from the numbering introduced in §2.3 and Figure 2-1).

	<i>Trends</i>	<i>Modelled</i>
1	Erosion of the Boschplaat	Not reproduced
2	Large sedimentation Westgat	Partly reproduced ^(a)
3	Strong erosion northern and southern part of Boschgat	Not reproduced ^(b)
4	Westward migration Borndiep. Accretion along the Ameland coast	Not reproduced ^(c)
5	Erosion western flank of Borndiep (eastern side of Koffiebonenplaat);	Not reproduced ^(c)
6	Strong erosion Bornrif	Partly reproduced ^(d)
7	Strong accretion eastern side Bornrif Strandhaak	Partly reproduced ^(e)
8	Erosion coastline facing east of Strandhaak	Reproduced
9	Accretion along the northeast side of the ETD	Partly reproduced ^(f)
10	Erosion northwestern side of ETD	Not reproduced ^(f)
11	Accretion central part Bornrif	Not reproduced ^(g)
12	Erosion south of Dantziggat	Not reproduced ^(h)
13	In basin pronounced changes along the tidal channels	Partly reproduced ^(h)

Remarks:

- (a) The sedimentation, infilling of the western part of Westgat is accurately reproduced. Sedimentation near the connection of Westgat and Borndiep is not accurately modelled.
- (b) In the measurements, the channel Boschgat shows a pronounced deepening south of the tip of Boschplaat. This erosion is not reproduced. In addition, the model predicts a distinct deepening of the area between Boschplaat and Borndiep.
- (c) In the measurements the Borndiep shows a westward movement. Erosion of Koffiebonenplaat and sedimentation along the western tip of Ameland. In the model the opposite trend occurs, an eastward movement with sedimentation along the Koffiebonenplaat and erosion of the Ameland coast.
- (d) In the model erosion of the entire Bornrif shoal occurs, while in the measurements this is focussed along the location of Oostgat channel. The model predicts stronger erosion in this channel, however this erosion is confined along the Strandhaak.
- (e) Some of the accretion along the tip of the Bornrif Strandhaak is reproduced. The area of accretion is smaller than observed. Eastward both model and observations indicate the presence of an area of erosion.
- (f) The pattern of erosion of the north-western margin of the ebb-tidal delta (ETD), and accretion to the east is not accurately reproduced in the model. The entire ebb-delta front accretes, no erosion is observed.
- (g) Accretion of the central part of Bornrif is not predicted by the model. The model shows a distinct erosion which plausibly contributes to the accretion of the delta front (sediments are pushed seaward).
- (h) Dynamics along the main channels in the basins are predicted in the model. However model resolution may not be sufficient to fully capture the observed developments. In general accretion dominates and no clear areas of erosion occur.

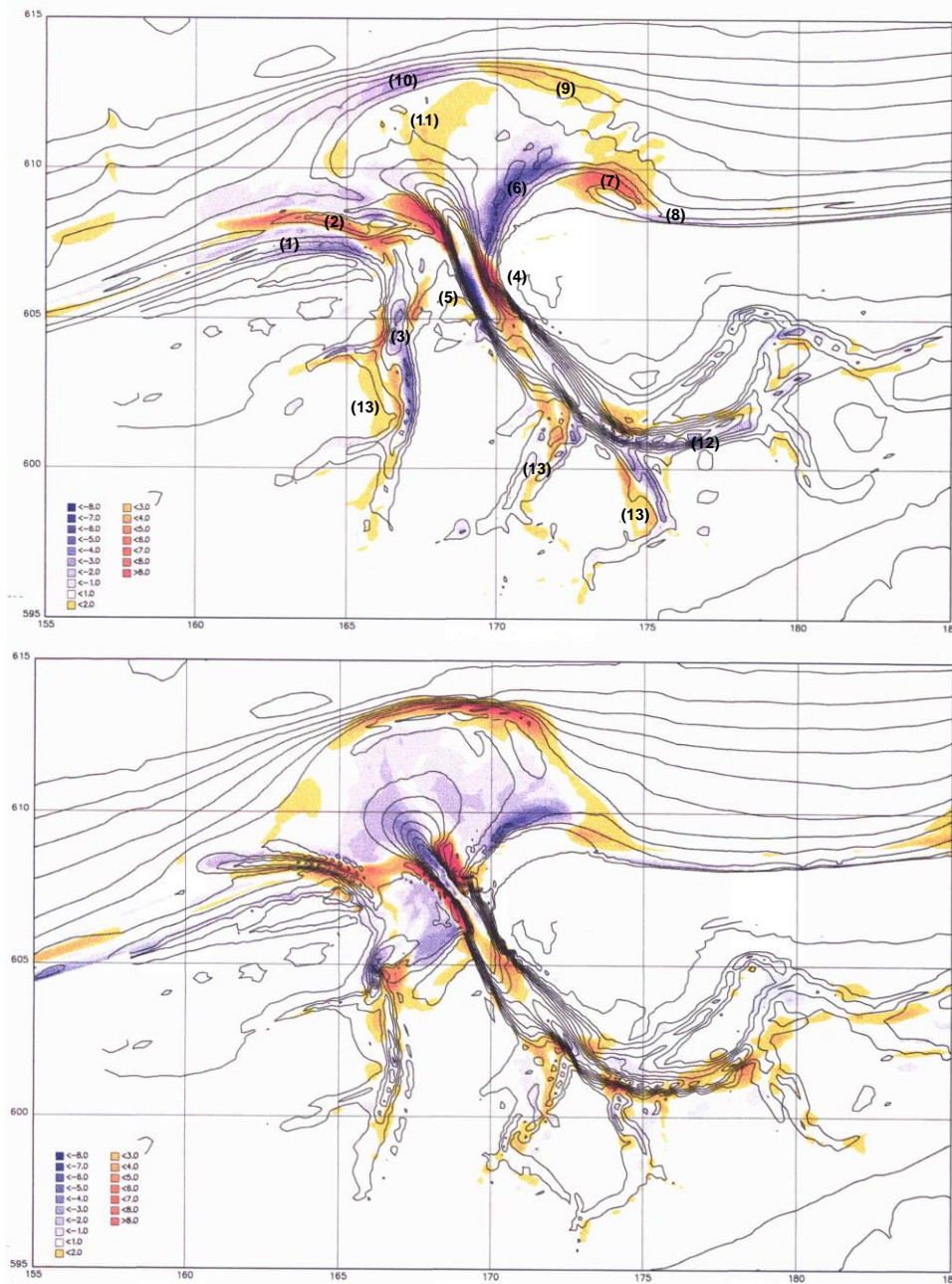


Figure 4-1: Measured (top panel) and modelled (bottom panel) bathymetric changes in m/year over the time frame 1989-1996.

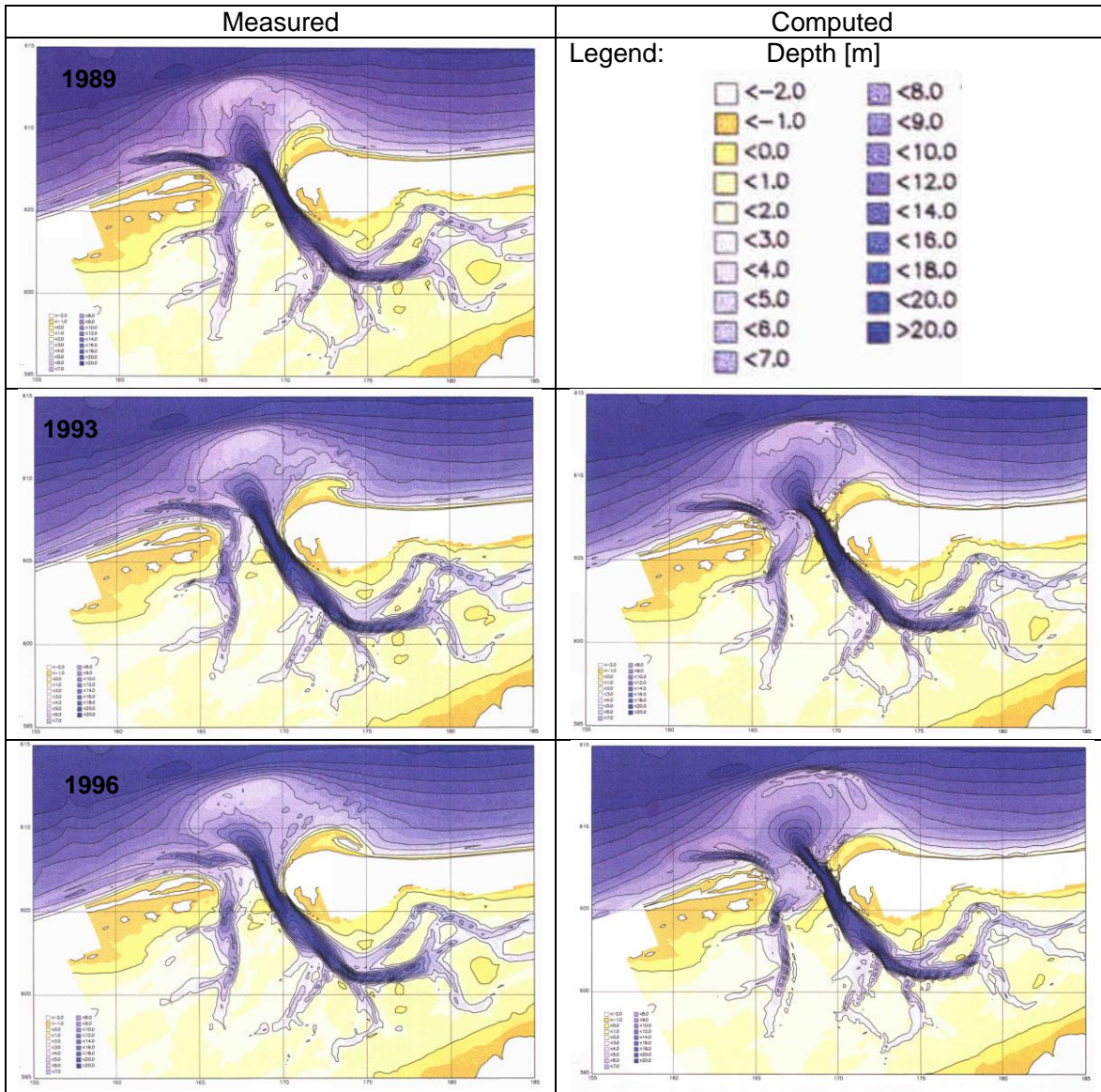


Figure 4-2: Overview of observed bathymetries for 1989, 1993 and 1996 (left column) and computed bathymetry in 1993 and 1996 (right column).

4.2 De Fockert (2008)

4.2.1 General description

De study of the De Fockert (2008) is the first comprehensive modelling study carried out since the studies of Steijn and Roelvink (1999). Three sets of morphodynamic computations were performed using the Delft3D Online Morphology model. Firstly, for validation, a simulation was made over the 1989-1999 time frame, and hindcast simulations were performed for the 1993-1999 and 1999-2002/2006 periods. Table 4-3 presents a brief overview of the model settings.

Results are summarized in Table 4-4 and shown in Figure 4-3, Figure 4-4 and Figure 4-5.

Table 4-3: Parameter settings Ameland model De Fockert (2008).

Parameter	Value or remarks
Model system	Delft3D Online Sediment
Grid dimensions	348x324
Resolution	30x40 (inlet) 300x350 (offshore)
Tidal Schematisation	Based on harmonic analysis of 24hr50m (close to spring tide)
Flow boundary condition	Water level / Neumann
Bed composition	1 Fraction ($d_{50} = 200 \mu\text{m}$)
Timestep flow model	15 s
Roughness	Space varying based on TRANSPOR 2004
Horizontal viscosity	1.0 m ² /s
No. wave runs per hour	3 (every 20 minutes)
No. wave conditions	12 wave conditions (based on SON); see Chapter 3.4.5.
Wave coefficients	SWAN – 3 rd generation Battjes & Janssen wave breaking GAMS =1 ALFA = 0.73
Wind	Schematized wind conditions per wave condition
Transport formulation	TR2004 (van Rijn, 2007)
Transport Time step	Every flow time step (15 s)
Duration of simulation	7 years Time frames: 1989-1993 1993-1999 1999-2002/2006
Morphodynamic timestep	180 – 270

De Fockert (2008) presents the following conclusions and remarks:

- Similarly to the older study a morphological tide and morphological wave climate are used to force the model. The morphological tide is based on the elongated tide approach as prescribed in Latteux (1995). Based on sedimentation-erosion patterns a tide was selected that closely resembles the spring tide. The hindcast simulations show that this tide overestimates the transports through the Borndiep compared to the neap-spring cycle.
- The yearly-averaged morphological wave climate accurately represents the total wave climate.

- The 'parallel online approach' is an efficient method to perform long-term morphodynamic simulations. However, with the large morphac values applied, the model can be sensitive for small morphological changes outside the area of interest.
- The model is able to predict the short term (<5 years) in an accurate way, while the longer-term (>5 years) shows some unrealistic behaviour.
- The two locations that need attention in the model are the ebb-tidal delta and the Bornrif area. The migration of the ebb-tidal delta can be explained by the selection of the morphological tide and by the larger discharges in the Borndiep, while the development of the Bornrif can be seen as a consequence of the depth-averaged model settings.
- A good morphological model needs a well calibrated hydrodynamic model.

4.2.2 Model results

Calibration: 1989-1999

The bathymetries and sedimentation-erosion patterns shown in Figure 4-4 and Figure 4-3 illustrate the observed and predicted morphological changes over the 1989-1993 and 1993-1999 time frames. The main findings of the model-data comparison are summarized in Table 4-4 and in the bullets below.

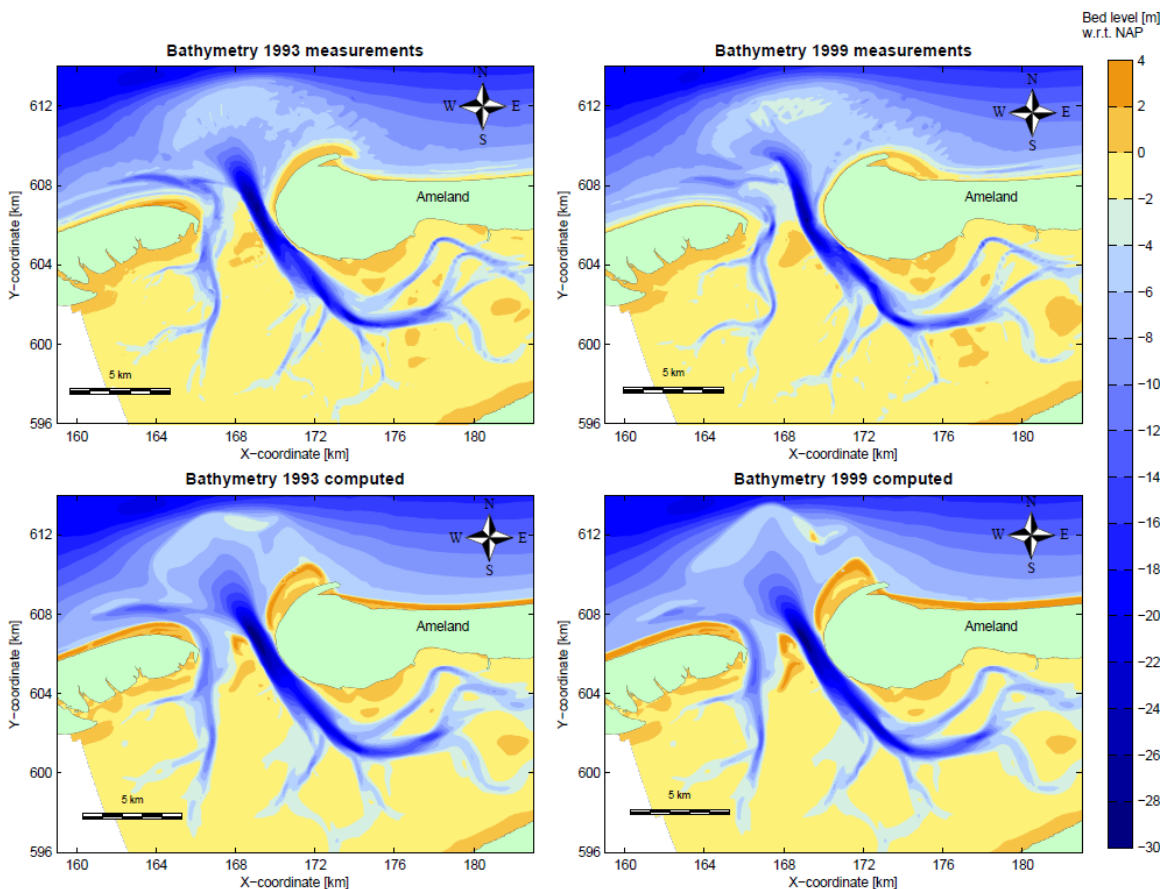


Figure 4-3: Measured bathymetry in 1993 and 1999 (top panels) and model predictions (bottom panels).

Table 4-4: Summary of the comparison of measured and modelled morphodynamic changes (see Figure 4-4 for numbering. Note that this numbering deviates from the numbering introduced in §2.3 and Figure 2-1).

	Trends	1989- 1993	1993- 1999	1999- 2002
1	Erosion of the Boschplaat	+	+/-	+/-
2	Large sedimentation Westgat	+	+	+
3	Channel migration southern part of Boschgat	+/-	+/-	+/-
4	Westward migration Borndiep. Accretion along Ameland coast and erosion Koffiebonenplaat	-	+/-	-
5	Strong erosion Bornrif (along Strandhaak)	-	-	+/-
6	Accretion/stable central platform Bornrif	+/-	-	+
7	Erosion northwestern side of ETD	-	-	-
8	Accretion along the northeast side of the ETD	-	-	+/-
9	Accretion at the tip of the Strandhaak	-	-	+/-
10	Erosion east of strandhaak	-	-	+/-
11	In basin pronounced changes along the tidal channels	-	-	-

- (1) Erosion along the Boschplaat is (partly) reproduced by the model. In the model we observe a small strip of accretion in the upper part of the profile that does not occur in reality. This accretion is most likely related to a profile change in the model (steepening). An inaccurate representation of the changes along the dry water line is a known limitation in Delft3D. The erosion during the first half of the simulation (1989-1993) is better represented compared to the second half. Over the 1993-1996 timeframe only erosion at the tip of Boschplaat is modelled. This is likely due to the model inaccuracies in the nearshore (see remarks below).
- (2) The large accretion in the Westgat channel is well reproduced by the model.
- (3) The model is able to compute erosion of the Boschgat in the basin. The areas of sedimentation are not reproduced.
- (4) The channel behaviour of Borndiep is not reproduced. In the measurements a clear accretion along the Ameland coast and erosion of Koffiebonenplaat is observed. Neither of these features are modelled.
- (5) Erosion of the Bornrif Strandhaak is not accurately reproduced. In the model accretion prevails, which likely results from a steepening of the surfzone (model artefact).
- (6) A stable central part of Bornrif occurs in both model and measurements. The area of local accretion is not reproduced by the model.
- (7) Erosion of the north-west side of the ebb-tidal delta is not reproduced. The model predicts an opposite behaviour. Accretion along the ebb-delta front due to a seaward outbuilding.
- (8) Accretion along the north-eastern side of the ebb-tidal delta is not accurately reproduced. Accretion takes place, but this is not comparable to the observed changes.
- (9) Eastward outbuilding / migration of the Strandhaak is not observed.
- (10) The area of localized erosion facing the tip of the Strandhaak is not reproduced. The model predicts a strong accretion of the coastline, which results from a steepening of the shoreline (see earlier remarks).
- (11) Dynamics of the basin are not well reproduced. In general, the observed changes are significantly larger than the predicted change. The input bed

schematization may play an important role as the basin tends to have smaller grain diameters that are more mobile.

Although, the details of the morphodynamic changes are not accurately reproduced, this hindcast simulation shows that the model is capable of reproducing a stable ebb-tidal delta. In addition, the observed morphodynamic changes are in the same order of magnitude as the observations. The main deviations between observations and model results can be related to two major deficiencies in the model.

Firstly, an inaccurate description of the bed dynamics in the nearshore (surfzone). This is a known limitation of the model and may partly be related to the depth-averaged description. In general the model tends to flatten and over steepen the nearshore (surfzone) areas. This often leads to strong accretion along the shoreline and some localized erosion offshore due to the shift in the profile. This behaviour is clearly visible in the model. Large coastline changes are observed during the first phase of the simulation. As the coastline shifts to a morphodynamic model equilibrium the changes in the second part of the computation are smaller as can be observed in the 1993-1999 results. The steep model shorelines prohibit a clear coastline erosion as was observed in the measurements. This influences both the evolution of Boschplaat, but also the evolution of the Strandhaak.

Secondly, part of the observed ebb-delta dynamics are related to a landward and eastward migration of the delta platform. This displacement is not predicted by the model. The model shows an opposite trend with a general westward outbuilding. It is likely that overestimated tidal currents are responsible for this outbuilding.

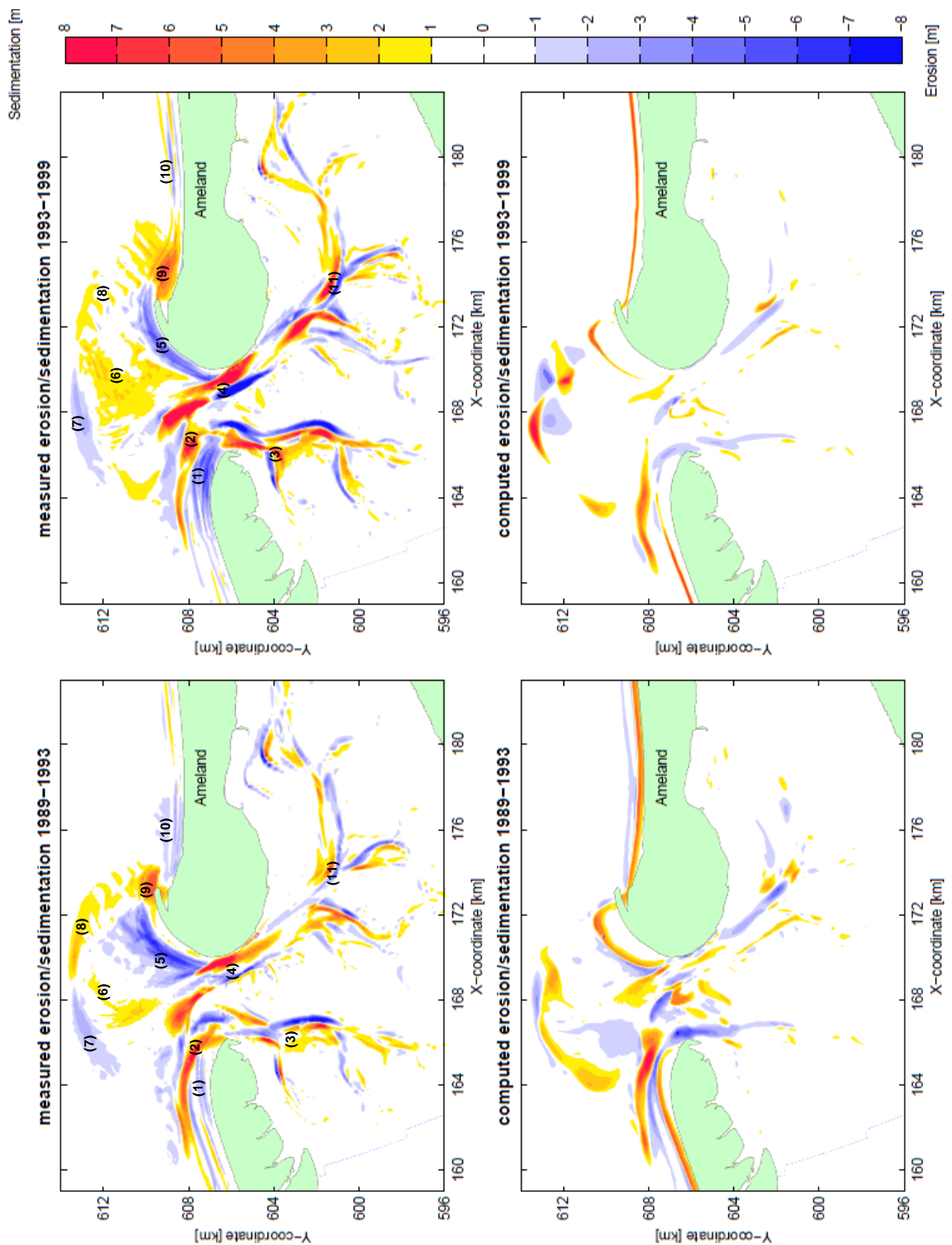


Figure 4-4: Measured and modelled sedimentation-erosion patterns for the 1989-1993 and 1993-1999 time frames.

Model results for the 1999-2002 time-frame

An additional validation simulation was made over the 1999-2006 timeframe. De Fockert limits its analysis to the 1999-2002 timeframe as results become increasingly erroneous. The sedimentation-erosion patterns shown in Figure 4-5 summarize the observed and predicted morphological changes through 2002. More explanation is provided below.

- (1) Erosion along the Boschplaat is (partly) reproduced by the model. In both the model and measurements erosion of the nearshore occurs. The landward movement of the tip of Boschplaat is not accurately reproduced.
- (2) Ongoing sedimentation in the Westgat is predicted (and overestimated) by the model. The model tends to build an unrealistic ebb-chute due to excessive scour of Boschgat.
- (3) The model is able to compute migration of the Boschgat in the basin. However, the model tends to form a larger channel in the inlet gorge. This channel formation results in a large mismatch between model and measurements around Westgat.
- (4) The channel behaviour of Borndiep is not reproduced. In the measurements a clear accretion along the Ameland coast is observed. This is not modelled. The erosion in the central part of the inlet, facing the of Koffiebonenplaat, is modelled.
- (5) Erosion of the Bornrif strandhaak is not accurately reproduced. Although both model and measurements show a narrow strip of erosion. In the model, this erosion is likely caused by a steepening of the local shore-face rather than a general trend of erosion. Onshore transports are likely overestimated.
- (6) Both model and measurements show a stable, central part of the Bornrif platform.
- (7) Erosion of the north-west side of the ebb-tidal delta is not reproduced. The model predicts an opposite behaviour. Accretion along the ebb-delta front due to a seaward outbuilding.
- (8) Accretion along the north-eastern side of the ebb-tidal delta is not accurately reproduced. Accretion takes place, but this is not comparable to the observed changes.
- (9) Accretion takes place at the tip of the Strandhaak, but an eastward outbuilding / migration of the Strandhaak is not clearly observed.
- (10) The general trend of shoreline erosion along the Ameland coast, east of the Strandhaak, is not clearly reproduced by the model.
- (11) Dynamics of the basin are not well reproduced. In general, the observed changes are of the same order of magnitude, but the trends of sedimentation or erosion are not accurately represented.

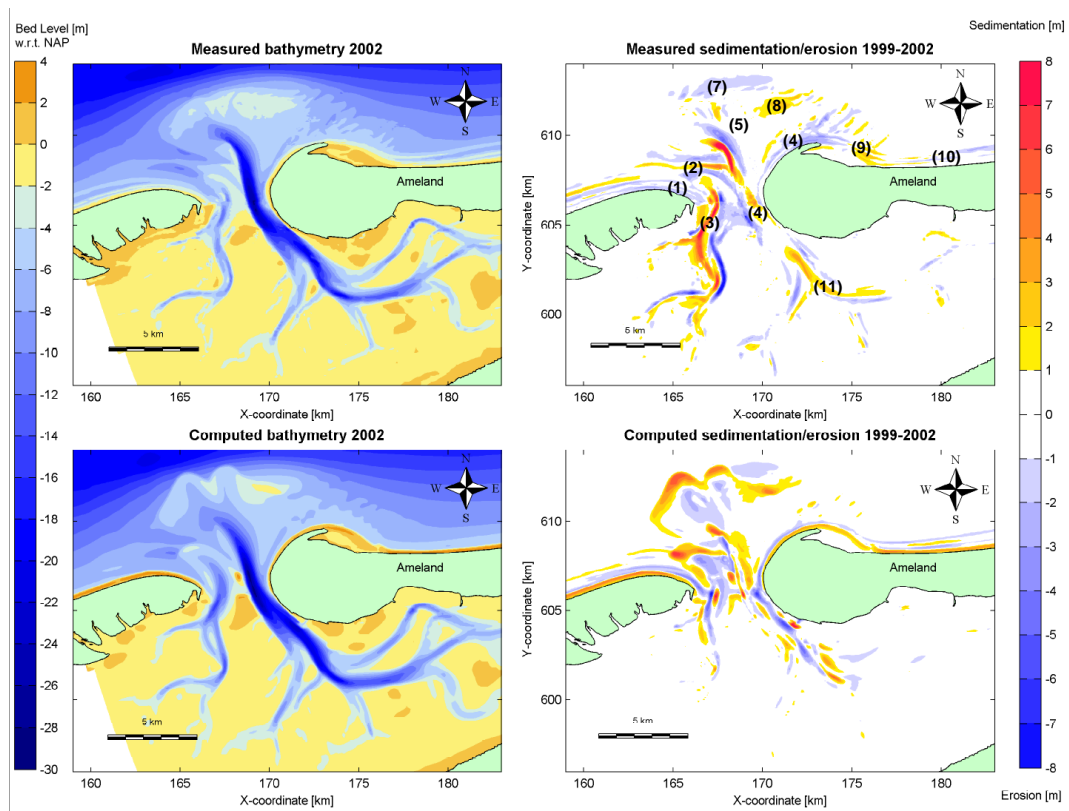


Figure 4-5 right panels: Measured (top) and computed 2002 bathymetry (bottom). Left panels: Measured (top) and modelled (bottom) sedimentation-erosion pattern over the timeframe 1999-2002.

4.3 Teske (2013)

Although, the study of Teske focusses on a longer timescales it provides additional insight in the functioning of the Van Rijn 2007 transport formulation. Therefore the main findings are presented here. Teske (2013), summarized in Elias and Teske (2015), provides an extensive analysis of the use of the Van Rijn 1993 (TR93) and Van Rijn 2007 (TR04) transport relations for long-term (80 year simulations) of Ameland inlet. By using TR04, we can include additional wave-driven transports, which are essential to improve predictions of the ebb-tidal delta evolution (ongoing research). The model domain is similar to Jiao with simplified tidal boundary conditions. All simulations are started from a bathymetry based on the 2005 Vaklodingen (Figure 4-6).

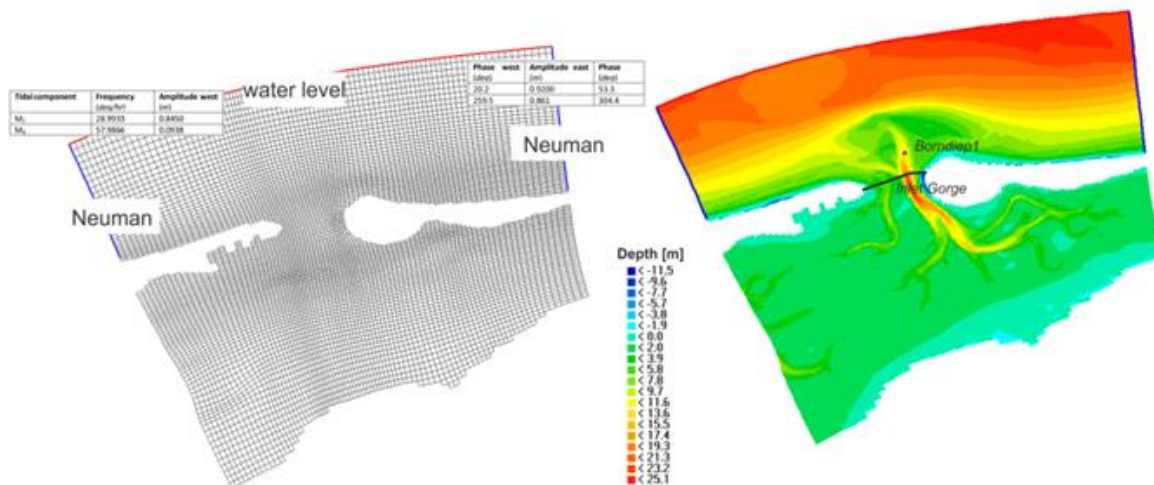


Figure 4-6: Model grid and bathymetry used in the study of Teske (2013).

The main conclusions from this study are (see Figure 4-7 for results):

1. The use of the Van-Rijn 2007 (TR04) sediment transport formulation improves of the morphologic development of the model regardless of the roughness definition and transverse bed-slope factor.
2. By using TR04 (default settings) incision of the main channel was greatly reduced compared to TR93. An additional reduction of channel scour was achieved by using a bedform-related roughness (Trt) predictor. Models using Trt roughness displayed stable channels in the first 40 years of simulation. Channel deepening after 40 years was likely related to the morphologic changes and feedback into the simulation of these. The Trt roughness shows a large variation over the inlet domain that cannot be captured by a constant Chézy or Manning coefficient.
3. Even with a single, homogenous sediment fraction of 200 μm or 300 μm stable channels were found with the combined use of TR04 in combination with Trt roughness.
4. In these models, the transverse bed-slope (AlfaBn) coefficient is still an effective parameter to fine-tune the channel development, but to retain representative cross-sections AlfaBn should not exceed 25.
5. Stable channels can also be obtained by using multiple sediment fractions. However, using a realistic fraction distribution did not improve channel stability compared to the homogenous bed as the fine sediments are eroded from the system rapidly and deposited on the ebb-tidal delta. Adding a coarser sediment fraction (or starting from an initial equilibrium fraction distribution) tends to stabilize the runs efficiently. For realistic simulations of the complete inlet system, graded sediments are likely essential due to the increased, more genuine, morphological response in both energetic and non-energetic areas.

6. All model results presented in this study showed a dominance of the suspended-load transports in the inlet gorge, even for the medium to coarse sand fractions. Typically, model input schematizations focus on the tidal residual and tidal asymmetry-related flow and transports. These net transports dominate the bed-load transports, but may be insufficient to characterize the net suspended transports in which additional mechanisms such as settling lag and scour lag may occur.

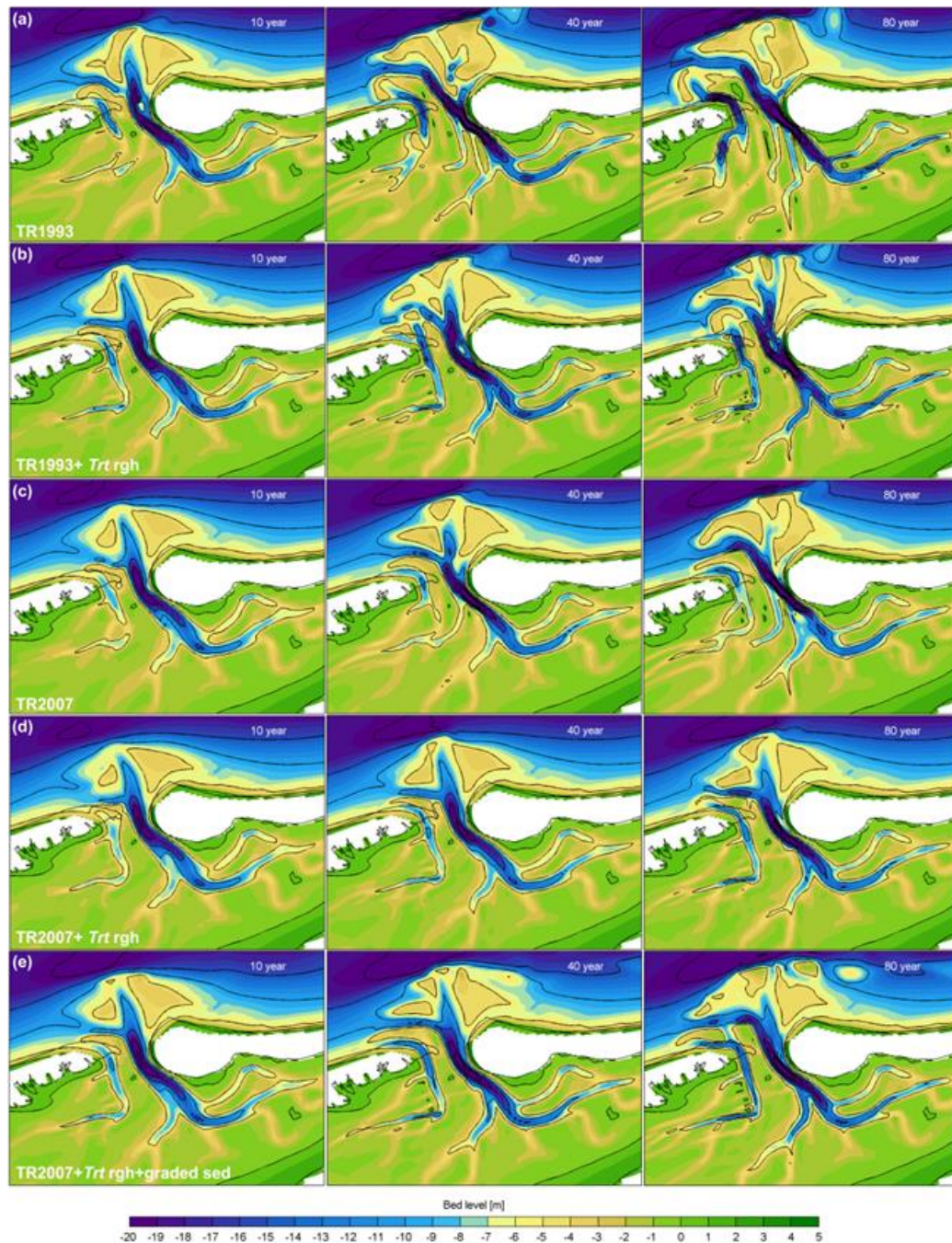


Figure 4-7: Morphologic development after 10, 40 and 80 years (left to right) for simulations using a uniform sediment fraction of $300 \mu\text{m}$ and (a) TR93 and uniform $C 65 \text{ m}0.5/\text{s}$, (b) TR93 and Trt bed roughness, (c) TR07 and uniform $C 65 \text{ m}0.5/\text{s}$, (d) TR07 and Trt bed roughness and (e) TR07, Trt bed roughness and a 25m bed with multi-fraction sediment distribution of $100, 200, 300$ and $400 \mu\text{m}$ (25% each).

4.4 Jiao (2014)

4.4.1 General description

The goal of the study of Jiao (2014) was to further improve the medium-term morphodynamic predictions of the Ameland model using the findings of Teske (2013). The Fockert (2008) model was used as a base. Jiao conduct a series of sensitive tests with various morphodynamic parameter settings, and with changes to the forcing boundary conditions (with a focus on tides). The improved tidal boundary conditions were explained in Chapter 3.4.3. Model simulations were run over the 1999-2011 timeframe using the Van Rijn 2007 transport formulation including bed-roughness predictor. Bed sediments were characterised by two sediment fractions (250 and 400 μm).

Table 4-5: Parameter settings Ameland model Jiao (2008).

Parameter	Value or remarks
Model system	Delft3D Online Sediment
Grid dimensions	174x162
resolution	60x80 (inlet) 600x700 (offshore)
Tidal Schematisation	Based on harmonic analysis of 24hr50m (see Chapter ??)
Flow boundary condition	Water level / Neumann
Bed composition	2 Fractions ($d_{50} = 250$ and $400 \mu\text{m}$)
Timestep flow model	60 s
Roughness	Space varying based on TRANSPOR 2004
Horizontal viscosity	$1.0 \text{ m}^2/\text{s}$
No. wave runs per hour	3 (every 20 minutes)
No. wave conditions	12 wave conditions (based on SON); see Chapter 3.4.5
Wave coefficients	SWAN – 3 rd generation Battjes & Janssen wave breaking GAMS =1 ALFA = 0.73
Wind	Schematized wind conditions per wave condition
Transport formulation	TR2004 (van Rijn, 2007)
Transport Time step	Every flow time step (15 s)
Duration of simulation	7 years Time frames: 1999 - 2005 2005 – 2011
Morphodynamic timestep	200

4.4.2 Model results

Figure 4-8, Figure 4-9 and Figure 4-10 show the final results for the morphodynamic predictions. In general, the response along the island tips of Ameland and Terschelling is well-modelled. The ebb-tidal delta shows less correspondence.

Table 4-6: Comparison of measured and modelled morphodynamic changes Jiao (2014). See Figure 4-9 for numbering.

	Trends	1999-2005	1999-2011
1	Erosion of the Boschplaat	+	+/-
2	Sedimentation Kofmansbult	-	-
3	Channel migration southern part of Boschgat	+/-	+/-
4	Accretion Borndiep	+	+/-
5	Strong erosion Bornrif (along Strandhaak)	+/-	+/-
6	Accretion/stable central platform Bornrif	-	-
7	Erosion northwestern side of ETD	-	-
8	Accretion along the northeast side of the ETD	-	+/-
9	Accretion at the tip of the Strandhaak	+/-	+
10	Erosion east of Strandhaak	-	-
11	In basin pronounced changes along the tidal channels	-	-

The erosion of the Boschplaat is reasonably well modelled (Table 4-6, 1). Both the model and measurements show a retreat of the Boschplaat although rates are somewhat underestimated. The accretion in the Boschgat region is well modelled (3). The pronounced deepening of Boschgat does not seem to occur in the measurements. Both the measurements and model show an accretion in Borndiep (4). Excessive scour of the main channels, a common problem in tidal inlet models, is not observed in the results. The distinct formation of the Kofmansbult ebb-shield is not clearly observed in the model (2). This maybe be related to the major difference in response in the behaviour of Bornrif. Similar to the study of De Fockert a seaward outbuilding of Bornrif is modelled. As a result, the ebb-delta front erodes and is pushed seaward (6,7,8). The observed onshore and eastward retreat are therefore not modelled. The modelled bathymetric response of Bornrif Bankje is likely a response to this deficiency and is therefore not accurately modelled (8). The erosion of the Bornrif Strandhaak over the 1999-2011 timeframe is well modelled. Similar patterns of erosion and accretion eastward (5,9) occur. The limited variability in the basins model results may be related to sediment composition present with d_{50} of 250 μm as in reality finer sediments are present in the basin (11).

Figure 4-10 summarizes the changes over the 1999-2011 time-frame by means of the sediment budget. In total the modelled erosion is near equal to the observations. However large deviations between the various elements can be observed. The sediment budget confirms that largest differences occur on the central – seaward ebb-delta. Changes along the coastlines are comparable. The difference in accretion along Ameland may partly be related to the nourishments that were not accounted for in the model. Especially along Boschgat sediment accumulation is overestimated.

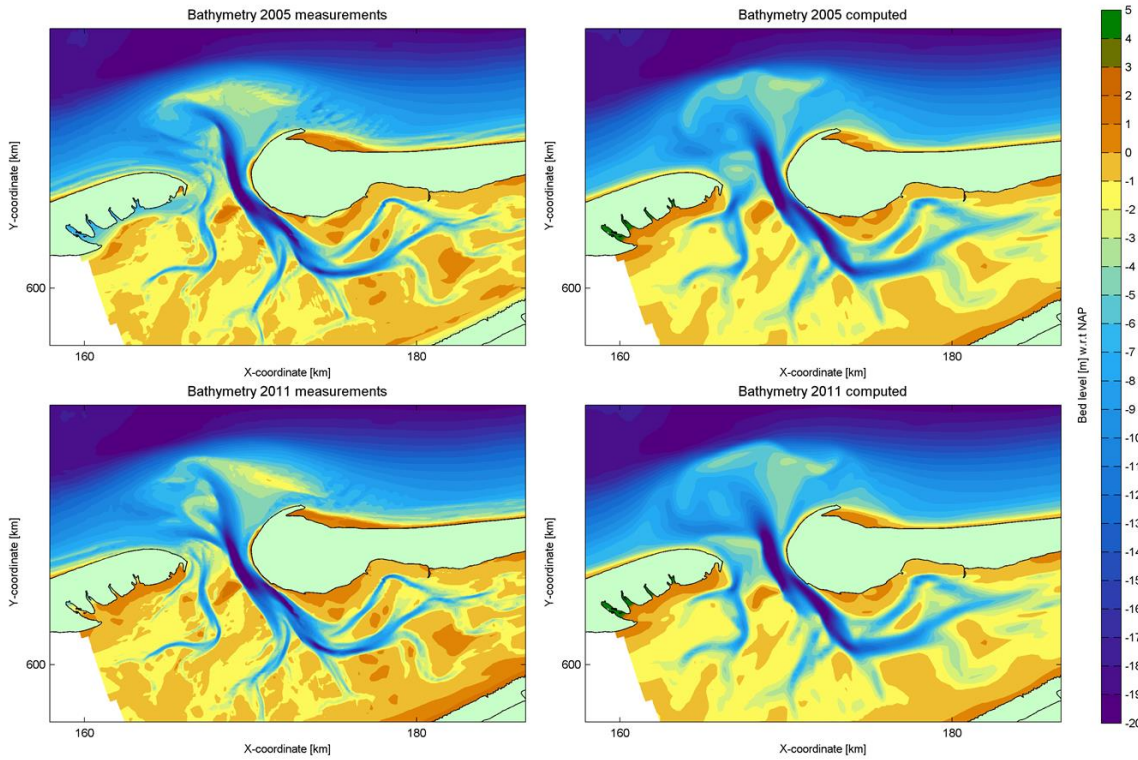


Figure 4-8: Measured (left panels) and modelled (right panels) bathymetries in 2005 (top) and 2011 (bottom).

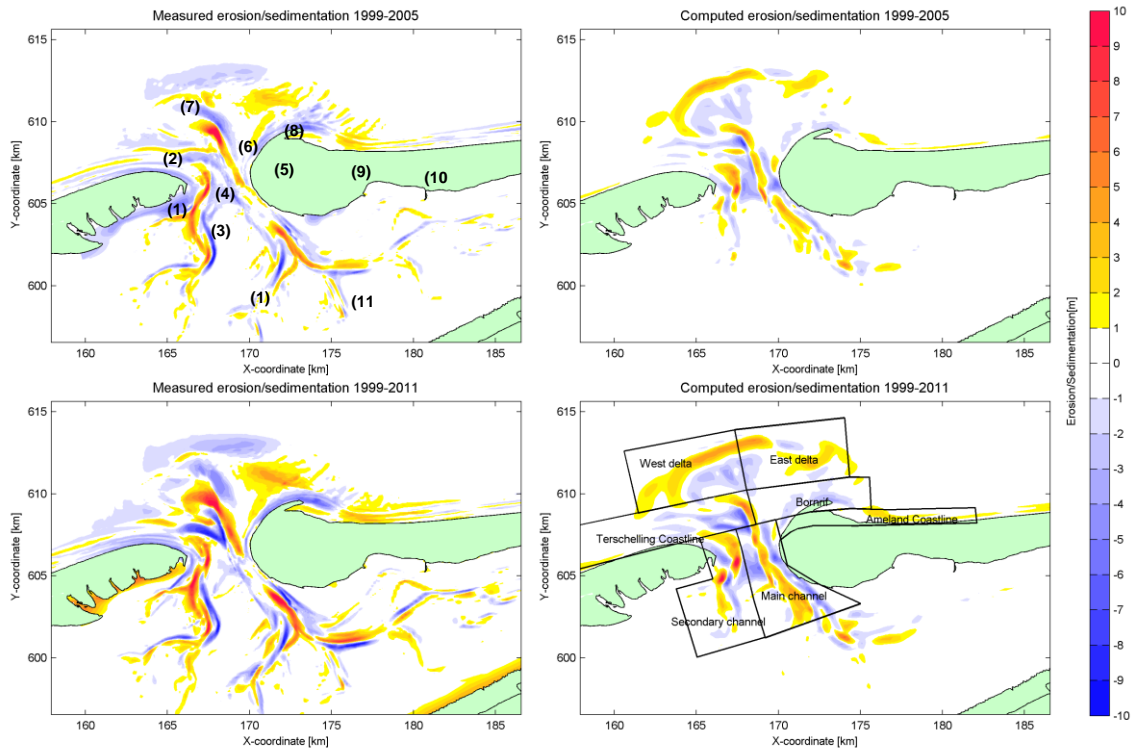


Figure 4-9: Measured (left panels) and modelled (right panels) sedimentation-erosion pattern over the timeframes 1999-2005 (top) and 1999-2011 (bottom).

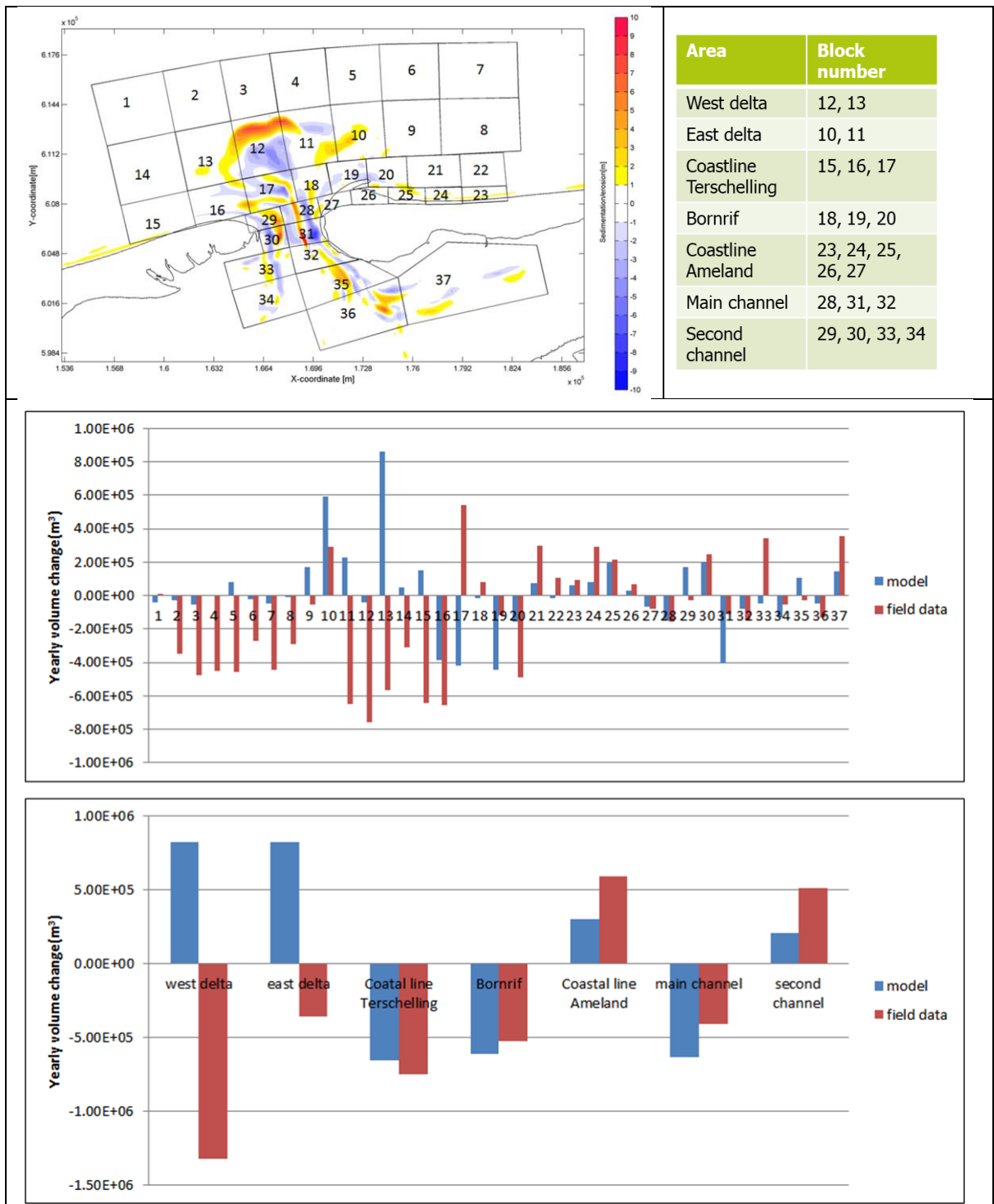


Figure 4-10: A summary of the modelled (blue bars) and measured (red bars) volume changes for selected polygons over the (1999-2011) timeframe. See top panel for location of individual polygons (middle panel). The summary polygons (Bottom panel) are shown in Figure 4-9.

5 Results for the bench-mark morphodynamic model simulation of Ameland Inlet

5.1 Introduction

In this Chapter, we present the results for the “bench-mark simulation”. We provide the results of the present-day Ameland model schematisation, with the latest settings and schematisations available. It may be a bit surprising that the bench-mark is based on the low-resolution version of the Ameland grids. However, we feel that the increased runtime efficiency of the model allows more efficient implementation of improvements as data and knowledge becomes available.

Typically, morphodynamic model studies are cumbersome due to the long runtimes involved. Runtimes over a week (to weeks) are no exception. This imposes a major limitation on the amount of runs that can be made. Very often the model can only be run once or twice. Especially if model results deviate from what is expected (not uncommon in morphodynamic models), this leaves a lot of uncertainty in the interpretation of the results. One of the major advantages of the present model setup for Ameland is the efficiency of the morphodynamic computation. In low-resolution the model takes ~24hrs to run for 8 years. These fast run times allows us to do sensitivity testing, while doing the analysis. These tests can help identify model limitations or point to possible areas of improvement.

Results for the bench-mark simulation and brief analysis of the results are presented in Chapter 5.2. In Chapter 5.3 we present the results of an initial series of sensitivity tests.

Table 5-1: Summary parameter settings bench-mark Ameland model.

Parameter	Value or remarks
Model system	Delft3D Online Sediment
Grid dimensions	174x162
resolution	60x80 (inlet) 600x700 (offshore)
Tidal Schematisation	Based on Jiao (2014)
Flow boundary condition	Water level / Neumann
Bed composition	4 Fractions ($d_{50} = 100, 200, 300$ and $400 \mu\text{m}$) Space-varying
$f_{FACTORS}$ sediment transport	$f_{SUS} = 1.0$, $f_{BED} = 1.0$, $f_{SUSW} = 0.2$ and $f_{BEDW} = 0.2$
Timestep flow model	60 s
Roughness	Space varying based on TRANSPOR 2004
Horizontal viscosity	$1.0 \text{ m}^2/\text{s}$
No. wave runs per hour	3 (every 20 minutes)
No. wave conditions	12 wave conditions (based on SON); see Chapter 3.4.5
Morphological wave climate	De Fockert (2008) – DF2008
Wave coefficients	SWAN – 3 rd generation Battjes & Janssen wave breaking GAMS = 1 ALFA = 0.73
Wind	Schematized wind conditions per wave condition
Transport formulation	TR2004 (van Rijn, 2007)
Transport Time step	Every flow time step (15 s)
Duration of simulation	8 years (Time frames: 2016 - 2025)
Morphodynamic timestep	600

5.2 Model Results

Using the settings presented in Chapter 3, a new morphodynamic simulation was carried out. This benchmark starts from the 2016 bathymetry and uses the settings as proposed by Bak (2017) as a basis. These settings contain the improved tidal boundary conditions derived by Jiao (2014). In line with the recommendations of Teske (2013) the latest iteration of the Van Rijn 2007 transport formulation, including the effects of the bottom roughness predictor were used. To prevent excessive scour in the initial stages of the prediction a detailed space-varying bed composition based on 4 fractions was applied following the recommendations of Van der Wegen (2011). Van der Wegen shows that in order to successfully generate a bed that suits the hydrodynamic conditions, the initial distribution of the fractions over the domain should be close to the observed distribution. Model simulations use a high morfac value of 600, since testing revealed that higher values yield instabilities, while differences with lower value morfacs are negligible. As an initial bathymetry the 2016 bed was applied, and run over 7 days of hydrodynamic time, which represents 8 years of morphodynamic change. A summary of basic model settings is presented in Table 5-1.

Figure 5-1 and Figure 5-2 show the final results for the morphodynamic prediction. While the main trends are summarized in Table 5-2.

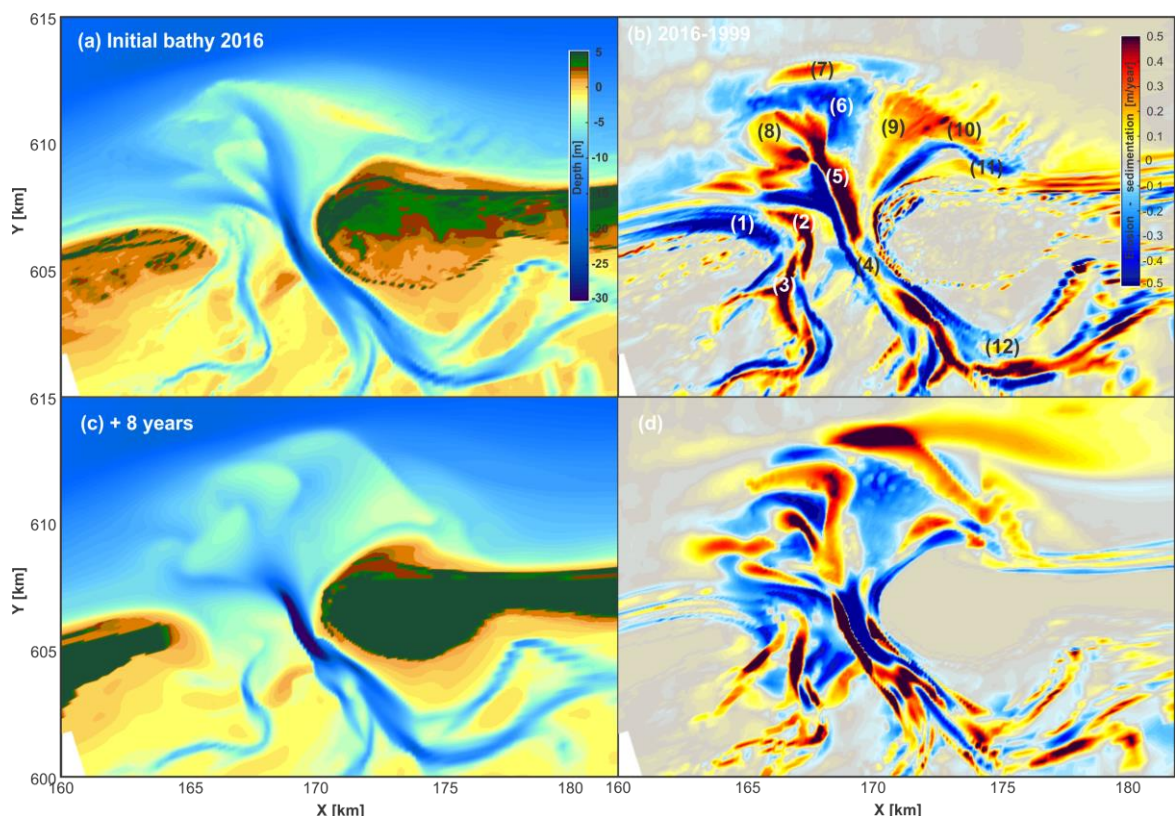


Figure 5-1: (a) Initial bathymetry at start of the model (2016). (b) Observed trends in sedimentation-erosion based on the 1999-2016 time frame. Modelled bed level (c) and morphodynamic changes (d) after 8 years of simulation.

Table 5-2: Comparison of measured and modelled morphodynamic changes for the Bench-mark simulation. For numbering see Figure 5-1b.

	Trends	Bench-mark
1	Erosion of the Boschplaat (island coast and tip)	+/-
2	Sedimentation Boschgat (inlet)	-
3	Eastward migration of Boschgat (basin) and shoal formation	+
4	Westward migration Borndiep	-
5	Accretion of Akkepollegat	+/-
6	Scour ebb-tidal delta front and eastward rotation Akkepollegat outflow	+/-
7	Localized sedimentation due to rotation Akkepollegat	+
8	Formation of an ebb-schild on Kofmansbult	+/-
9	Accretion central part of Bornrif	+/-
10	Formation, and landward/ eastward migration of Bornrif Bankje	+/-
11	Eastward migration, areas of erosion and accretion Bornrif Strandhaak	+/-
12	Large (channel) variability in the basin	+/-

Comparison of the modelled 2025 bathymetry with the 2016 bathymetry shows a significant, plausibly unrealistic change of the bed level (Figure 5-1). However if we compare the dominant changes of the main elements on the ebb-tidal delta, we can identify some common characteristics between the model prediction and the observed behaviour of the ebb-tidal delta. As “observed behaviour” we use the sedimentation-erosion trends over the 1999-2016 timeframe. Table 5-2 summarizes the results. With exception of Borndiep the model is capable of (partly) representing the observed trends. In more detail:

- (1) Erosion of the Boschplaat. The model is capable of eroding the tip of the Boschplaat. This erosion is underestimated. Especially the retreat of the island coastline is only partly modelled.
- (2) Sedimentation Boschgat. In previous models, Boschgat tended to excessively scour the platform between Boschplaat and Borndiep. In the benchmark simulation this platform is retained. Clear sedimentation such as observed in the measurements does not occur. Only smaller channels fill in while the overall height is however. In contrast to earlier studies no large, deep channels develop.
- (3) Migration Boschgat channel (basin). The migration of the basin part of Boschgat is well modelled. A clear trend of eastward channel migration is observed and accretion areas resemble the observed trends. The smaller channel along Boschgat is however not fully retained in the model. This may partly be due to the low grid resolution. Partly this may be a result from inaccuracies of modelling of the Boschplaat response.
- (4) Migration Borndiep. A significant difference in behaviour of the central part of Borndiep occurs. The model tends to over deepen the channel. In addition, an opposite trend of sedimentation is observed along the westward flank of the channel.
- (5) Accretion of Akkepollegat. The model is capable of predicting accretion in Akkepollegat. Along the western margin of Akkepollegat a clear area of sedimentation occurs that pushes the channel in eastward direction. The migration of the channel seems unrealistically high, but the general trend is represented.
- (6) Scour ebb-tidal delta front. Scour of the ebb-delta front is not clearly observed. Erosion is related to a reorientation of the delta rather than a general trend of scour. It appears that sedimentation rates are overpredicted by the model. This results in larger than observed sedimentation of the ebb-tidal delta.

- (7) Rotation of Akkepollegat. This rotation is clearly observed and results from the migration of the Kofmansbult (ebb-shield).
- (8) Kofmansbult. Formation and migration of the Kofmansbult is clearly observed. In general, the rates are overestimated, but the forcing mechanisms seem present. The model results here are for a large part controlled by a secondary ebb-chute that formed near Westgat. Plausibly over predicted accretion and migration of this ebb-shield results in large changes around the Kofmansbult. Although magnitudes are likely overestimated, the trends seem to represent the observed behaviour.
- (9) Accretion Bornrif. Accretion of the central part of Bornrif is not observed. The model overpredicts seaward expansion of the ebb-tidal delta. This results in scour of the central part and overestimated deposition seaward.
- (10) Landward migration Bornrif Bankje. Such migration is observed but excessive sediment accumulation dominates the results (see point 9).
- (11) Erosion of the Strandhaak. Eastward dispersion of the Strandhaak is modelled. However, an unrealistic accretion at the tip of the Strandhaak is predicted.
- (12) Basin dynamics. In general both model and measurements indicated a large variability around the channels in the basin.

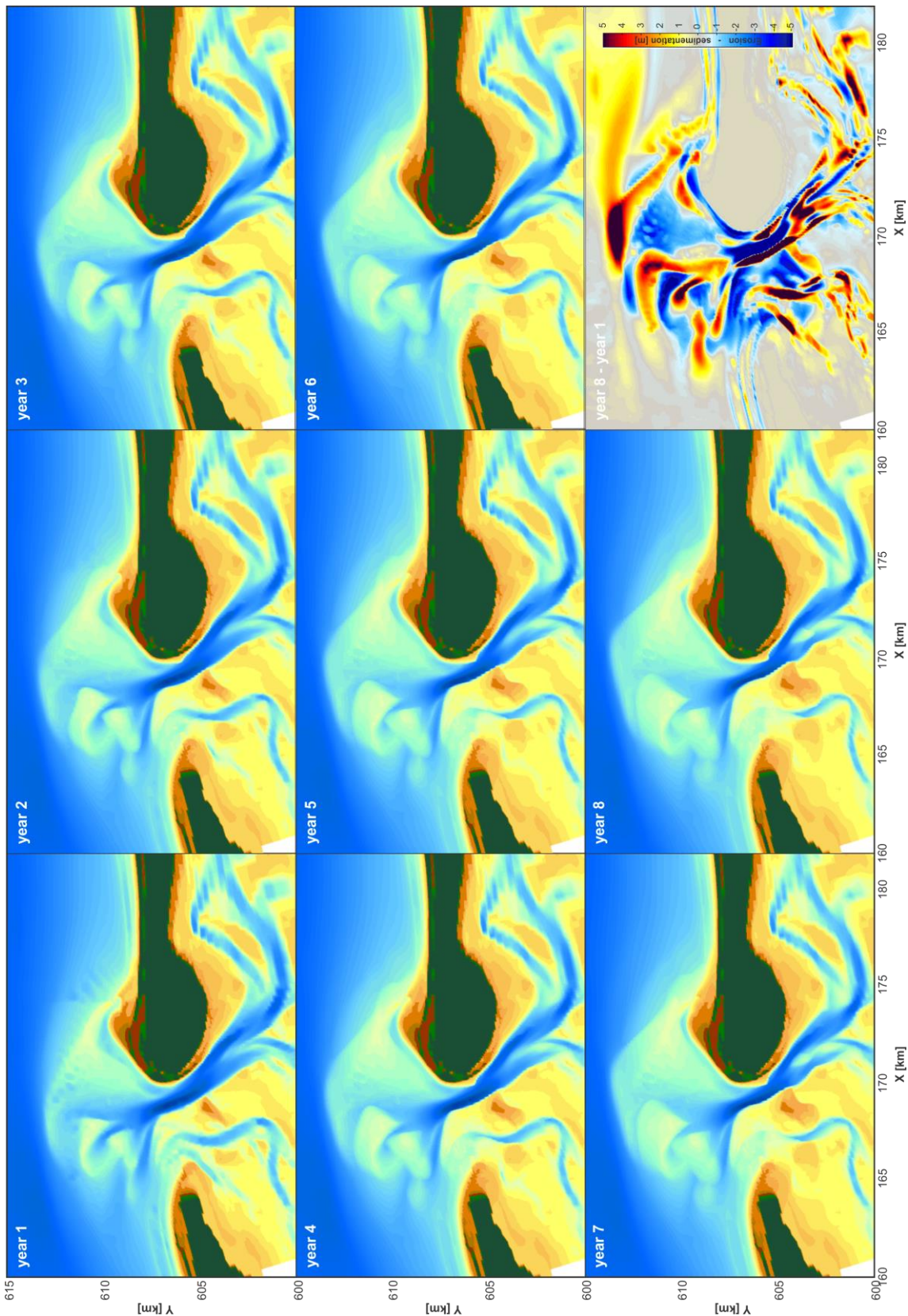


Figure 5-2: Modelled bed levels for each simulated year (1-8) and the total sedimentation and erosion after 8 years of simulation.

5.3 Sensitivity Testing

Note that for sensitivity testing not all parameter settings are equal to the benchmark. Therefore it may not be possible to randomly compare results.

5.3.1 Effect of wave climate

Research question:

What is the influence of the morphological wave climate on the model results? Compare the results obtained for the wave climate of De Fockert (2008) – DF2008 versus the wave climate schematisation of Steijn and Roelvink (1999) – SR1999.

Parameter settings:

Identical to the benchmark simulation. Uses the SR1999 wave climate schematisation (see Chapter 4.1 for details). Two simulations were made (1) a hind cast over the 1999-2008 timeframe (Figure 5-3) and (2) a “bench-mark” simulation starting from the 2016 bathymetry (Figure 5-4).

Table 5-3: Parameter settings sensitivity testing – wave climate.

Parameter	Value or remarks
Tidal Schematisation	Based on Jiao (2014)
Bed composition	4 Fractions (d50 = 100, 200, 300 and 400 µm) Space varying
$f_{FACTORS}$ sediment transport	$f_{SUS}= 1.0$, $f_{BED}= 1.0$, $f_{SUSW}= 0.2$ and $f_{BEDW}= 0.2$
Morphological wave climate	Steijn and Roelvink (1999) – SR1999
Duration of simulation	8 years
Initial bathymetry	Hindcast : 1999 Benchmark : 2016

Analysis

Using the wave climate derived by Steijn and Roelvink (1999) shows a noticeable difference in sedimentation-erosion pattern of the hindcast (Figure 5-3) versus the bench-mark simulation (Figure 5-4). Especially in the hindcast the ebb-delta is dominated by a seaward expansion. Sediments are eroded from Bornrif and the main channels and deposited seaward forming a large area of accretion at the seaward margin of the ebb-delta. The erosion of the two island tips, at Boschplaat and at Bornrif is well represented by the model.

Comparing the overall patterns of sedimentation and erosion for the benchmark simulations (Figure 5-1 versus Figure 5-4) show remarkable similar characteristics. In both cases the ebb-delta growth is likely to be overestimated. The deformation of the ebb-shield and Akkepollegat dominate the local developments. Table 5-4 summarizes the results of both simulations. More remarks are given below:

- (1) Erosion of the Boschplaat. Both climates reproduce the erosion of the island tip at Boschplaat. Erosion with SR1999 is smaller compared to DF2008. The smaller changes lead to a more realistic prediction of the basin part. Both models underestimate the erosion along the shoreline.
- (2) Sedimentation Boschgat. Both models produce similar results. The SR1999 hind cast simulation shows a good representation of the sequence of erosion-sedimentation-erosion (going from Boschplaat to Borndiep).
- (3) Migration Boschgat channel (basin). Both simulations predict the migration of the basin part of Boschgat.

- (4) Migration Borndiep. Not modelled in both simulations. This is a tidally driven process, changes in the wave-climate will not resolve this inconsistency.
- (5) Accretion of Akkepollegat. Both models produce accretion in Akkepollegat. The SR1999 simulation retains a larger depth. The SR1999 hindcast simulation shows the initial formation of two small ebb-chutes at approximately the correct locations.
- (6) Scour ebb-tidal delta front. Both models do not show scour of the ebb-delta. Erosion is related to a reorientation of the delta rather than a general trend of scour. It appears that sedimentation rates are overpredicted in both models, but is the smallest in SR1999.
- (7) Rotation of Akkepollegat. Similar rotation in both models.
- (8) Kofmansbult. Formation and migration of the Kofmansbult is clearly observed in both schematisations.
- (9) Accretion Bornrif. Accretion of the central part of Bornrif is not observed. The model overpredicts seaward expansion of the ebb-tidal delta. This expansion is smallest for SR1999.
- (10) Landward migration Bornrif Bankje. SR1999 predicts the displacement of Bornrif Bankje over the ebb-tidal delta. This migration occurs on the Bornrif platform rather than along the margin of Bornrif.
- (11) Erosion of the Strandhaak. Eastward dispersion of the Strandhaak is modelled. However, an unrealistic accretion at the tip of the Strandhaak is predicted.
- (12) Basin dynamics. In general, both models produce similar variability around the channels in the basin.

Table 5-4: Comparison of measured and modelled morphodynamic changes using SF2008 (see Figure 5-1) and SR 1999 (see Figure 5-4) wave climatology's.

	Trends	SF2008	SR1999
1	Erosion of the Boschplaat (island coast and tip)	+/-	+/-
2	Sedimentation Boschgat (inlet)	-	+/-
3	Eastward migration of Boschgat (basin) and shoal formation	+	+
4	Westward migration Borndiep	-	-
5	Accretion of Akkepollegat	+/-	+/-
6	Scour ebb-tidal delta front and eastward rotation Akkepollegat outflow	+/-	+/-
7	Localized sedimentation due to rotation Akkepollegat	+	+
8	Formation of an ebb-schild on Kofmansbult	+/-	+/-
9	Accretion central part of Bornrif	+/-	+/-
10	Formation, and landward/ eastward migration of Bornrif Bankje	-	+
11	Eastward migration, areas of erosion and accretion Bornrif Strandhaak	+/-	+/-
12	Large (channel) variability in the basin	+/-	+/-

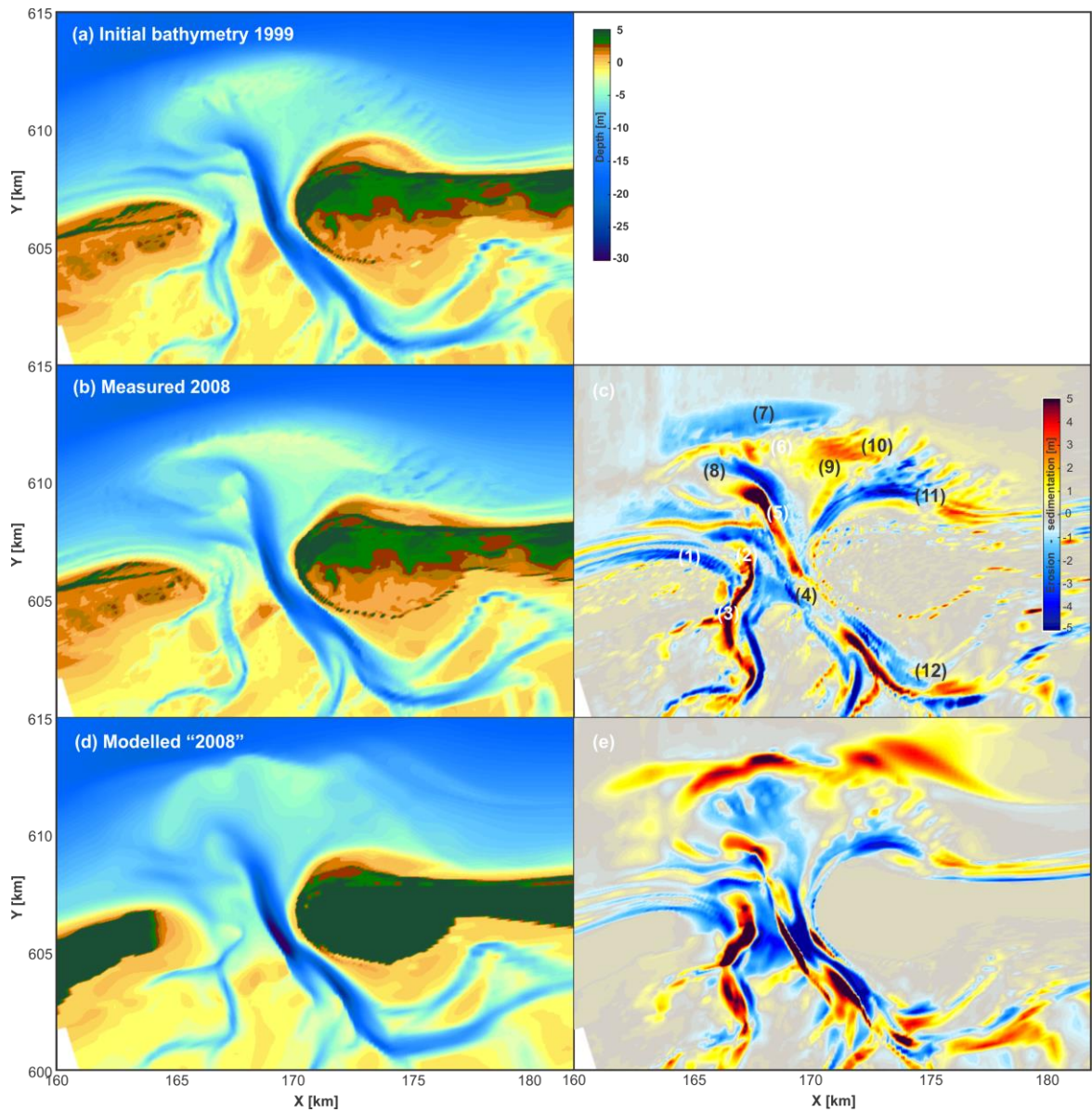


Figure 5-3: Hind cast Effect of wave climatology on morphodynamic change of the ebb-tidal delta (hindcast simulation). (a) Initial bathymetry in 1999, (b) measured bathymetry in 2008, (c) measured sedimentation-erosion pattern 1999-2008, (d) modelled bathymetry in 2008, and (e) modelled sedimentation-erosion patterns between 1999-2008.

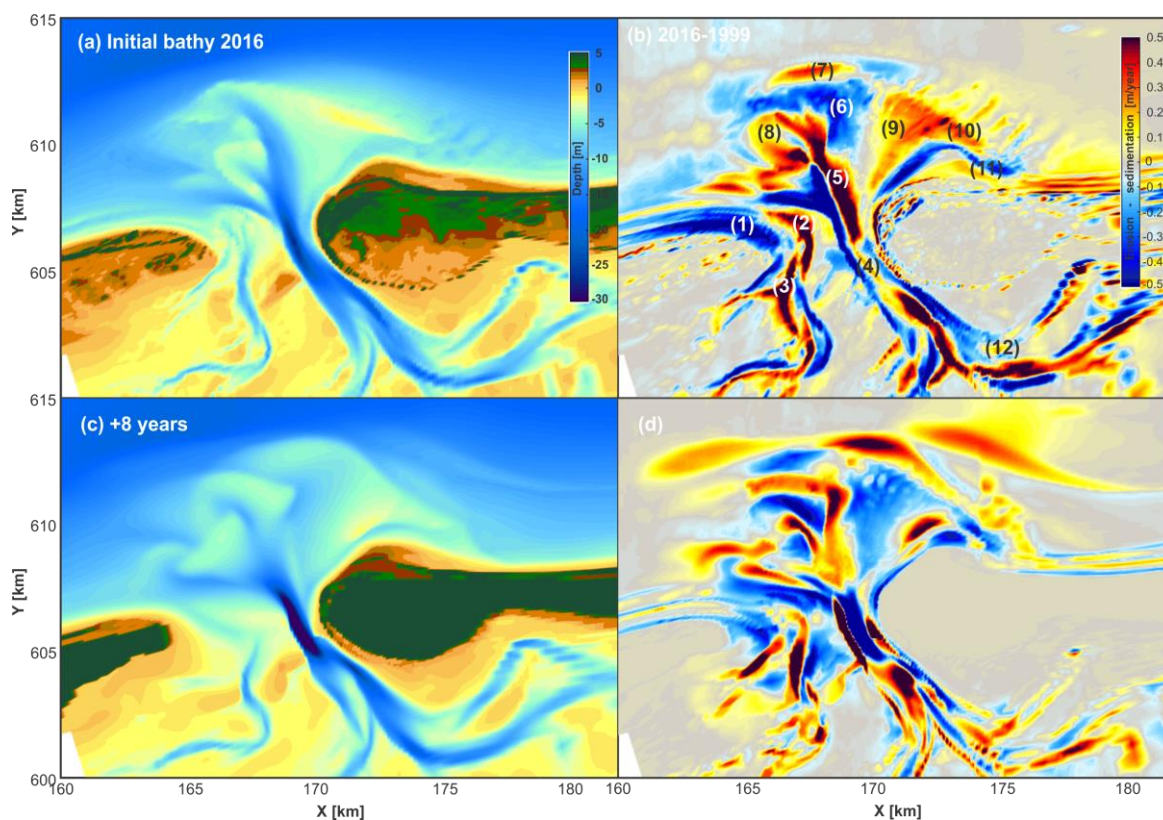


Figure 5-4: Bench-mark Effect of wave climatology on morphodynamic change of the ebb-tidal delta. (a) Initial bathymetry in 2016, (b) measured sedimentation-erosion trends over the timeframe 199-2016 (in m/year), (d) modelled bathymetry in "2025", and (e) modelled sedimentation-erosion rates (in m/year).

5.3.2 Effect of individual wave heights on long-term morphology

Research question:

What is the influence of littoral drift and waves on the ebb-delta shoal development?

Parameter settings:

These simulations run with a uniform wave height from a westerly direction (270°) and significant wave-heights varying between 0 and 3 m. Except for the wave heights, all simulations run the bench-mark settings, including the 4-fraction sediment distribution.

Table 5-5: Parameter settings sensitivity testing – waves.

Parameter	Value or remarks
Tidal Schematisation	Based on Jiao (2014)
Bed composition	4 Fractions (d50 = 100, 200, 300 and 400 µm) Space varying
$f_{FACTORS}$ sediment transport	$f_{SUS}= 0.7$, $f_{BED}= 0.7$, $f_{SUSW}= 0.3$ and $f_{BEDW}= 0.3$
Morphological wave climate	Uniform wave climate (a). Tide only (b). $H_{sig} = 1$ m, $H_{dir} = 270^\circ$ (c). $H_{sig} = 2$ m, $H_{dir} = 270^\circ$ (d). $H_{sig} = 3$ m, $H_{dir} = 270^\circ$
Duration of simulation	8 years
Initial bathymetry	1999

Analysis:

Figure 5-5 provides an overview of the model results. For reference a tide-only (no waves) simulation has been added to the model results. The results for the $H_s=3$ m may not be fully representative as here an abundant sediment supply plausibly related to the sediment boundary specification governs the development of the system. Unless otherwise mentioned, the analysis focusses on the wave heights up to 2m and the 4 areas indicated by (1) to (4) in Figure 5-5(upper right panel)

(1) Erosion of Boschplaat

The tide only simulation predicts an erosion of the tip of the Boschplaat. The addition of 1 or 2 m waves adds coastline erosion along the seaward shore. The largest waves overestimate an outbuilding of the coast which is likely introduced by boundary effects.

(2) All simulations indicate an accretion of the ebb-delta front. Waves from this pronounced angle do not introduce a retreat of the ebb-delta. Addition of waves alters the observed accretion at the outflow of Akkepollegat to erosion.

(3) Erosion of Borndiep. All simulations show large changes in Borndiep. The largest (3m) waves are capable of pushing the Akkepollegat eastward. Introducing scour on the eastward side of the channel.

(4) Erosion of the Bornrif Strandhaak due to tides is limited. Introducing waves produces an area of erosion on the westward side and increasing accretion to the east of the tip of the Strandhaak.

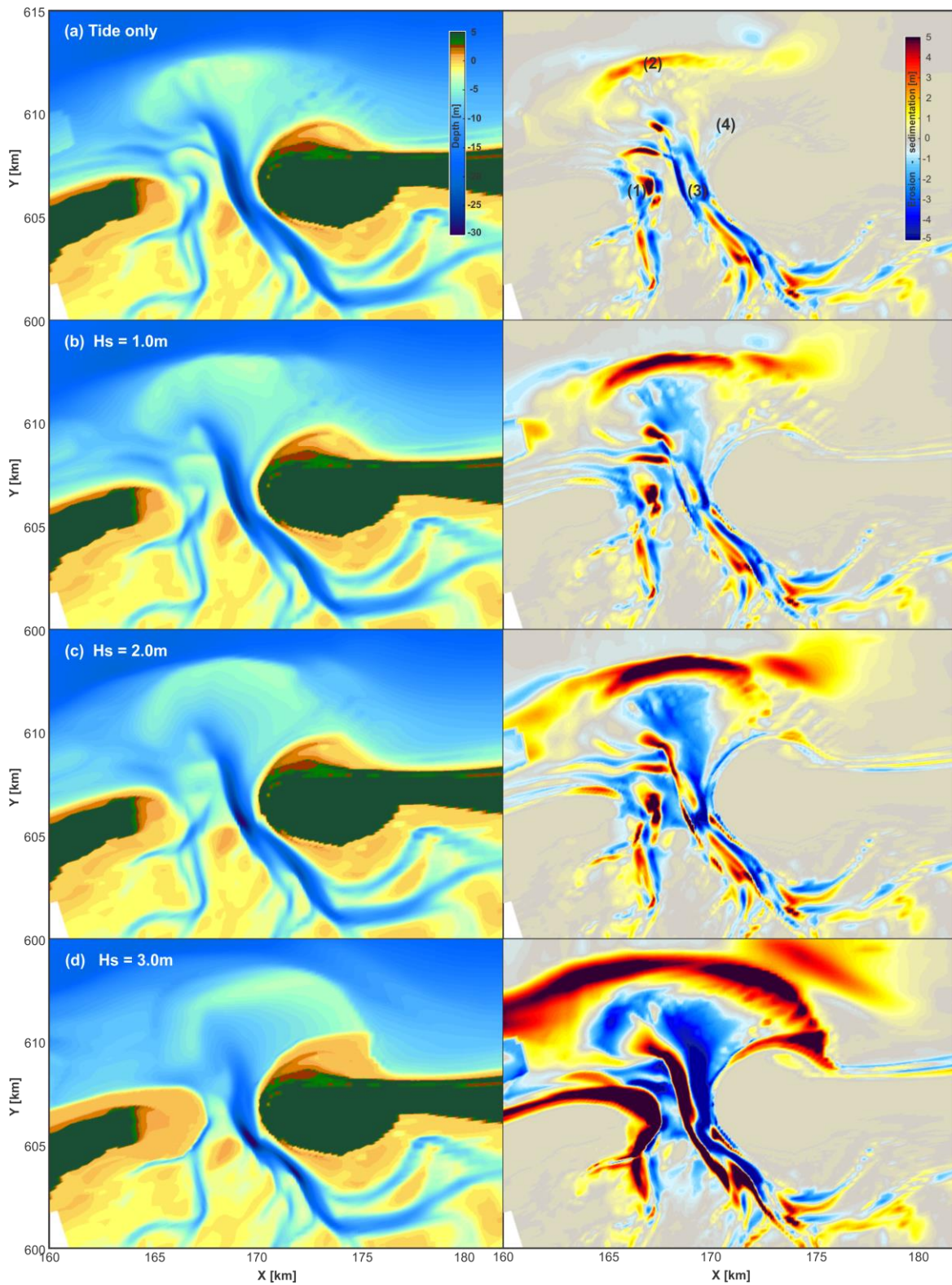


Figure 5-5: Effect of wave-height on morphodynamic change of the ebb-tidal delta. Model results after 10-years of simulation with (a) Tide only simulation, (b) Hsig = 1m, (c) Hsig=2m and (d) Hsig = 3m.

5.3.3 Effect of sediment transport tuning factors

Research question:

What is the influence of the factors f_{SUS} , f_{BED} , f_{SUSW} and f_{BEDW} on the morphodynamic response?

Parameter settings:

These simulations run with a uniform wave height $H_{sig} = 2.0$ m from a westerly direction (270°). All simulations run the bench-mark settings, including the 4-fraction sediment distribution. The sediment transport tuning factor settings are summarized in Table 5-6.

Table 5-6: Parameter settings sensitivity testing – wave climate.

Parameter	Value or remarks				
Tidal Schematisation	Based on Jiao (2014)				
Bed composition	4 Fractions ($d_{50} = 100, 200, 300$ and $400 \mu\text{m}$)				
	Space varying				
	Run	f_{SUS}	f_{BED}	f_{SUSW}	f_{BEDW}
$f_{FACTORS}$ sediment transport	(a)	0.7	0.7	0.3	0.7
	(b)	0.7	0.7	1	1
	(c)	0.3	0.1	0.3	0.7
Morphological wave climate	De Fockert (2008) – DF2008				
Duration of simulation	8 years				
Initial bathymetry	1999				

Analysis:

Figure 5-6 shows that minor differences are present between simulations (a) and (b). Most noticeable differences occur along the higher shoals and coastlines, where higher settings of f_{SUSW} and f_{BEDW} increase accretion. This effect is as expected, since these calibration factors influence the sediment transports due to wave-asymmetry. By definition these are onshore directed. With the imposed H_{sig} of 2 m, these factors do not (significantly) alter the patterns and magnitudes in the deeper parts of the ebb-delta and on the Bornrif shoal.

By decreasing the f_{SUS} and f_{BED} the total sedimentation and erosion can be significantly influenced. However, the patterns do not significantly alter. Similar results of different magnitude are observed in the sediment-erosion plots.

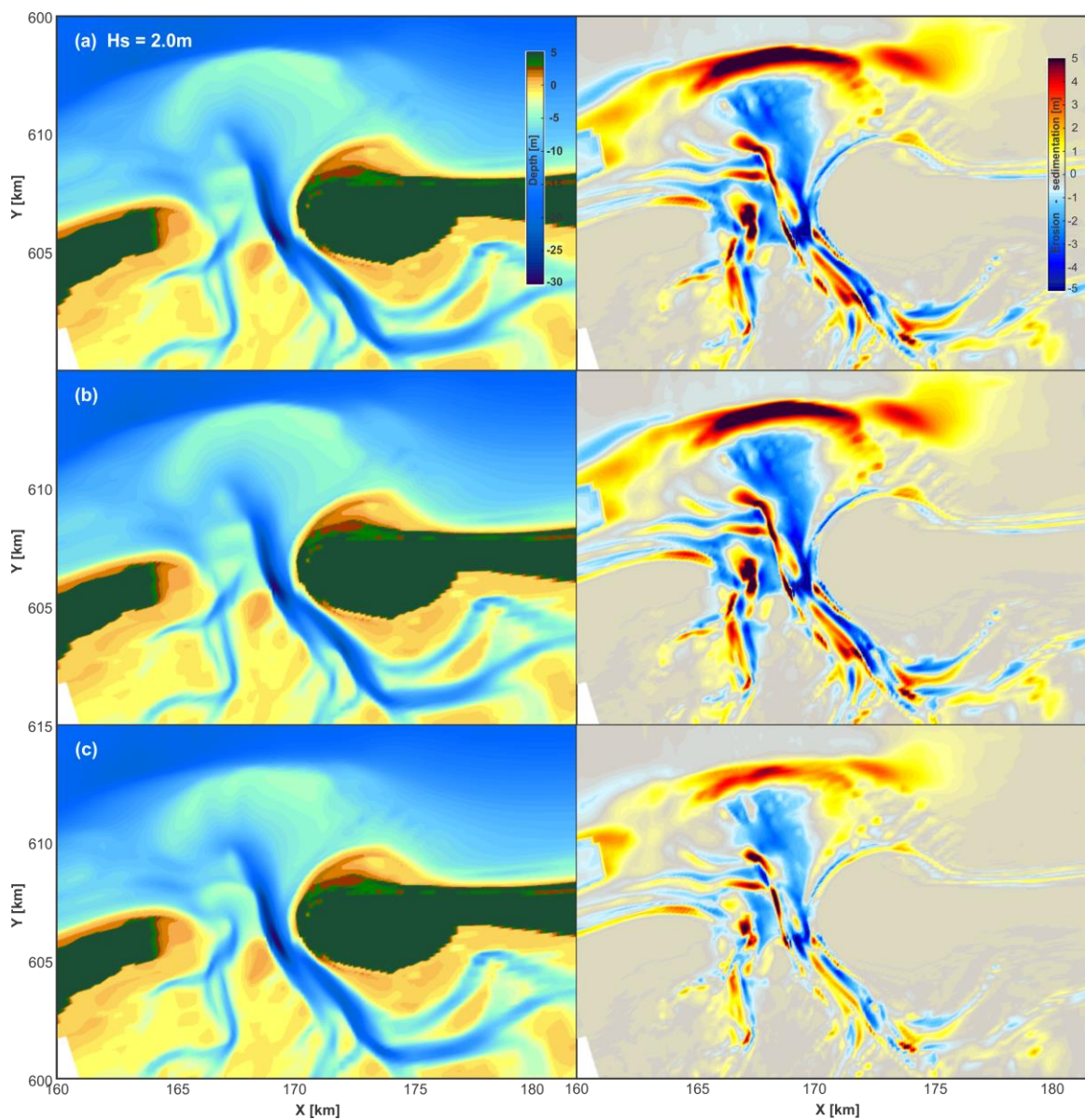


Figure 5-6: Effect of sediment transport tuning factors on morphodynamic change of the ebb-tidal delta. Model results after 10-years of simulation. For settings see Table 5-6.

5.3.4 Effect of initial bathymetry

Research question:

What is the influence of the initial bathymetry on the morphodynamic response.

Parameter settings:

These simulations run with the morphological wave climate. An initial uniform distribution of 2 sediment fractions (200 and 300 μm) with a thickness of 20 m (unlimited supply) is present. These results can therefore not be directly compared with the benchmark simulation.

Table 5-7: Parameter settings sensitivity testing – initial bathymetry.

Parameter	Value or remarks
Tidal Schematisation	Based on Jiao (2014)
Bed composition	4 Fractions (d50 = 100, 200, 300 and 400 μm) Space varying
$f_{FACTORS}$ sediment transport	$f_{SUS}= 0.7$, $f_{BED}= 0.7$, $f_{SUSW}= 0.3$ and $f_{BEDW}= 0.3$
Morphological wave climate	De Fockert (2008) – DF2008
Duration of simulation	8 years
Initial bathymetry	(a) 1999 (b) 2005 (c) 2011

Analysis:

Figure 5-7 illustrates the sensitivity of the modelled ebb-delta response to the initial bathymetry. Distinctively different patterns and bathymetries develop for the various starting years.

(1,2,3) Starting from 1999 or 2005 results in scour of Boschgat. Using the 2011 bathy retains the shallow platform.

(4) In all model's excessive scour occurs in Borndiep along Robben Eiland.

(5,6,7) All bathymetries show a tendency of Akkepollegat to rotate eastward. Largest accretion is observed for the 2011 bathy.

(8) The 2011 bathymetry propagates the existing ebb-shield seaward. The resulting is shoal is less pronounced than reality. No clear ebb-shield and chute are formed starting from 1999 or 2005 bathymetry.

(9,10) Starting from the 2005 bathymetry reproduces the migration of Bornrif Bankje most accurately. Starting from the 2011 bathymetry generates a Bankje, that nearly attached to the Strandhaak. The shape and size are different from the measured Bankje. The 1999 bathymetry forms a shoal on the platform but not at the correct location, or with the correct characteristics.

(11) All models show an eastward outbuilding of the Bornrif Strandhaak. Clear erosion is not observed.

Table 5-8: Comparison of measured and modelled morphodynamic changes. For numbering see Figure 5-7.

	Measured	1999	2005	2011
1	Erosion of the Boschplaat (island coast and tip)	+/-	+/-	+/-
2	Sedimentation Boschgat (inlet)	-	+/-	+/-
3	Eastward migration of Boschgat (basin) and shoal formation	+	+	+
4	Westward migration Borndiep	-	-	-
5	Accretion of Akkepollegat	+/-	+/-	+/-
6	Scour ebb-tidal delta front and eastward rotation Akkepollegat outflow	+/-	+/-	+/-
7	Localized sedimentation due to rotation Akkepollegat	+	+	+
8	Formation of an ebb-schild on Kofmansbult	+/-	+/-	+/-
9	Accretion central part of Bornrif	+/-	+/-	+/-
10	Formation, and landward/ eastward migration of Bornrif Bankje	-	+	+
11	Eastward migration, areas of erosion and accretion Bornrif Strandhaak	+/-	+/-	+/-
12	Large (channel) variability in the basin	+/-	+/-	+/-

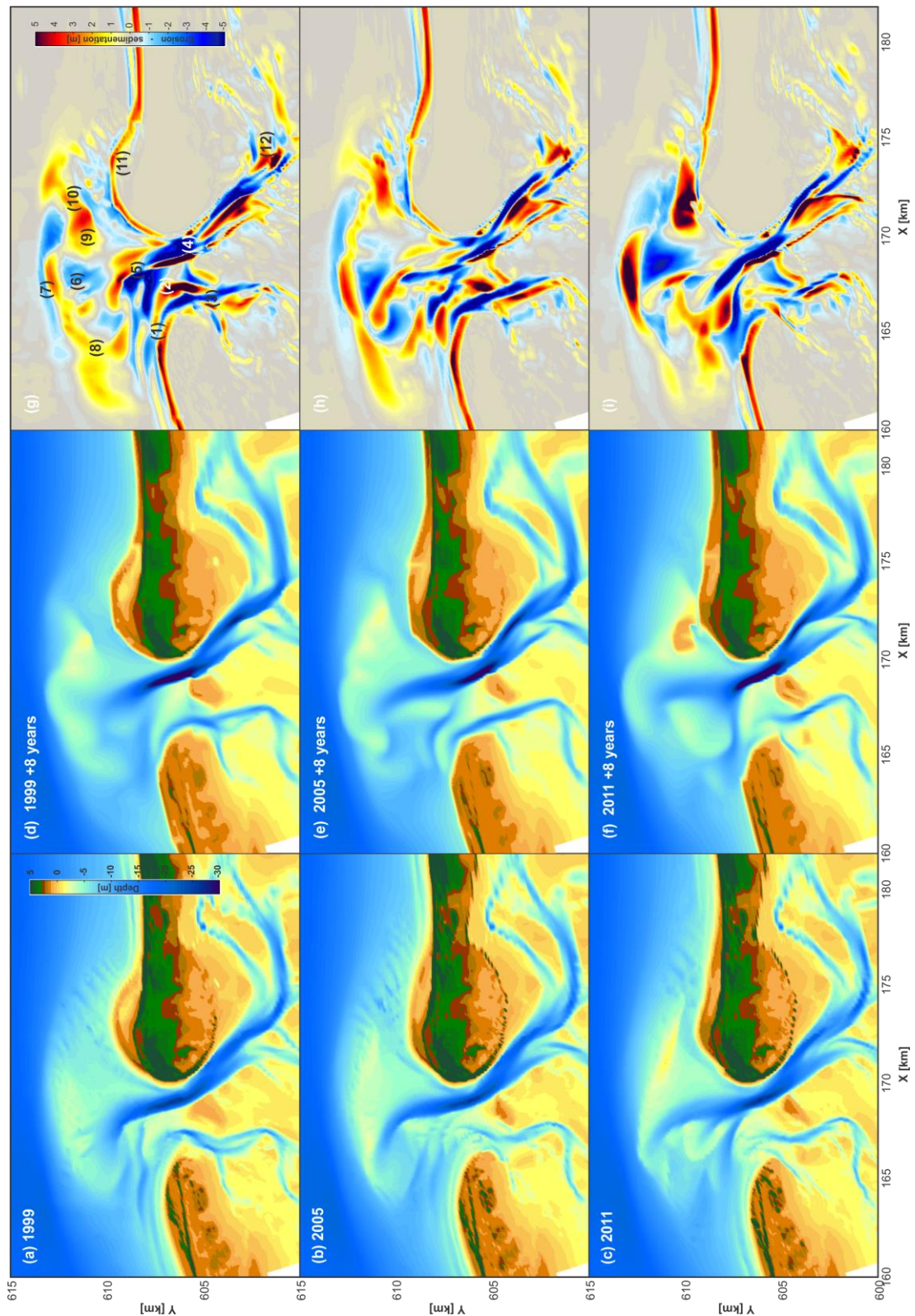


Figure 5-7: Effect of initial bathymetry of the ebb-tidal delta. (a,b,c) Initial model bathymetry for the years 1999, 2005 and 2011. (d,e,f) modelled bathymetries after 8 years of simulation, and (g,h,i) modelled morphodynamic changes.

5.3.5 Effect of reduced tides

Research question:

What is the influence of the morphological tide schematisation on the morphodynamic response.

Parameter settings:

Table 5-9: Parameter settings sensitivity testing – tides.

Parameter	Value or remarks
Tidal Schematisation	Based on Jiao (2014) (a)..-10% reduction of tidal range (b)..-20% reduction of tidal range (c)..-30% reduction of tidal range (d)..-50% reduction of tidal range
Bed composition	4 Fractions (d50 = 100, 200, 300 and 400 µm) Space varying
$f_{FACTORS}$ sediment transport	$f_{SUS} = 0.7$, $f_{BED} = 0.7$, $f_{SUSW} = 0.3$ and $f_{BEDW} = 0.3$
Morphological wave climate	De Fockert (2008) – DF2008
Duration of simulation	8 years
Initial bathymetry	1999

Analysis:

All runs show a similar morphodynamic response (Figure 5-8) to the reduction of the tide. Reduction of the morphological tide results in an onshore movement from the ebb-delta front. This movement increases as tides reduce. In addition, on the central Bornrif platform a shall shoal develops illustrating the changes balance between tidal and wave forcing. These runs illustrate the importance of a correct schematisation of the morphological tide. The observed over predicted ebb-delta growth may indicate that the tidal schematisation is not accurate enough.

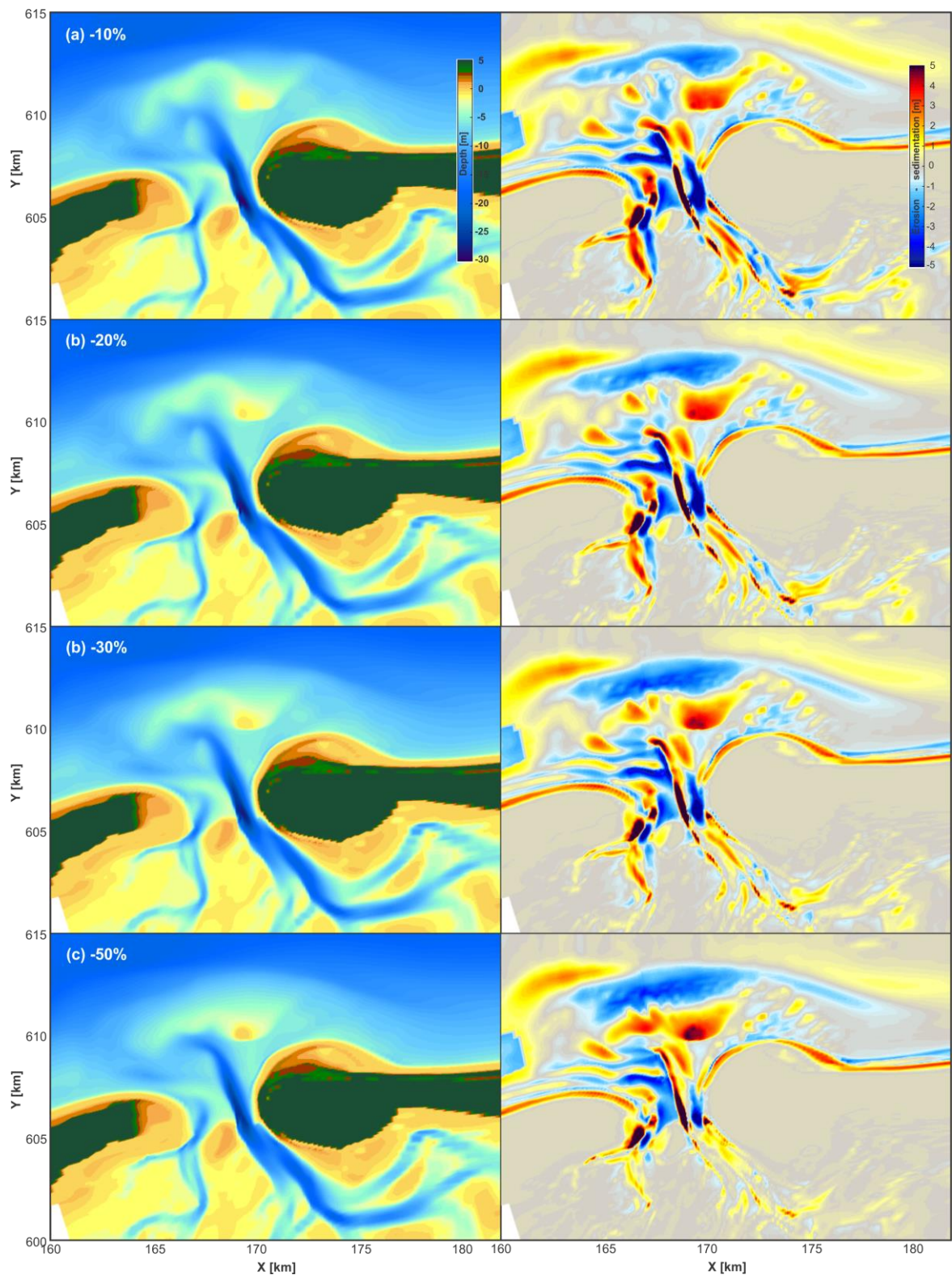


Figure 5-8: Effect of reduction of the morphological tide on morphodynamic change of the ebb-tidal delta. Model results after 10-years of simulation with (a) 10%, (b) 20%, (c) 30% and (d) 50% reduction.

5.4 Discussion

An impressive achievement obtained in the series of successive studies of Ameland is the improvement in model speed and stability. Starting from the initial Delft3D MOR model back in 1999, the Ameland model has developed into a highly efficient process-based model using a combination of an optimized (low-resolution) grid and innovative morphological acceleration approach. Medium-term (5-10 years), stable morphodynamic model simulations are now feasible with acceptable run times. This capability allows for sensitivity testing with the full morphodynamic model. Initial tests, presented in this report already provide insight in how to improve the bench-mark model (without changing the model formulations).

The model results presented in the bench-mark simulation show that morphodynamically stable simulations over a timescale of 5 to 10 years can be obtained with Delft3D. The use of a parallel online approach, in combination with a low-resolution model grid allows us to run with acceptable runtimes (~24 hrs/simulation). The bench-mark study specifically aims to identify which trends and patterns in morphodynamic behaviour can or cannot be reproduced. This approach is only feasible due to the increased efficiency of the numerical models (and computer hardware). By selecting a highly efficient bench-mark model we can easily implement, test and verify new insights, model developments and advances as these are obtained in the Kustgenese 2.0 project.

A simple comparison of bed-levels reveals a major short-coming of the bench-mark model. The modelled morphodynamic changes are significantly larger than the observed values. If one compares the range of bed-level variations in the measurements relative to the morphodynamic prediction after 8-years, one must conclude that the model results are well outside the range of the predicted values; the main channel is too deep and the spatial extend of the ebb-tidal delta, and the configuration of the shoal areas lie well beyond the measured values. However, comparing the observed trends, in the bench-mark simulation and all sensitivity tests, shows that the model is well capable of reproducing the dominant trends. Although not modelled perfectly, the model is capable to predict the erosion of the tip of the Boschplaat (but not the adjacent coast). Starting from the 2016 bathymetry (which includes the Kofmansbult ebb-shield), the model is also capable of reproducing the migration of the ebb-shield and the eastward rotation of the adjacent Akkepollegat. The related morphodynamic changes are likely overestimated, which distorts the Bornrif area and the associated processes. As a result, the bed-level itself seems incorrect, however the underlying processes are probably well modelled.

The morphodynamic response observed in the bench-mark model overpredicts the seaward expansion of the ebb-tidal delta; the ebb-tidal delta develops beyond measured limits. The basic processes controlling the shape of an ebb-tidal delta are well known (see a recent summary by Hayes & FitzGerald, 2013). In principle, the ebb-tidal delta facing the inlet is shown to reflect the ratio between wave- versus tidal energy. Conceptual descriptions by e.g. Hayes (1975, 1979), Oertel (1975) and Hubbard et al. (1979) show that wave-dominated ebb-tidal deltas tend to be pushed closer to the inlet throat. In the model, it is likely that the balance between the offshore directed tidal component and the onshore directed wave-driven transports is not resolved accurately.

5.5 Next steps in Kustgenese 2.0 research

5.5.1 Validate the morphological tide

Sensitivity simulations with reduced tides show that landward retreat of the ebb-tidal delta (keeping similar patterns) occurs as the tides decrease. An improved schematization of the morphological tide may be needed to improve model results. Although, De Fockert (2008) and Jiao (2004) have extensively investigated the correct morphological tide settings, both of the methods use a “closed” basin as a starting point. A justification of this choice was given by Hartsuiker and Wang (1999), based on the results of their hydrodynamic model no significant flow over the tidal divides was observed. The more recent study of Duran Matute et al. (2014) illustrates that a closed boundary at the Terschelling tidal divide does not really exist. In this study, model simulations driven by tides, wind and temperature over the 2009-2010 timeframe were made and estimates of the tidal prisms through the individual inlets and over the Terschelling watershed are presented. The averaged tidal prism through Ameland inlet was estimated at $383 \times 10^6 \text{ m}^3$ (mcm), with a net seaward residual of 12 mcm. The tidal prism over the watershed is 33 mcm, an order of magnitude smaller. However, the eastward residual flow of 23 mcm is comparable in magnitude to the residual flow through the inlet.

In addition, Jiao (2014) selected an arbitrary month as a basis for the tide schematisation. Additional steps to obtain a more accurate description of the long-term average uses as an input for the morphological tide are presented by Hartsuiker and Wang (1999). These additional steps include:

- (1) Select a representative year to represent the 18.6 year (Saros) tide cycle. Based on their analysis the year 1992 best represent this cycle.
- (2) Select a representative spring-neap cycle within the representative year. The month of may best represent the yearly cycle.
- (3) Choose the representative “double tide” that best describes the spring-neap cycle.

Note that the steps above are meant to get to a more accurate morphological tide. Prior to this analysis, the underlying model will be extensively calibrated, validated and evaluated with the measurements (flow, water levels) obtained from the Kustgenese campaigns. These measurements are essential for the exact definition of the various parameter settings.

5.5.2 Validate the Morphological wave-climate schematisation

Firstly, the difference in morphodynamic change between the bench-mark study using the DF2008 versus SR1999 wave climate, shows the importance of the wave schematization. Secondly, the model fails to reproduce much of the smaller-scale behaviour of shoals. For example the formation and migration of Bornrif Bankje that propagates as a distinct small, high shoal over the platform is likely controlled by wave events that specifically target the Bankje. Due to the wave sheltering of the ebb-tidal delta. It is possible that a wider range of wave heights needs to be included to account for specific (smaller scale) alterations of the individual shoals. In the present wave-climate schematisations this is not accounted for. The schematization of SR1999 is likely too simplistic, while the schematization of DF2008 is focused on the larger scale patterns.

In the past wave climates needed to be reduced to make these simulations feasible at all. But with the improved runtimes, we may need to revisit the classification techniques to more accurately account for the wave processes.

5.5.3 Grid resolution

Simulations with varying bathymetry show that importance of the initial state for the final model result. The model is capable of propagating the ebb-shield if present in the initial bathymetry, but not capable of reproducing the formation of the ebb-shield. It is well possible that this deficiency is related to the low-resolution grids used that may not contain or resolve the small-scale physics needed to develop these smaller-scale features.

5.5.4 Sediment transport tuning factors.

Once the morphological boundary conditions are set, the sensitivity test reveal that fine-scale tuning of the results can be obtained with the sediment calibration factors. More sensitivity testing on the correct settings of these parameters is needed. A focus needs to be on coastline erosion, as the model fails to reproduce island retreat accurately.

5.5.5 Initial bed composition.

The model reveals an excessive scour of the Borndiep channel. This may partly be related to the morphological tide schematization. Partly, this may be related to the bed composition that is not in equilibrium with the flow. More testing is needed to assess if bed compositions can be composed that are closer to the model equilibrium condition. Reducing excessive scour of the main channels will also reduce the overpredicted tides in the ebb-tidal delta.

5.6 Concluding Remarks

- Stable morphodynamic simulations on the medium-term timescales (5-10 years) can be obtained.
- Using a parallel-online approach and low resolution model grids allows us to perform these runs in an acceptable runtime (~24 hrs/simulation).
- The bench-mark model overpredicts the morphodynamic changes. The bed level changes exceed the observations. However, most of the important trends are reproduced.
- To more accurately predict the morphodynamic changes, the following improvements will be considered in the next steps (prioritisation may be needed if not all can be included):
 - Investigate the relative contribution of tides and waves. A more accurate morphological tide and/or morphological wave climate may be needed.
 - Improve the morphological wave-climate schematization to resolve the wave-driven transport over the ebb-tidal delta in more detail. This may improve the prediction of the smaller shoal areas.
 - Investigate the bed composition schematisation. Scour of the main channels still occurs, which may contribute to a larger sediment supply to the ebb-tidal delta.
 - Investigate the importance of the basin boundaries, open versus closed on the water sheds. This may alter the morphological tide prediction.
- A performance (skill) indicator needs to be developed and agreed upon acknowledging and reflecting a) system understanding, b) process understanding, c) model goals (i.e. target variables) related to the question to be answered, and d) model specific characteristics. The performance indicator may be a combination of subjective and objective evaluation(s).

6 References

- Booij, N., R. C. Ris, and L. H. Holthuijsen (1999), A third-generation wave model for coastal regions, Part I: Model description and validation, *J. Geophys. Res.*, 104(C4), 7649–7666, doi:10.1029/98JC02622.
- Bak, J. (2017). Nourishment strategies for the Ameland Inlet. Msc. Report, Delft University of Technology, 126 pp.
- Dastgheib, A. (2012). Long-term process-based morphological modelling of large tidal basins, Ph.D. Thesis, UNESCO-IHE, Delft, The Netherlands.
- De Fockert, A. (2008). Impact of relative sea level rise on the Ameland inlet Morphology, Master thesis, Delft University, Delft, The Netherlands.
- Eckart, C., (1958). Properties of water, Part II. The equation of state of water and sea water at low temperatures and pressures. *American Journal of Science*, 256, pp. 225-240.
- Elias, E.P.L., (2006). Morphodynamics of Texel Inlet. Ph.D. Thesis, Delft University of Technology, Faculty of Civil Engineering and Geosciences (Delft): 261 pp.
- Elias, E.P.L. and Hansen, J. (2012). “Understanding processes controlling sediment transports at the mouth of a highly energetic inlet system (San Francisco Bay, CA),” *Marine Geology*, 345, 207-220.
- Elias, E.P.L., Teske, R., Van der Spek, A., Lazar, M., (2015). Modelling tidal inlet morphodynamics on medium time scales, *Proceedings of Coastal Sediments 2015*, San Diego, USA.
- Elias, E.P.L. (2017a). Understanding the present-day morphodynamics of Ameland inlet. Report 120339-006, Deltares, Delft, 46pp.
- Elias, E.P.L. (2017b). *Kustgenese 2.0; available measurements and bathymetric data at Ameland inlet*, The Netherlands Report 120339-007, Deltares, Delft, 46pp.
- Hartsuiker and Wang (1999), *Morfologische ontwikkelingen in het Zeegat van Ameland: toetsing van hypothesen*. Alkyon / Delft Hydraulics, A450/Z2652, 161 pp.
- Hibma, A., (2004). Morphodynamic modelling of channel-shoal systems, *Communications on Hydraulic and Geotechnical Engineering*, vol. 04-3, Delft University of Technology, Delft, 122p

Holthuijsen, L.H., Booij, N., and Ris, R.C., (1993). A spectral wave model for the coastal zone. Proc. of the 2nd Int. Symposium on Ocean Wave Measurement and Analysis, New Orleans, 630-641.

Jiao, J., (2014). Morphodynamics of Ameland Inlet. Medium-term Delft3D modelling. MSc thesis Delft University of Technology. 10 September 2014.

Latteux, B., (1995). Techniques for long-term morphological modeling under tidal action. Marine Geology, 126, 129-141.

Leendertse, J. J. (1987), A three-dimensional alternating direction implicit model with iterative Fourth order dissipative non-linear advection terms, Rep. WD-3333-NETH, Rijkswaterstaat, Hague, Netherlands.

Lesser, G.R., Roelvink, J.A., Van Kester, J.A.T.M., Stelling, G.S., (2004). Development and validation of a three-dimensional model. Coastal Engineering 51: 883–915.

Lesser, G.R. (2009). “An approach to medium-term coastal morphological modelling,” Ph.D. Thesis, UNESCO-IHE, Delft, The Netherlands.

Pawlowicz, R., B. Breardsley, and S. Lentz (2002), Classical tidal harmonic analysis including error estimates in MATLAB using T_TIDE, Comput. Geosci., 28(8), 929–937, doi:10.1016/S0098-3004(02)00013-4.

Ris, R.C., Booij, N., Holthuijsen, L.H., (1999). A third-generation wave model for coastal regions, part II: verification. Journal of Geophysical Research 104 (C4), 7649–7666.

Roelvink, J.A., (1999), Morfodynamic simulations of the tidal inlet “Zeegat van Ameland”. Report 1: Validation of Delft2D-MOR. Alkyon/WL Delft Hydraulics, A505/Z2731. 68 pp.

Roelvink, J.A., (2006). Coastal morphodynamic evolution techniques. Coast. Eng. 53, 177–187.

Steijn R.C., Roelvink. J.A. (1999), Morfodynamische berekeningen voor het zeegat van Ameland. Rapport A505/Z2731.

Stelling, G. S. (1984), On the construction of computational methods for shallow water flow problems, PhD dissertation, 35 pp., Hauge Univ. of Appl. Sci., Hague, Netherlands.

Teske, R., (2013). Tidal inlet channel stability in long term process based modelling. MSc traineeship report, thesis University of Utrecht, July 2013.

van der Wegen, M., Jaffe, B.E., Roelvink, J.A., (2011). Process-based, morphodynamic hindcast of decadal deposition patterns in San Pablo Bay, California, 1856–1887. J. Geophys. Res. 116, F02008. <http://dx.doi.org/10.1029/2009JF001614>.

Van Rijn, L.C., (1993). Principles of sediment transport in Rivers, Estuaries and Coastal Seas. Aqua Publications, Amsterdam. Van Rijn (2000)

Van Rijn, L.C., (2002). Approximation formulae for sand transport by currents and waves and implementation in DELFT-MOR, Report Z3054.20. WL\Delft Hydraulics, Delft.

Van Rijn, L.C., (2007a). Unified view of sediment transport by currents and waves. I: Initiation of motion, bed roughness, and bed-load transport. *Journal of Hydraulic Engineering* 133, 19.

Van Rijn, L.C., (2007b). Unified view of sediment transport by currents and waves. II: Suspended transport. *Journal of Hydraulic Engineering* 133, 22.

Van Rijn, L.C., (2007c). Unified view of sediment transport by currents and waves. III: Graded beds. *Journal of Hydraulic Engineering* 133, 15.

Walstra, D.J. and Van Rijn, L.C. (2003). Modeling of sand transport in Delft3D, Report Z3624. WL\Delft Hydraulics, Delft.

Wang, Z.B., Louters, T. and De Vriend, H.J., 1995. Morphodynamic modelling for a tidal inlet in the Wadden Sea, *Marine Geology* 126, 289-300.

WANG, Y. (2015) Coupling bedform roughness with decadal morphodynamics of Ameland Inlet Yunwei Wang. MSc thesis, Delft University of Technology.

Wang, Y., YU, Q., Jiao, J., Tonnon, P.K., Wang, Z.B. and Gao, S. (2016) Coupling bedform roughness and sediment grain-size sorting in modelling of tidal inlet incision. *Marine Geology*, 381, 128–141. doi:10.1016/j.margeo.2016.09.004